Franziska Vogl MSc

Janus-faced oxidized phospholipids: Toxic mediators in macrophages and skin cancer cells

DISSERTATION

zur Erlangung des akademischen Grades

Doktorin der Naturwissenschaften

eingereicht an der

Technischen Universität Graz

Betreuer

Ao.Univ.-Prof. Dr.phil. Albin Hermetter

Institut für Biochemie

Graz, September 2014

Danksagung

Die vorliegende Arbeit wurde im Zeitraum von April 2011 bis September 2014 am Institut für Biochemie an der Technischen Universität Graz durchgeführt.

Betreuer dieser Arbeit war Univ.-Prof. Dr. Albin Hermetter, dem ich an dieser Stelle meinen Dank dafür aussprechen möchte, dass er mir die Möglichkeit gegeben hat, meine Dissertation in seiner Arbeitsgruppe zu verfassen.
Ich konnte jederzeit, wenn Fragen auftauchten, auf ein offenes Ohr und hilfreiche Anregungen und Lösungsansätze zählen. Seine herausragende fachliche Expertise auf dem Gebiet der Lipidforschung, seine vielen Ideen und zahlreiche spannende Diskussionen haben maßgeblich zu dem Gelingen der von mir bearbeiteten Projekte beigetragen.

Weiters möchte ich mich bei der gesamten Arbeitsgruppe Hermetter und den vielen lieben Kolleginnen und Kollegen, mit denen ich während meiner Dissertationszeit zusammenarbeiten durfte, bedanken. Die freundliche Atmosphäre und die methodischen Hilfestellungen im Labor haben zu einem sehr angenehmen und kollegialen Arbeitsklima beigetragen. Mein besonderer Dank gilt in diesem Zusammenhang Elfriede Zenzmaier, Claudia Ramprecht und Daniel Koller.

Ich möchte mich auch herzlich bei meinen Eltern und bei Martin für ihre fortwährende Unterstützung und ihren Zuspruch während meiner Dissertationszeit bedanken.

EIDESSTATTLICHE ERKLÄRUNG

AFFIDAVIT

Ich erkläre an Eides statt, dass ich die vorliegende Arbeit selbstständig verfasst, andere als die angegebenen Quellen/Hilfsmittel nicht benutzt, und die den benutzten Quellen wörtlich und inhaltlich entnommenen Stellen als solche kenntlich gemacht habe. Das in TUGRAZonline hochgeladene Textdokument ist mit der vorliegenden Dissertation identisch.

I declare that I have authored this thesis independently, that I have not used other than the declared sources/resources, and that I have explicitly indicated all material which has been quoted either literally or by content from the sources used. The text document uploaded to TUGRAZonline is identical to the present doctoral dissertation.

Datum / Date	Unterschrift / Signature

Abstract

Oxidized phospholipids (oxPL) are components of cell membranes and plasma lipoproteins. They are toxic in vascular cells and contribute to the development of atherosclerosis. POVPC (1-palmitoyl-2-(5-oxovaleroyl)-*sn*-glycero-3-phosphocholine) and PGPC (1-palmitoyl-2-glutaroyl-*sn*-glycero-3-phosphocholine) are main components of oxidized low-density lipoprotein. These compounds contain short-chain carboxylic acid residues in position *sn*-2 of glycerol that are responsible for their specific biochemical properties. Sustained exposure to PGPC and POVPC induces apoptosis in cultured macrophages, as well as in cultured melanoma and non-melanoma skin cancer cells. It was the aim of this doctoral thesis to identify molecular mechanisms of oxPL toxicity to improve our understanding of oxPL (patho)biochemistry in these cells.

In the first part of this doctoral thesis we found that oxPL-induced apoptotic cell death in cultured RAW 264.7 macrophages is associated with the formation of apoptotic ceramide and time-dependent activation of effector caspases. We identified protein kinase C-delta (PKCδ) as a key pro-apoptotic kinase which is causally related to activation of caspase-3 and -7 in macrophages under the influence of oxPL. SiRNA-mediated knockdown of PKCδ resulted in decreased caspase activation by oxPL in these cells. Direct interaction between PKCδ and oxPL in live cells was determined from codiffusion of RFP-tagged PKCδ and fluorescently labeled oxPL.

The second part of this doctoral thesis was devoted to the molecular mechanisms of oxPL toxicity in skin cancer cells. PGPC and POVPC preferably induce apoptosis in skin cancer cells compared with differentiated progenitor cells. The primary protein targets of fluorescent oxPL have been determined in human squamous carcinoma cells. Next to other identified candidates, several proteins from the heat shock protein (Hsp) family and the protein disulfide isomerase (PDI) family have been identified. We found that PGPC inhibited the enzymatic activities of Hsps and PDI *in vitro*. POVPC also reduced HSP activity, but activated PDI. In line with the observed modification

and dysfunction of ER-associated proteins (PDI, some Hsps), expression levels of ER-stress markers were upregulated in oxPL-treated cells. Finally, oxPL affected the expression of ceramide synthase 4 which is an enzyme of *de novo* ceramide synthesis and also localizes to the ER. Ceramides are mediators of apoptotic cell death elicited by PGPC and POVPC.

The cytotoxic activities of oxPL may be regarded janus-faced since their ultimate consequences may be positive or negative, depending on the (patho)physiological context. In vascular cells oxPL promote initiation and progression of atherosclerosis. Their cytotoxic activities in skin cancer cells make them promising candidates as anti-cancer drugs.

Zusammenfassung

Oxidierte Phospholipide sind Bestandteile von Zellmembranen und Lipoproteinen. Diese Substanzen wirken toxisch auf vaskuläre Zellen und tragen zur Entstehung von Arteriosklerose bei. POVPC (1-Palmitoyl-2-(5-Oxovaleroyl)-*sn*-glycero-3-phosphocholin) und PGPC (1-Palmitoyl-2-Glutaroyl-*sn*-glycero-3-phosphocholin) sind wichtige biologisch aktive Bestandteile von oxidierten Lipoproteinen geringer Dichte (oxLDL). Sie tragen eine verkürzte Acylkette in der *sn*-2-Position des Glycerols, die ihre jeweiligen biochemischen Eigenschaften bestimmt. Wenn kultivierte Makrophagen und Hautkrebszellen längere Zeit oxidierten Phospholipiden ausgesetzt sind, wird in diesen Zellen apoptotischer Zelltod ausgelöst. Ziel dieser Doktorarbeit war es, molekulare Mechanismen zu identifizieren, die für die toxischen Effekte der oxidierten Phospholipide in kultivierten Zellen verantwortlich sind, um die Pathobiochemie dieser Verbindungen besser zu verstehen.

Im ersten Teil dieser Doktorarbeit konnten wir zeigen, dass der durch oxidierte Phospholipide ausgelöste Zelltod in Makrophagen mit der Bildung des apoptotischen Mediators Ceramid und der zeitabhängigen Aktivierung von Effektor-Caspasen einhergeht. Wir haben herausgefunden, dass die Protein Kinase C-delta (PKCδ) ein Schlüsselenzym in der Lipid-induzierten Apoptose darstellt. PKCδ steht in kausalem Zusammenhang mit der Lipid-abhängigen Aktivierung der Caspasen-3 und -7. In PKCδ-Knockdown-Zellen wurde eine geringere Caspase-Aktivierung durch oxidierte Phospholipide gemessen als in Kontrollzellen. Auf der Basis der Codiffusion von RFP-markierter PKCδ und fluoreszierenden oxidierten Phospholipiden konnten wir in lebenden Zellen eine direkte Interaktion zwischen Lipiden und PKCδ nachweisen.

Der zweite Teil dieser Doktorarbeit befasste sich mit den molekularen Mechanismen, die für die Toxizität oxidierter Phospholipide in Hautkrebszellen verantwortlich sind. Die oxidierten Phospholipide PGPC und POVPC lösen in Hautkrebszelllinien Apoptose aus, beeinflussen aber die Viabilität von differenzierten Vorläuferzellen weit weniger. In kultivierten Plattenepithelkarzinomzellen der Haut haben wir jene Proteine

identifiziert, die molekulare Targets von fluoreszenzmarkierten oxidierten Phospholipiden repräsentieren. Unter diesen Targetproteinen befinden sich Abkömmlinge der Hitzeschockproteinfamilie (Hsps) und Proteindisulfidisomerasen (PDIs). Wir konnten zeigen, dass PGPC die enzymatische Aktivität von Hitzeschockproteinen und einer Proteindisulfidisomerase hemmte. POVPC hemmte ebenfalls Hsps, aktivierte aber die PDI. In Übereinstimmung mit der beobachteten Modifizierung und Dysfunktion von ER-assoziierten Proteinen wurden in den Lipid-behandelten Zellen erhöhte Expressionslevel von ER-Stress-Markern detektiert. Die oxidierten Phospholipide beeinflussten auch die Expression der Ceramidsynthase 4, die ein Enzym der *de novo* Ceramidsynthese darstellt und ebenfalls im ER lokalisiert ist. Ceramide sind Mediatoren der Apoptose, die durch PGPC und POVPC ausgelöst wird.

Die toxische Wirkung von oxidierten Phospholipiden hat zwei Seiten, da sie abhängig vom (patho)physiologischen Kontext positive oder negative Konsequenzen haben kann. In vaskulären Zellen sind oxidierte Phospholipide maßgeblich an der Entstehung von Arteriosklerose beteiligt. Hingegen können diese Substanzen wegen ihrer zytotoxischen Effekte auf Hautkrebszellen als viel versprechende Wirkstoffkandidaten in der Krebstherapie angesehen werden.

Table of Contents

CHAPTER 3

OXPL MODULATE ENZYME ACTIVITIES OF CHAPERONES AND PROTEIN DISULFIDE ISOMERASE *IN VITRO* AND IN CULTURED SKIN CANCER CELLS

APPENDIX

PROTEIN TARGETS OF BY-POVPE IN CULTURED RAW 264.7 MACROPHAGES

List of Figures

List of Tables

Chapter 1

General Introduction

1.1 Oxidized phospholipids

1.1.1 Structure and formation of oxidized phospholipids

Glycerophospholipids are the main component of cellular membranes. The classes of glycerophospholipids differ by the polar alcohols esterified to the diacyl-*sn*-glycerophospholipid backbone. These compounds include phosphatidic acid, phosphatidylethanolamine, phosphatidylserine, phosphatidylcholine, phosphatidyl-glycerol, phosphatidylinositol and cardiolipin.

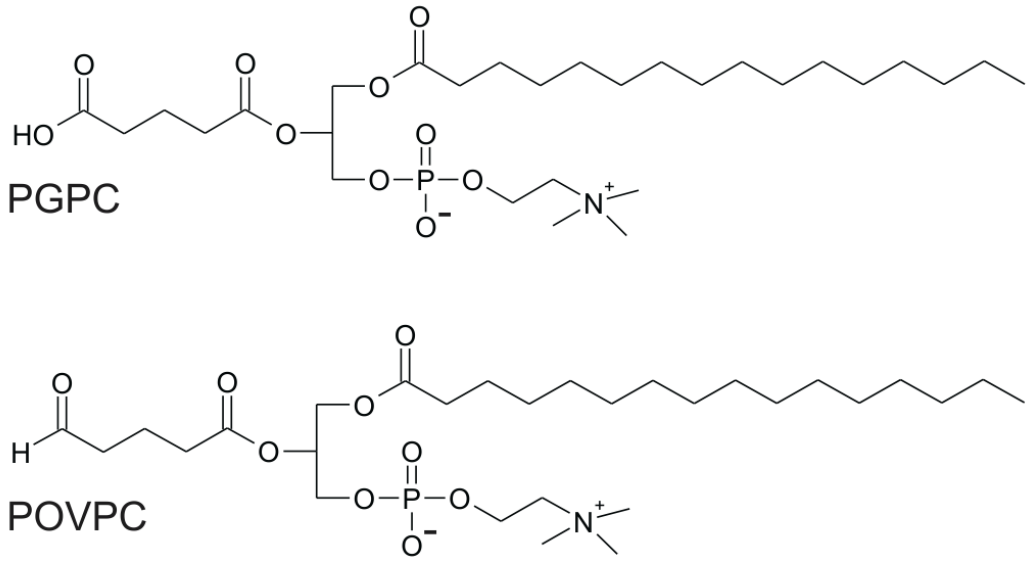

Figure 1.1 Chemical structures of the oxidized phospholipids PGPC and POVPC.

1-palmitoyl-2-glutaroyl-sn-glycero-3-phosphocholine (PGPC)
1-palmitoyl-2-(5-oxovaleroyl)-sn-glycero-3-phosphocholine (POVPC)

In eukaryotic phospholipids the *sn*-1 position of the glycerol backbone is either linked to an acyl residue via an ester bond or to an alk(en)yl residue via an (enol)ether bond. Saturated fatty acids are usually found at the *sn*-1 position of the glycerol backbone. The *sn*-2 position is frequently linked to an unsaturated fatty acid. The polyunsaturated fatty acids (PUFAs) at the *sn*-2 position of the glycerol are the most sensitive targets of free radical attack due to their bisallylic hydrogen atoms. Since phosphatidylcholine is

one of the main phospholipids in animal tissues (Christie, 1985), many oxidized phospholipids identified *in vivo* contain a choline headgroup.

Enzyme-catalyzed and non-enzymatic reactions lead to the formation of a plethora of different reaction products. The resultant oxidatively modified lipids differ by the degree of modification, hydrophobicity, chemical reactivity, physical properties and biological activities (Fruhwirth *et al.*, 2007). The truncated phospholipids represent an important subclass of reaction products. POVPC (1-palmitoyl-2-(5-oxovaleroyl)-*sn*-glycero-3-phosphocholine) and PGPC (1-palmitoyl-2-glutaroyl-*sn*-glycero-3-phosphocholine) are two important derivatives of fragmented phospholipids (Figure 1.1). They are biologically active components of oxidized low-density lipoprotein (see 1.2.1) and significantly contribute to the toxicity of this particle in the vascular wall (Watson *et al.*, 1997; Subbanagounder *et al.*, 2000; Loidl *et al*., 2003).

1.1.2 Biophysical properties and biochemical reactivity of oxPL

The truncated phospholipids PGPC and POVPC show highly similar structures. Both lipids are generated from 1-palmitoyl-2-arachidonoyl-*sn*-glycero-3-phosphatidylcholine (PAPC) under oxidative stress. They contain a long-chain carboxylic acid at the *sn*-1 position and a short-chain carboxylic acid at the *sn*-2 position of the glycerol backbone. Subbanagounder *et al.* have shown that the acyl group at the *sn*-2 position determines the specific bioactivity of PGPC and POVPC (Subbanagounder *et al.*, 2000). The structures of these two oxPL only differ by the functional group at the ω-end of the truncated *sn*-2 acyl residue. In this position, PGPC carries a carboxyl group, whereas POVPC contains an aldehyde function. This small structural difference leads to a significant change in chemical reactivity and to a different conformation in membranes.

In a lipid bilayer, the amphiphiles POVPC and PGPC are anchored to the phospholipid phase only by one long hydrophobic acyl chain. The negatively charged *sn*-2 carboxylate group of carboxylate phospholipids (e.g. PGPC) protrudes into the aqueous phase. In contrast, the less polar aldehyde function of aldehydo-phospholipids

(e.g. POVPC) resides in the lipid-water interface of the bilayer (Beranova *et al.*, 2010; Khandelia and Mouritsen, 2009; Wong-Ekkabut *et al.*, 2007; Greenberg *et al.*, 2008). PGPC can only physically interact with biomolecules in its immediate vincinity via its carboxyl group. In contrast, POVPC can undergo Schiff base formation with -NH_2 groups of proteins and aminophospholipids such as phosphatidylethanolamine and phosphatidylserine (Stemmer *et al.*, 2012; Hermetter *et al.*, 2013). These lipid-lipid modifications (I.) and lipid-protein modifications (II.) have structural and functional consequences for the affected biomolecules.

I.) Lipid-lipid modifications: Schiff base formation between the carbonyl group of POVPC and the amino group of phosphatidylethanolamine results in lipid products with three tails and two heads. The insertion of such adduct lipids into bilayers of POPC increases the average cross-sectional area per lipid and decreases bilayer thickness. Schiff base formation between lipids can alter the concentration, homeostasis and localization of phosphatidylserine and ethanolamine-phospholipids in membranes. As a consequence, several membrane-associated processes including fusion and budding may be influenced. (Hermetter *et al.*, 2013) Changes in lipid geometry and polarity give rise to changes in membrane organization and curvature. Rhode *et al.* showed that fluorescent PGPC induces the formation of endosomes within seconds (Rhode *et al.*, 2009). These supramolecular lipid-lipid interactions can be explained by phospholipid geometry: PGPC is conically shaped since it contains a large head group and only a small hydrophobic tail (*sn*-1 acyl chain). As a consequence, it facilitates the formation of curved membrane regions leading to endosome segregation.

II.) Lipid-protein modifications: Not only membrane lipids are affected by lipid modification, proteins are targeted by lipid peroxidation products as well (see Figure 1.2). Lysine, histidine and cysteine residues have been shown to undergo Michael addition with unsaturated lipid aldehydes (e.g. hydroxyalkenals) (Grimsrud *et al.*, 2008; Fruhwirth *et al.*, 2007). Aldehydo-phospholipids can form Schiff bases with

nucleophilic -NH_2 groups of lysines, since at physiological pH a fraction lysines is at least partially deprotonated.

Protein modification with lipid oxidation products may influence protein function. Protein inactivation by 4-HNE-modification has been shown for several membrane transporters as well as enzymes, such as isocitrate dehydrogenase, thioredoxin or glutathione peroxidase. (Grimsrud *et al.*, 2008) In addition, Cathepsin B (Crabb *et al.*, 2002), Hsp90 (Carbone *et al.*, 2005), Hsp72 (Carbone *et al.*, 2004) and protein disulfide isomerase (Muller *et al.*, 2013) are inactivated by modification with reactive aldehydes. PoxnoPC (1-palmitoyl-2-(9'-oxo-nonanoyl)-*sn*-glycero-3-phosphocholine) can covalently react with phospholipase A2 via Schiff base formation and enhance the activity of this enzyme in DPPC (1,2-dipalmitoyl-*sn*-glycero-3-phosphocholine) membranes (Code *et al.*, 2010).

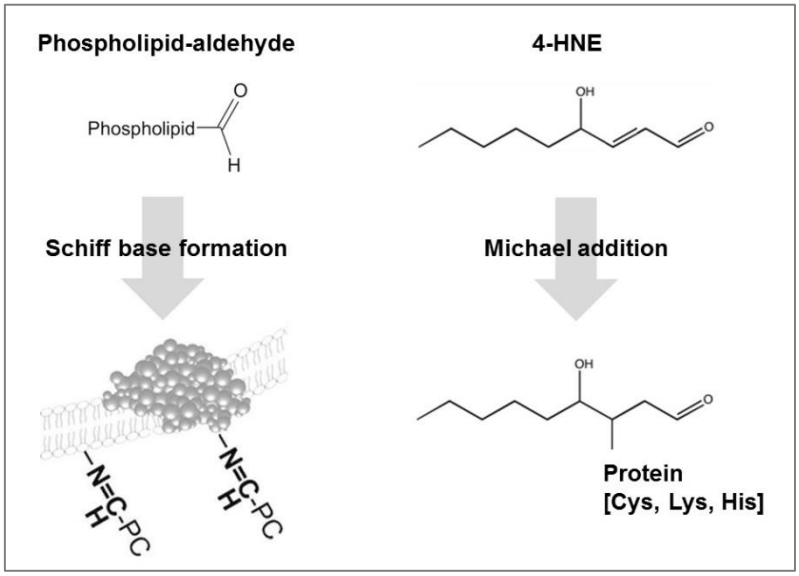

Figure 1.2 Schematic representation of Schiff base formation and Michael adduct formation.

Phospholipid aldehydes can undergo covalent Schiff base formation with free amino groups of proteins and aminophospholipids in cellular membranes (left side). 4-hydroxynonenal (4-HNE) can form Michael adducts with cysteine, lysine or histidine residues of proteins (right side).

Furthermore, lysine modification with lipid aldehydes is well studied for apoB on the surface of oxLDL. During LDL oxidation, lipid peroxidation products become covalently attached to apolipoprotein B (apoB). Oxidized phospholipids containing ω-aldehydoacyl groups at the *sn*-2 position bind to lysine residues of apoB and thereby mask the positive charge of the lysine clusters of apoB (Gillotte *et al.*, 2000). Steinbrecher *et al.* have shown that there is a progressive decrease in the number of reactive lysine ε-amino groups during oxidation of LDL (Steinbrecher *et al.*, 1987). As a consequnce, oxLDL is rendered more negatively and is no longer recognized by the classical apoB receptor and oxLDL is taken up by macrophage scavenger receptors (Gillotte *et al.*, 2000).

Cellular proteins are also modified by aldehydo-oxPL. OxPL protein targets have been identified in endothelial cells (Gugiu *et al.*, 2008) and in RAW 264.7 macrophages (Stemmer *et al.*, 2012). Both studies show that only a limited subfraction of the total proteome was targeted by oxPL. In macrophages, many of the detected proteins are relevant to apoptotic signaling and stress response. (Stemmer *et al.*, 2012) In this work the focus is on one of the identified proteins, namely protein kinase C-delta (PKCδ), which is a kinase involved in apoptotic signaling (see Chapter 2).

1.2 Oxidized phospholipids in arteriosclerosis

1.2.1 OxLDL and oxPL in the development of arteriosclerosis

One major risk factor for the development of arteriosclerosis is the oxidative modification of plasma LDL (low density lipoprotein). The biological function of LDL is to transport cholesterol from the liver to peripheral tissue. Native LDL is taken up by cells via LDL receptors (apoprotein B/E receptor) which recognize the apolipoprotein B-100 on the particle. (Goldstein and Brown, 2009) In contrast to native LDL, modified LDL is not recognized by the apoB receptor anymore, but it can be taken up by scavenger receptors of macrophages (Brown and Goldstein, 1979) (see below).

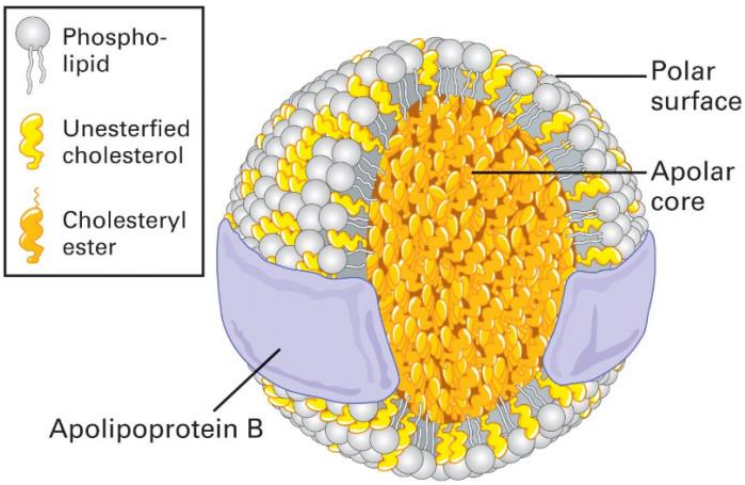

Figure 1.3 Structure of low density lipoprotein (LDL).

LDL consists of a hydrophobic core containing mainly cholesteryl esters and triacylglycerides. The core is surrounded by a phospholipid monolayer and one apolipoprotein B-100 molecule. This figure was taken from: Molecular Cell Biology, Sixth Edition, ©2008 W.H. Freeman and Company.

LDL consists of protein and lipid components (Figure 1.3). The particle is surrounded by a phospholipid monolayer containing phosphatidylcholine, cholesterol and sphingomyelin. A single apolipoprotein B-100 molecule (apoB100) is bound to the

polar surface. The hydrophobic core of the LDL particle contains cholesteryl esters and triacylglycerols.

Under conditions of oxidative stress, the protein and lipid components of LDL are subject to modification. Depending on the extent of modification, minimally modified LDL (mmLDL) and extensively oxidized LDL (oxLDL) are formed. In mmLDL, mostly the lipids are modified by phospholipid aldehydes and other electrophiles (e.g. HNE, MDA). In oxLDL, the protein components are affected by oxidative modification as well. The bioactive compounds in oxLDL include phospholipid products (e.g. *sn*-2 short chain PAPC oxidation products such as POVPC and PGPC), free fatty acid oxidation products (HODE, HPODE, HETE, HPETE, isoprostanes and the aldehydes HNE and MDA) and oxysterols (e.g. cholesteryl ester hydroperoxides and aldehydes) (Levitan *et al.*, 2010). The oxPL POVPC and PGPC (Figure 1.1) are present in mmLDL (Berliner *et al.*, 2001) and have been found in atherosclerotic lesions (Watson *et al.*, 1997).

Since the protein component (apoB) is hardly modified in mmLDL, this particle is still recognized by the apoB receptor (Salvayre *et al.*, 2002; Levitan *et al.*, 2010; Gillotte *et al.*, 2000). OxLDL in contrast, is not recognized by the apoB receptor anymore but can be taken up by macrophages via several receptors including scavenger receptors and Toll-like receptors (TLRs) (Fruhwirth *et al.*, 2007; Levitan *et al.*, 2010). Specifically, scavenger receptor A (SR-A) and CD36 are the main scavenger receptors responsible for the uptake of modified LDL into macrophages (Kunjathoor *et al*., 2002). Macrophage scavenger receptors recognize apoptotic and necrotic cells and mediate clearance of these cells by phagocytosis. It has been shown that oxidized phospholipids linked to apoB serve as ligands for macrophage receptors. OxPL containing ω-aldehydo carboxylic acids in position *sn*-2 may react with free -NH_2 groups of lysine residues on the surface of oxLDL (Gillotte *et al*., 2000) and as a consequence make the particle a ligand for scavenger receptors.

Depending on the degree of modification and on lipid concentration, oxidized LDL elicits proliferative or apoptotic effects. At low concentrations, oxLDL prevents apoptosis and induces cell proliferation. In contrast, high concentrations of oxLDL induce apoptosis and necrosis in macrophages. (Steinbrecher *et al*., 2004) In the subendothelial space, oxLDL attracts monocytes that subsequently differentiate into macrophages. These cells massively take up oxLDL and undergo foam cell formation (Figure 1.4).

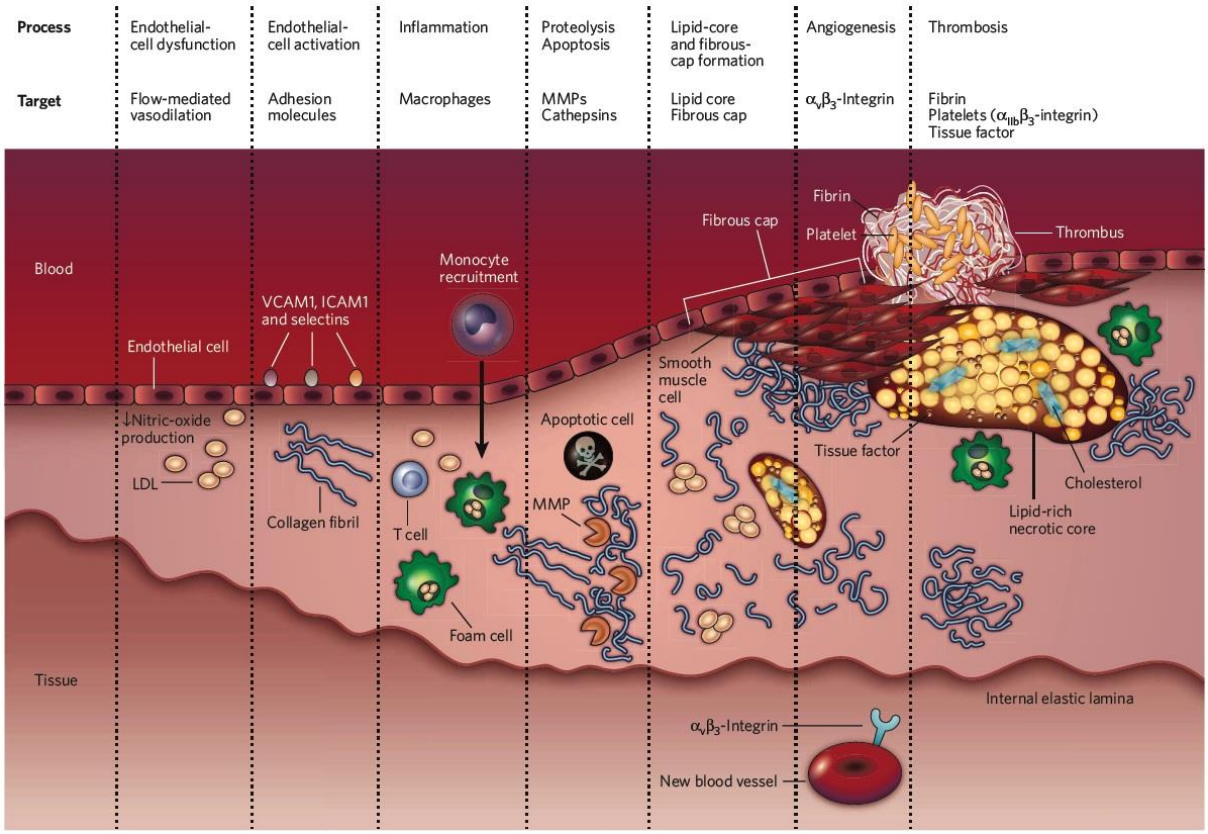

Figure 1.4 The development of an atherosclerotic lesion.

The progression of an atherosclerotic lesion is shown in a simplified form, developing from a normal blood vessel (far left) to a vessel with an atherosclerotic plaque and superimposed thrombus (far right). (Figure and legend from Sanz and Fayad (Sanz and Fayad, 2008)).

Accumulation of lipid-loaded macrophages is characteristic for early atherosclerotic lesions, termed “fatty streaks”. Migration of smooth muscle cells into the fatty streak leads to the formation of a more complex atherosclerotic lesion. (Glass and Witztum,

2001; Sanz and Fayad, 2008; Ross, 1999) These atherosclerotic lesions contain high concentrations of oxidized phospholipids and apoptotic/ necrotic macrophages (Berliner *et al.*, 2001; Watson *et al.*, 1997). During the initiation and progression of arteriosclerosis, several cell types are involved including monocytes, macrophages, endothelial cells, vascular smooth muscle cells and lymphocytes. Inflammation, deposition of cell debris and oxidized lipids in the blood vessel wall leads to the development of atherosclerotic plaques, resulting in a reduced cross-section of the arteries. Advanced atherosclerotic lesions are prone to plaque rupture followed by thrombosis and occlusion of blood vessels. These events may finally result in cardiovascular complications as myocardial infarction and stroke. (Glass and Witztum, 2001; Sanz and Fayad, 2008; Ross, 1999)

1.2.2 Effects of PGPC and POVPC on cultured vascular cells

Our group showed that the oxPL PGPC and POVPC induce apoptosis in vascular smooth muscle cells (VSMCs) (Loidl *et al.*, 2003; Loidl *et al.*, 2004; Fruhwirth *et al.*, 2006; Moumtzi *et al.*, 2007), in primary macrophages as well as in RAW 264.7 macrophage like cells (Stemmer *et al.*, 2012). In all these cells, induction of apoptosis by oxPL is mediated by the apoptotic messenger ceramide, which is generated at least in part by activation of aSMase (for VSMCs see Loidl *et al.*, 2003; for macrophages see Stemmer *et al.*, 2012). In cultured RAW 264.7 macrophages, the oxPL seem to activate at least two ceramide synthesizing pathways. In the early phase of signaling, they trigger ceramide generation by fast activation of aSMase. PGPC and POVPC also activate specific subsets of ceramide synthase isoforms that correlate with a rise in cellular ceramide levels. (Halasiddappa *et al.*, 2013) Ceramide synthases generate ceramide via the *de novo* pathway and/ or recycling pathways (Levy and Futerman, 2010). It was speculated that the latter ceramide pool is involved in the late (execution) phase of apoptosis.

In rat vascular smooth muscle cells, it was shown that mmLDL as well as PGPC and POVPC activate signaling components of stress response and apoptotic cell death including p38 MAPK and JNK (Loidl *et al.*, 2003). Activation of MAPK and JNK

results in the activation of the executor caspase-3 and -7 (Loidl *et al*., 2003), directly leading to apoptotic cell death. POVPC and PGPC also influence cell physiology on the transcriptional level, although to a different extent. Gene expression analysis using microarrays showed that PGPC affects the expression of hundreds of genes, whereas POVPC exerts only minor effects on the transcriptome level (Koller *et al.*, PhD thesis, TU Graz, 2013). POVPC is likely to act on the proteome level. It can form Schiff bases with primary amino groups of proteins and aminophospholipids. Thereby POVPC influences the structure and function of these biomolecules (see 1.1.2 Biophysical properties and biochemical reactivity of oxPL).

In summary, oxPL affect cell physiology and viability by molecular and supramolecular effects. From fluorescence microscopic studies it is known that they are easily taken up to the plasma membrane of vascular cells (Stemmer *et al.*, 2012; Moumtzi *et al.*, 2007). After cellular uptake, they modulate membrane organization, induce vesicle formation, interact with proteins and phospholipids, and as a consequence activate a cascade of intracellular signaling molecules (see above). The oxPL interfere with cellular metabolism on the transcriptome, proteome and lipidome level. The apoptotic mediator ceramide plays a specific role in this scenario with respect to cell death in vascular (and cancer) cells. Acid sphingomyelinase (aSMase) seems to be a key enzyme since its inhibition attenuates the apoptotic response to oxPL. From several reports in the literature, evidence is available that aSMase may be activated by upstream enzymes, e.g. PKCδ (Zeidan and Hannun, 2007). Chapter 2 is devoted to the role of this enzyme in oxPL-induced cell death.

1.3 Effects of oxidized phospholipids on skin cancer cells

1.3.1 Classification of skin cancer

Skin cancer may be divided into two broad categories: melanoma and non-melanoma skin cancer. The latter group includes basal cell carcinoma, squamous cell carcinoma and premalignant lesions, such as actinic keratosis and Bowen's disease. The most common types of skin cancers are basal cell skin cancer, squamous cell skin cancer and melanoma. Compared to non-melanoma skin cancer, melanomas occur less frequently, but they are generally associated with poor prognosis. (National Cancer Institute (NCI) booklet, 2010) The two major risk factors for development of skin cancer are exposure to environmental factors (mainly UV radiation) and genetic predisposition (Saladi and Persaud, 2005).

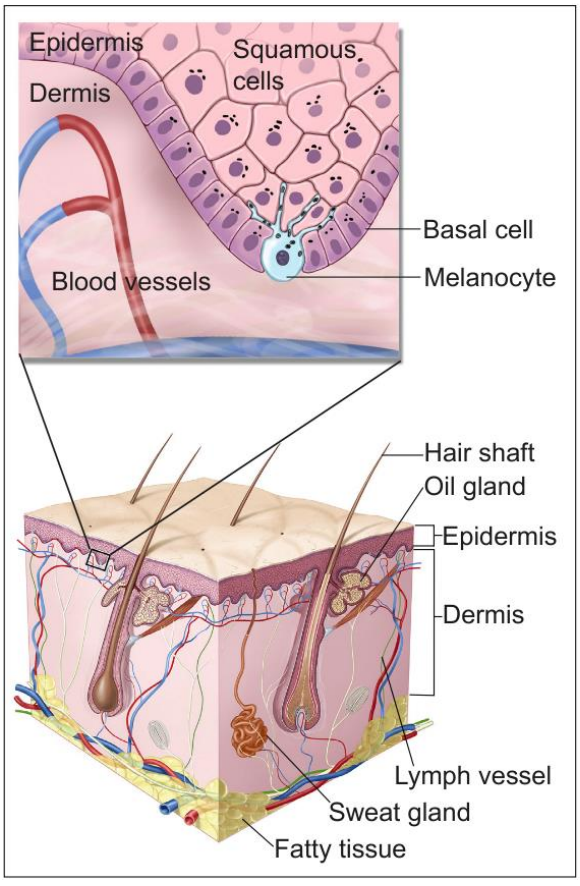

Figure 1.5 Anatomy of the skin.

The skin is composed of two primary layers: the epidermis and the dermis. Keratinocytes are the major cells of the epidermis. Basal cells (undifferentiated basal keratinocytes) and melanocytes are also present in the epidermis. A thin basement membrane separates the epidermis and dermis. The dermis contains many types of cells and structures, such as blood vessels, lymph vessels, and sweat glands. Figure was taken from National Cancer Institute (NCI) booklet (NIH Pubblication No. 10-7625, 2010).

The human skin consists of two main layers, the epidermis and the dermis (Figure 1.5). Skin cancer develops from the outermost layer of the skin, the epidermis. The different classes of skin cancers are named after the type of cells that become malignant: Melanoma begins in melanocytes, basal cell skin cancer in the basal layer of the skin and squamous cell carcinoma in squamous cells.

Malignant cancer growth was recently defined by Hanahan and Weinberg. They postulated six hallmarks of tumorigenicity that are shared by most types of human tumors. These six capabilities are self-sufficiency from external growth signals, insensitivity to negative growth signals, resistance to apoptosis, limitless replicative potential, sustained angiogenesis, and acquisition of tissue invasiveness (Hanahan and Weinberg, 2010).

The studies in this work have been performed on SCC-13 squamous carcinoma cells (see Chapter 3). The cultured SCC-13 cell line is a tumorigenic keratinocyte line derived from a human squamous cell carcinoma (Rheinwald and Beckett, 1981). The biopsy was taken from a primary tumor in the face of a 56 year old female. Cultured SCC-13 cells show high tumor differentiation, an aneuploid chromosome set (hyperdiploid), p53 mutation and 100 % tumorigenicity (Masters and Palsson, 1998).

1.3.2 Cytotoxic effects of oxPL and alkylphospholipids on skin cancer cells

Treatment of skin cancer depends on the stage of disease, the type of skin cancer, the size and place of the tumor and medical history of the patient. The following interventions are possible therapies for skin cancer treatment: Surgery to remove the cancerous growth, chemotherapy to induce cancer cell death and to inhibit cancer cell growth, or photodynamic therapy (PDT) and radiation therapy to kill cancer cells using high-energy rays (National Cancer Institute (NCI) booklet, 2010).

In addition to the above mentioned therapies for the treatment of (skin) cancer, several experimental cancer drugs were tested over the years. These substances include the large group of alkyl-lysophospholipids (ALPs). ALPs are synthetic analogs of lysophosphatidylcholines. In ALPs the acyl-group of lysophosphatidylcholine is replaced with an alkyl-group. Typical analogs of such compounds are edelfosine,

miltefosine and perifosine (van Blitterswijk and Verheij, 2008). Already in the 1970s, the antitumor activities of ALPs on leukemic cells were discovered (Andreesen *et al.*, 1978). In the 1980s, ALPs were tested on human leukemia cells in the serum of a tumor patient (Berdel *et al.*, 1981) and the cytotoxic effects of ALPs on solid human malignant tumors were determined *in vitro* (Runge *et al.*, 1980). In head and neck squamous carcinoma cells, perifosine achieves antiproliferative properties by inducing cell cycle arrest (Patel *et al.*, 2002). Recently, a phase II trial of perifosine in patients with incurable or metastatic squamous cell carcinoma of the head and neck was conducted. However, the study did not obtain positive results for perifosine under the chosen experimental settings. (Argiris *et al.*, 2011) It seems that ALPs are most promising in combination with conventional cancer therapies. For example, ALPs increase the cancer cell sensitivity to radiotherapy *in vitro* and *in vivo* and are therefore used as radiosensitizers (van Blitterswijk and Verheij, 2008). Specifically, perifosine has been identified as radiosensitizer in squamous cell carcinoma (Vink et al., 2006).

OxPL share similar structural features with alkyl-lysophospholipids including a long hydrophobic hydrocarbon chain in position *sn*-1 and a large polar head group. Ramprecht *et al*., have extensively investigated the cytotoxic effects of the oxPL PGPC and POVPC as well as of their ether analogs E-PGPC and E-POVPC on various cultured skin cancer cell lines. These lipids have toxic effects on several human melanoma cell lines of different malignancies (SBcl2, WM35, WM9, WM164), on the murine melanoma cell line B16-BL6, and on squamous carcinoma cell lines (SCC-12, SCC-13). Oxidized phospholipids preferentially induce apoptosis in skin cancer cells, but not in healthy cells of the skin (Fom melanocytes and HaCaT keratinocytes). The toxicity of PGPC and POVPC was associated with efficient uptake of these lipids into cancer cells, activation of acid sphingomyelinase and the formation of the pro-apoptotic second messenger ceramide in most of the cell lines. (Ramprecht *et al.*, PhD thesis, TU Graz, 2013)

Chapter 3 of this work is devoted to the elucidation of the molecular mechanisms behind the cytotoxic effects of oxPL in cultured SCC-13 squamous carcinoma cells.

We found that the oxPL-induced apoptotic cell death in these cells is associated with upregulation of ER-stress markers. Furthermore the fluorescent oxPL BY-POVPE has been shown to target Hsps (heat shock proteins) and PDIs (protein disulfide isomerases) in SCC-13 cells. As a consequence, the oxPL modify (enzymatic functions of) Hsps and PDIs *in vitro* and *in vivo* (see Chapter 3).

OxPL and alkylphospholipids show similar biophysical interactions with the cellular plasma membrane due to their similarity in structure and polarity. The anti-tumorigenic potential of alkyl-(lyso)phospholipids is based on their interaction with membranes. Since they are amphiphiles and contain only one long *sn*-1 hydrocarbon chain, they easily insert into lipid bilayers. They accumulate in cellular membranes and thereby interfere with lipid metabolism (inhibition of phosphatidylcholine synthesis) and activate various signaling pathways. On the one hand, synthetic alkylphospholipids activate stress pathways, on the other hand, they downregulate proliferation pathways. Specifically, they inhibit MAP kinase/ ERK proliferative and phosphatidylinositol 3-kinase/ Akt survival pathways and they activate the JNK pathway, which leads to apoptosis in cancer cells. (van Blitterswijk and Verheij, 2008; van Blitterswijk and Verheij, 2013)

Interestingly, the toxicities of alkylphospholipids (van Blitterswijk and Verheij, 2008) as well as of oxPL (Ramprecht *et al.*, PhD thesis, TU Graz, 2013) are highly selective, sparing healthy cells. Their toxicities towards cancer cells may be due to the fact that tumor cells are metabolically very active and show high proliferation rates compared to normal cells. For this reason, normal cells also become sensitive to ALPs, as long as they are in a proliferative state. (van Blitterswijk and Verheij, 2008) Zerp *et al.* showed that ALP-induced apoptosis in vascular endothelial cells was dependent on the proliferative status of the cells and positively correlated with cellular lipid uptake. Nondividing cells failed to undergo apoptosis, whereas proliferating cells showed a 3-4-fold higher uptake and higher levels of apoptosis. (Zerp et al., 2008)

1.4 Role of macrophages in cancer

1.4.1 Physiological functions of macrophages

Macrophages are important cells of the immune response and are present in all tissues (e.g. Langerhans cells in the skin). The different subtypes of tissue macrophages differ by their cell morphology, their transcriptional profiles and their functions (Wynn *et al.*, 2013).

Macrophages are main components of the innate and adaptive immune response: They are capable of selectively recognizing pathogens and apoptotic cells via specific receptors to eliminate them by phagocytosis followed by intracellular degradation. As components of the adaptive immune response, macrophages present the degraded antigen fragments by MHC II molecules. T-cells may recognize these complexes via their T-cell receptors (TCRs). In addition to their key role in innate and adaptive immune response, macrophages are involved in tissue development and maintenance of tissue integrity and homeostasis. These functions are based on capacities of matrix remodeling and synthesizing growth and angiogenesis factors. In this context, macrophages are involved in bone morphogenesis, neural networking, angiogenesis, and the generation of adipose tissue (Pollard, 2009; Wynn *et al.*, 2013).

The diversity of macrophage localization and function makes them indispensable for normal body function. Therefore, defects in macrophage function are causally related to numerous pathophysiological conditions including tuberculosis, leishmaniasis, arteriosclerosis, rheumatoid arthritis, HIV infection and cancer (Pollard, 2009; Cassetta *et al.*, 2011; Wynn *et al.*, 2013).

1.4.2 Tumor-associated macrophages

Inflammation and cancer are closely linked: On the one hand, chronic inflammation can give rise to cancer development; on the other hand are tumors sites of inflammation since they are invaded by several classes of immune cells.

An inflammatory environment rich in immune cells, growth factors, and activated stroma promotes neoplastic risk due to sustained cell proliferation. By the secretion of chemokines, tumors attract a large variety of immune cells including neutrophils, dendritic cells, macrophages, eosinophils and mast cells, as well as lymphocytes. (Coussens and Werb, 2002; Condeelis and Pollard, 2006; Mantovani and Sica, 2010; Borrello *et al*., 2008)

Some of these cells have been shown to exert anti-tumor effects, others are correlated with poor prognosis of malignant disease. T lymphocytes belong to the first category. The density of these cells has been associated with a more favorable prognosis in some cancer types including e.g. colorectal cancer, ovarian cancer and melanoma (Sica *et al.*, 2008). In contrast, macrophages belong to the second, tumor-promoting category. Extensive macrophage infiltration in tumors has been shown to correlate with poor prognosis in most cancer types including carcinomas of the breast, cervix, and bladder (Bingle *et al.*, 2002). These macrophages which are found in close proximity of tumors or within a tumor are called tumor-associated macrophages (TAMs). In melanoma, macrophage infiltration is closely associated with the depth of invasion of primary melanoma. This correlation is partly due to macrophage-regulated tumor-associated angiogenesis. (Torisu *et al.*, 2000)

Tumor cells exploit mechanisms by which immune cells interfere with cancers, to further their colonization of the host (Coussens and Werb, 2002). In this context, macrophages have a pivotal role in tumor growth and invasion due to their direct communication and interaction with cancer cells (Sica *et al.*, 2008; Coussens and Werb, 2002; Mantovani and Sica, 2010). Condeelis and Pollard postulated six extrinsic traits conferred by macrophages that enhance tumor incidence, progression, and metastasis (Figure 1.6). These are 1.) chronic inflammation, 2.) matrix remodeling, 3.) tumor cell invasion, 4.) intravasation, 5.) angiogenesis, and 6.) seeding at distant sites (Condeelis and Pollard, 2006).

1.) Chronic inflammation caused by infections or by cigarette smoking promotes tumorigenesis since the recruitment of immune cells establishes a microenvironment that is mutagenic through the production of ROS. 2.) Tumors take advantage of the

matrix remodeling capacities of TAMs which facilitates their migration through the stroma. 3.) Invasive tumor cells and TAMs within primary mammary tumors of rats have been found to migrate together. 4.) In addition, macrophages enhance the capacity of tumor cells to enter blood vessels (intravasation). 5.) The correlation between local macrophage density and angiogenesis provides a hint for a role of macrophages in tumor angiogenesis. 6.) Finally, macrophages seem to be involved in metastasis since a high number of macrophages associated with metastases correlates with poor prognosis. (Condeelis and Pollard, 2006)

The role of macrophages in tumorigenesis is complex and still far from clear. Depending on their polarization, tumor-infiltrating macrophages produce different types of cytokines, which induce opposite effects on cancer growth. M2 macrophages promote tumor progression, whereas M1 macrophages show anti-tumor activities (Wang *et al.*, 2010).

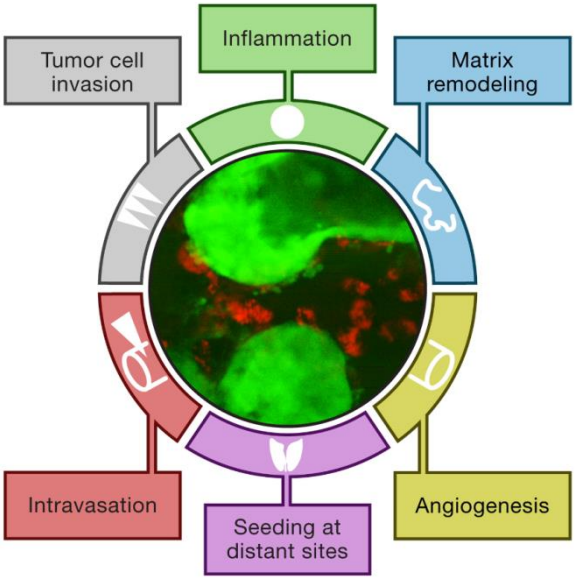

Figure 1.6 Six traits for malignancy promoted by macrophages.

Tumors direct macrophages to adopt a trophic role that facilitates six traits that are extrinsic to the intrinsic genetic changes of tumor cells. The wheel (in deference to Hanahan and Weinberg, 2000) can turn in either direction, allowing macrophages to contribute to invasion, intravasation, angiogenesis, and extravasation equally. The image in the center is a multiphoton micrograph of a mammary tumor (green) and associated macrophages (red) in a living mouse. (Figure and legend from Condeelis and Pollard (Condeelis and Pollard, 2006)).

Figure 2.1 in Chapter 1 shows the apoptotic effect of oxPL on cultured RAW 264.7 macrophages as determined by FACS measurements which correlated with activation of the effector caspases 3 and 7 (Figure 2.3). We found that oxPL exert their apoptotic

effects on several human skin cancer cell lines (melanoma cells and squamous skin cancer cells) as well (Ramprecht *et al.*, PhD thesis, TU Graz, 2013). In the context of arteriosclerosis, oxPL are pathogenic since they contribute to inflammation and apoptosis/ necrosis of vascular cells. In contrast, oxPL-toxicity in skin cancer cells may be beneficial. It opens new doors to develop strategies for selective inhibition of cancer growth and cancer treatment. In this particular case, oxPL based therapy could provoke a direct and an indirect antitumor effect. On the one hand, oxPL could exert a direct cytotoxic effect on skin cancer cells. On the other hand, these compounds could enhance macrophage cytotoxicity on tumor cells provided the latter cells maintain a tumoricidal phenotype (Wang *et al.*, 2010).

It has long been known that lysophospholipids efficiently activate antitumor activity of macrophages (Berdel et al., 1981; Yamamoto *et al.*, 1987; Ngwenya *et al.*, 1991; Bonjouklian *et al.*, 1986). For orally administered ether analogs of lysophospholipids it was shown that the high levels of macrophage activation correlated with their cytotoxic action on tumor cells (Ngwenya *et al.*, 1991). The macrophages of the skin are the Langerhans cells. If oxPL preparations are used for topical treatment of skin cancer, these cells are likely to be affected, too. Several reports in the literature have already described the effects of oxPL on dendritic cells (Bluml *et al.*, 2005).

1.5 References Chapter 1

Andreesen, R., Modolell, M., Weltzien, H.U., Eibl, H., Common, H.H., Lohr, G.W. & Munder, P.G. 1978, "Selective destruction of human leukemic cells by alkyl-lysophospholipids", *Cancer research,* vol. 38, no. 11 Pt 1, pp. 3894-3899.

Argiris, A., Karamouzis, M.V., Gooding, W.E., Branstetter, B.F., Zhong, S., Raez, L.E., Savvides, P. & Romkes, M. 2011, "Phase II trial of pemetrexed and bevacizumab in patients with recurrent or metastatic head and neck cancer", *Journal of clinical oncology : official journal of the American Society of Clinical Oncology,* vol. 29, no. 9, pp. 1140-1145.

Beranova, L., Cwiklik, L., Jurkiewicz, P., Hof, M. & Jungwirth, P. 2010, "Oxidation changes physical properties of phospholipid bilayers: fluorescence spectroscopy and molecular simulations", *Langmuir : the ACS journal of surfaces and colloids,* vol. 26, no. 9, pp. 6140-6144.

Berdel, W.E., Bausert, W.R., Fink, U., Rastetter, J. & Munder, P.G. 1981, "Anti-tumor action of alkyl-lysophospholipids (Review)", *Anticancer Research,* vol. 1, no. 6, pp. 345-352.

Berliner, J.A., Subbanagounder, G., Leitinger, N., Watson, A.D. & Vora, D. 2001, "Evidence for a role of phospholipid oxidation products in atherogenesis", *Trends in cardiovascular medicine,* vol. 11, no. 3-4, pp. 142-147.

Bingle, L., Brown, N.J. & Lewis, C.E. 2002, "The role of tumour-associated macrophages in tumour progression: implications for new anticancer therapies", *The Journal of pathology,* vol. 196, no. 3, pp. 254-265.

Bluml, S., Kirchberger, S., Bochkov, V.N., Kronke, G., Stuhlmeier, K., Majdic, O., Zlabinger, G.J., Knapp, W., Binder, B.R., Stockl, J. & Leitinger, N. 2005, "Oxidized phospholipids negatively regulate dendritic cell maturation induced by TLRs and CD40", *Journal of immunology (Baltimore, Md.: 1950),* vol. 175, no. 1, pp. 501-508.

Bonjouklian, R., Phillips, M.L., Kuhler, K.M., Grindey, G.B., Poore, G.A., Schultz, R.M. & Altom, M.G. 1986, "Studies of the antitumor activity of (2-alkoxyalkyl)- and (2-alkoxyalkenyl)phosphocholines", *Journal of medicinal chemistry,* vol. 29, no. 12, pp. 2472-2477.

Borrello, M.G., Degl'Innocenti, D. & Pierotti, M.A. 2008, "Inflammation and cancer: the oncogene-driven connection", *Cancer letters,* vol. 267, no. 2, pp. 262-270.

Brown, M.S. & Goldstein, J.L. 1979, "Receptor-mediated endocytosis: insights from the lipoprotein receptor system", *Proceedings of the National Academy of Sciences of the United States of America,* vol. 76, no. 7, pp. 3330-3337.

Carbone, D.L., Doorn, J.A., Kiebler, Z., Ickes, B.R. & Petersen, D.R. 2005, "Modification of heat shock protein 90 by 4-hydroxynonenal in a rat model of chronic alcoholic liver

disease", *The Journal of pharmacology and experimental therapeutics,* vol. 315, no. 1, pp. 8-15.

Carbone, D.L., Doorn, J.A., Kiebler, Z., Sampey, B.P. & Petersen, D.R. 2004, "Inhibition of Hsp72-mediated protein refolding by 4-hydroxy-2-nonenal", *Chemical research in toxicology,* vol. 17, no. 11, pp. 1459-1467.

Cassetta, L., Cassol, E. & Poli, G. 2011, "Macrophage polarization in health and disease", *TheScientificWorldJournal,* vol. 11, pp. 2391-2402.

Christie, W.W. 1985, "Rapid separation and quantification of lipid classes by high performance liquid chromatography and mass (light-scattering) detection", *Journal of lipid research,* vol. 26, no. 4, pp. 507-512.

Code, C., Mahalka, A.K., Bry, K. & Kinnunen, P.K. 2010, "Activation of phospholipase A2 by 1-palmitoyl-2-(9'-oxo-nonanoyl)-sn-glycero-3-phosphocholine in vitro", *Biochimica et biophysica acta,* vol. 1798, no. 8, pp. 1593-1600.

Condeelis, J. & Pollard, J.W. 2006, "Macrophages: obligate partners for tumor cell migration, invasion, and metastasis", *Cell,* vol. 124, no. 2, pp. 263-266.

Coussens, L.M. & Werb, Z. 2002, "Inflammation and cancer", *Nature,* vol. 420, no. 6917, pp. 860-867.

Crabb, J.W., O'Neil, J., Miyagi, M., West, K. & Hoff, H.F. 2002, "Hydroxynonenal inactivates cathepsin B by forming Michael adducts with active site residues", *Protein science : a publication of the Protein Society,* vol. 11, no. 4, pp. 831-840.

Fruhwirth, G.O., Loidl, A. & Hermetter, A. 2007, "Oxidized phospholipids: from molecular properties to disease", *Biochimica et biophysica acta,* vol. 1772, no. 7, pp. 718-736.

Fruhwirth, G.O., Moumtzi, A., Loidl, A., Ingolic, E. & Hermetter, A. 2006, "The oxidized phospholipids POVPC and PGPC inhibit growth and induce apoptosis in vascular smooth muscle cells", *Biochimica et biophysica acta,* vol. 1761, no. 9, pp. 1060-1069.

Gillotte, K.L., Horkko, S., Witztum, J.L. & Steinberg, D. 2000, "Oxidized phospholipids, linked to apolipoprotein B of oxidized LDL, are ligands for macrophage scavenger receptors", *Journal of lipid research,* vol. 41, no. 5, pp. 824-833.

Glass, C.K. & Witztum, J.L. 2001, "Atherosclerosis. the road ahead", *Cell,* vol. 104, no. 4, pp. 503-516.

Goldstein, J.L. & Brown, M.S. 2009, "The LDL receptor", *Arteriosclerosis, Thrombosis, and Vascular Biology,* vol. 29, no. 4, pp. 431-438.

Greenberg, M.E., Li, X.M., Gugiu, B.G., Gu, X., Qin, J., Salomon, R.G. & Hazen, S.L. 2008, "The lipid whisker model of the structure of oxidized cell membranes", *The Journal of biological chemistry,* vol. 283, no. 4, pp. 2385-2396.

Grimsrud, P.A., Xie, H., Griffin, T.J. & Bernlohr, D.A. 2008, "Oxidative stress and covalent modification of protein with bioactive aldehydes", *The Journal of biological chemistry,* vol. 283, no. 32, pp. 21837-21841.

Gugiu, B.G., Mouillesseaux, K., Duong, V., Herzog, T., Hekimian, A., Koroniak, L., Vondriska, T.M. & Watson, A.D. 2008, "Protein targets of oxidized phospholipids in endothelial cells", *Journal of lipid research,* vol. 49, no. 3, pp. 510-520.

Halasiddappa, L.M., Koefeler, H., Futerman, A.H. & Hermetter, A. 2013, "Oxidized phospholipids induce ceramide accumulation in RAW 264.7 macrophages: role of ceramide synthases", *PloS one,* vol. 8, no. 7, pp. e70002.

Hanahan, D. & Weinberg, R.A. 2000, "The hallmarks of cancer", *Cell,* vol. 100, no. 1, pp. 57-70.

Hermetter, A., Kopec, W. & Khandelia, H. 2013, "Conformations of double-headed, triple-tailed phospholipid oxidation lipid products in model membranes", *Biochimica et biophysica acta,* vol. 1828, no. 8, pp. 1700-1706.

Khandelia, H. & Mouritsen, O.G. 2009, "Lipid gymnastics: evidence of complete acyl chain reversal in oxidized phospholipids from molecular simulations", *Biophysical journal,* vol. 96, no. 7, pp. 2734-2743.

Koller, D. 2013, *Effects of Oxidized Phospholipids on Gene Expression and Sphingolipid Metabolism in RAW 264.7 macrophages*, Technical University of Graz.

Kunjathoor, V.V., Febbraio, M., Podrez, E.A., Moore, K.J., Andersson, L., Koehn, S., Rhee, J.S., Silverstein, R., Hoff, H.F. & Freeman, M.W. 2002, "Scavenger receptors class A-I/II and CD36 are the principal receptors responsible for the uptake of modified low density lipoprotein leading to lipid loading in macrophages", *The Journal of biological chemistry,* vol. 277, no. 51, pp. 49982-49988.

Levitan, I., Volkov, S. & Subbaiah, P.V. 2010, "Oxidized LDL: diversity, patterns of recognition, and pathophysiology", *Antioxidants & redox signaling,* vol. 13, no. 1, pp. 39-75.

Levy, M. & Futerman, A.H. 2010, "Mammalian ceramide synthases", *IUBMB life,* vol. 62, no. 5, pp. 347-356.

Loidl, A., Claus, R., Ingolic, E., Deigner, H.P. & Hermetter, A. 2004, "Role of ceramide in activation of stress-associated MAP kinases by minimally modified LDL in vascular smooth muscle cells", *Biochimica et biophysica acta,* vol. 1690, no. 2, pp. 150-158.

Loidl, A., Sevcsik, E., Riesenhuber, G., Deigner, H.P. & Hermetter, A. 2003, "Oxidized phospholipids in minimally modified low density lipoprotein induce apoptotic signaling via activation of acid sphingomyelinase in arterial smooth muscle cells", *The Journal of biological chemistry,* vol. 278, no. 35, pp. 32921-32928.

Mantovani, A. & Sica, A. 2010, "Macrophages, innate immunity and cancer: balance, tolerance, and diversity", *Current opinion in immunology,* vol. 22, no. 2, pp. 231-237.

Masters, J.R. & Palsson, B. 1998, *Human Cell Culture: Volume I: Cancer Cell Lines*, Edition I edn, Springer.

Moumtzi, A., Trenker, M., Flicker, K., Zenzmaier, E., Saf, R. & Hermetter, A. 2007, "Import and fate of fluorescent analogs of oxidized phospholipids in vascular smooth muscle cells", *Journal of lipid research,* vol. 48, no. 3, pp. 565-582.

Muller, C., Bandemer, J., Vindis, C., Camare, C., Mucher, E., Gueraud, F., Larroque-Cardoso, P., Bernis, C., Auge, N., Salvayre, R. & Negre-Salvayre, A. 2013, "Protein disulfide isomerase modification and inhibition contribute to ER stress and apoptosis induced by oxidized low density lipoproteins", *Antioxidants & redox signaling,* vol. 18, no. 7, pp. 731-742.

National Cancer Institute (NCI) booklet 2010, *What You Need To Know About Melanoma and Other Skin Cancers*, NIH Publication No. 10-7625 edn, U.S. Department of Health and Human Services.

Ngwenya, B.Z., Fiavey, N.P. & Mogashoa, M.M. 1991, "Activation of peritoneal macrophages by orally administered ether analogues of lysophospholipids", *Proceedings of the Society for Experimental Biology and Medicine.Society for Experimental Biology and Medicine (New York, N.Y.),* vol. 197, no. 1, pp. 91-97.

Patel, V., Lahusen, T., Sy, T., Sausville, E.A., Gutkind, J.S. & Senderowicz, A.M. 2002, "Perifosine, a novel alkylphospholipid, induces p21(WAF1) expression in squamous carcinoma cells through a p53-independent pathway, leading to loss in cyclin-dependent kinase activity and cell cycle arrest", *Cancer research,* vol. 62, no. 5, pp. 1401-1409.

Pollard, J.W. 2009, "Trophic macrophages in development and disease", *Nature reviews.Immunology,* vol. 9, no. 4, pp. 259-270.

Ramprecht, C. 2013, *Toxicity of Oxidized Phospholipids in Cultured Skin Cancer Cell Lines*, Technical University of Graz.

Rheinwald, J.G. & Beckett, M.A. 1981, "Tumorigenic keratinocyte lines requiring anchorage and fibroblast support cultured from human squamous cell carcinomas", *Cancer research,* vol. 41, no. 5, pp. 1657-1663.

Rhode, S., Grurl, R., Brameshuber, M., Hermetter, A. & Schutz, G.J. 2009, "Plasma membrane fluidity affects transient immobilization of oxidized phospholipids in endocytotic sites for subsequent uptake", *The Journal of biological chemistry,* vol. 284, no. 4, pp. 2258-2265.

Ross, R. 1999, "Atherosclerosis--an inflammatory disease", *The New England journal of medicine,* vol. 340, no. 2, pp. 115-126.

Runge, M.H., Andreesen, R., Pfleiderer, A. & Munder, P.G. 1980, "Destruction of human solid tumors by alkyl lysophospholipids", *Journal of the National Cancer Institute,* vol. 64, no. 6, pp. 1301-1306.

Saladi, R.N. & Persaud, A.N. 2005, "The causes of skin cancer: a comprehensive review", *Drugs of today (Barcelona, Spain : 1998),* vol. 41, no. 1, pp. 37-53.

Salvayre, R., Auge, N., Benoist, H. & Negre-Salvayre, A. 2002, "Oxidized low-density lipoprotein-induced apoptosis", *Biochimica et biophysica acta,* vol. 1585, no. 2-3, pp. 213-221.

Sanz, J. & Fayad, Z.A. 2008, "Imaging of atherosclerotic cardiovascular disease", *Nature,* vol. 451, no. 7181, pp. 953-957.

Sica, A., Allavena, P. & Mantovani, A. 2008, "Cancer related inflammation: the macrophage connection", *Cancer letters,* vol. 267, no. 2, pp. 204-215.

Steinbrecher, U.P., Gomez-Munoz, A. & Duronio, V. 2004, "Acid sphingomyelinase in macrophage apoptosis", *Current opinion in lipidology,* vol. 15, no. 5, pp. 531-537.

Steinbrecher, U.P., Witztum, J.L., Parthasarathy, S. & Steinberg, D. 1987, "Decrease in reactive amino groups during oxidation or endothelial cell modification of LDL. Correlation with changes in receptor-mediated catabolism", *Arteriosclerosis (Dallas, Tex.),* vol. 7, no. 2, pp. 135-143.

Stemmer, U., Dunai, Z.A., Koller, D., Purstinger, G., Zenzmaier, E., Deigner, H.P., Aflaki, E., Kratky, D. & Hermetter, A. 2012, "Toxicity of oxidized phospholipids in cultured macrophages", *Lipids in health and disease,* vol. 11, pp. 110-511X-11-110.

Stemmer, U. & Hermetter, A. 2012, "Protein modification by aldehydophospholipids and its functional consequences", *Biochimica et biophysica acta,* vol. 1818, no. 10, pp. 2436-2445.

Subbanagounder, G., Watson, A.D. & Berliner, J.A. 2000, "Bioactive products of phospholipid oxidation: isolation, identification, measurement and activities", *Free radical biology & medicine,* vol. 28, no. 12, pp. 1751-1761.

Torisu, H., Ono, M., Kiryu, H., Furue, M., Ohmoto, Y., Nakayama, J., Nishioka, Y., Sone, S. & Kuwano, M. 2000, "Macrophage infiltration correlates with tumor stage and angiogenesis in human malignant melanoma: possible involvement of TNFalpha and IL-1alpha", *International journal of cancer.Journal international du cancer,* vol. 85, no. 2, pp. 182-188.

van Blitterswijk, W.J. & Verheij, M. 2013, "Anticancer mechanisms and clinical application of alkylphospholipids", *Biochimica et biophysica acta,* vol. 1831, no. 3, pp. 663-674.

van Blitterswijk, W.J. & Verheij, M. 2008, "Anticancer alkylphospholipids: mechanisms of action, cellular sensitivity and resistance, and clinical prospects", *Current pharmaceutical design,* vol. 14, no. 21, pp. 2061-2074.

Vink, S.R., Lagerwerf, S., Mesman, E., Schellens, J.H., Begg, A.C., van Blitterswijk, W.J. & Verheij, M. 2006, "Radiosensitization of squamous cell carcinoma by the alkylphospholipid perifosine in cell culture and xenografts", *Clinical cancer research : an official journal of the American Association for Cancer Research,* vol. 12, no. 5, pp. 1615-1622.

Wang, Y.C., He, F., Feng, F., Liu, X.W., Dong, G.Y., Qin, H.Y., Hu, X.B., Zheng, M.H., Liang, L., Feng, L., Liang, Y.M. & Han, H. 2010, "Notch signaling determines the M1 versus M2 polarization of macrophages in antitumor immune responses", *Cancer research,* vol. 70, no. 12, pp. 4840-4849.

Watson, A.D., Leitinger, N., Navab, M., Faull, K.F., Horkko, S., Witztum, J.L., Palinski, W., Schwenke, D., Salomon, R.G., Sha, W., Subbanagounder, G., Fogelman, A.M. & Berliner, J.A. 1997, "Structural identification by mass spectrometry of oxidized phospholipids in minimally oxidized low density lipoprotein that induce monocyte/endothelial interactions and evidence for their presence in vivo", *The Journal of biological chemistry,* vol. 272, no. 21, pp. 13597-13607.

Wong-Ekkabut, J., Xu, Z., Triampo, W., Tang, I.M., Tieleman, D.P. & Monticelli, L. 2007, "Effect of lipid peroxidation on the properties of lipid bilayers: a molecular dynamics study", *Biophysical journal,* vol. 93, no. 12, pp. 4225-4236.

Wynn, T.A., Chawla, A. & Pollard, J.W. 2013, "Macrophage biology in development, homeostasis and disease", *Nature,* vol. 496, no. 7446, pp. 445-455.

Yamamoto, N., Ngwenya, B.Z., Sery, T.W. & Pieringer, R.A. 1987, "Activation of macrophages by ether analogues of lysophospholipids", *Cancer immunology, immunotherapy : CII,* vol. 25, no. 3, pp. 185-192.

Zeidan, Y.H. & Hannun, Y.A. 2007, "Activation of acid sphingomyelinase by protein kinase Cdelta-mediated phosphorylation", *The Journal of biological chemistry,* vol. 282, no. 15, pp. 11549-11561.

Zerp, S.F., Vink, S.R., Ruiter, G.A., Koolwijk, P., Peters, E., van der Luit, A.H., de Jong, D., Budde, M., Bartelink, H., van Blitterswijk, W.J. & Verheij, M. 2008, "Alkylphospholipids inhibit capillary-like endothelial tube formation in vitro: antiangiogenic properties of a new class of antitumor agents", *Anti-Cancer Drugs,* vol. 19, no. 1, pp. 65-75.

Chapter 2

Protein kinase C-delta knockdown decreases oxPL-induced apoptosis in macrophages

Vogl F[a], Humpolícková J[b], Amaro M[b], Koller D[a], Köfeler H[c], Zenzmaier E[a], Hof M[b], Hermetter, A[a].

a Institute of Biochemistry, Graz University of Technology, Graz, Austria

b Heyrovský Institute of Physical Chemistry, Academy of Sciences of the Czech Republic, Prague, Czech Republic

c Center for Medical Research, Core Facility for Mass Spectrometry, Medical University of Graz, Graz, Austria

2.1 Abstract

The short-chain oxidized phospholipids (oxPL) 1-palmitoyl-2-glutaroyl-*sn*-glycero-3-phosphocholine (PGPC) and 1-palmitoyl-2-(5-oxovaleroyl)-*sn*-glycero-3-phosphocholine (POVPC) are bioactive components of oxidized LDL. OxPL are cytotoxic for vascular cells and contribute to atherogenesis.

In macrophages, the network of toxic oxPL-signaling is still largely unknown. To address this problem, we have recently identified the protein targets of a fluorescent POVPC analog in macrophages. In this study, we investigated the contributions of two target proteins, namely caspase-3 and protein kinase C-delta (PKCδ), to oxPL-induced cell death in RAW 264.7 macrophages. We found a time-dependent activation of caspase-3 and -7 that correlates with the formation of apoptotic ceramide. PKCδ also participates in this process. This enzyme is a kinase involved in acid sphingomyelinase (aSMase) regulation. It can act as pro- or anti-apoptotic kinase, depending on cell type and stimulus. PKCδ knockdown by siRNA was associated with decreased caspase activation compared to control cells.

Single molecule fluorescence microscopy provided direct evidence for oxPL-PKCδ interaction. Codiffusion of fluorescently labeled oxPL and RFP-tagged PKCδ in live cells could be determined from two-color cross-correlation number and brightness (ccN&B) analysis of molecular motions. Finally, we detected colocalization of PKCδ-RFP and aSMase-GFP in macrophages. This observation supports the assumption of a functional relationship between PKCδ and aSMase.

In summary, we identified PKCδ as a proapoptotic kinase in oxPL-induced apoptosis in RAW 264.7 macrophages. Notably, the direct association of bioactive lipids with their protein targets seems to play a role in PKCδ signaling function.

2.2 Introduction

The oxidized phospholipids (oxPL) 1-palmitoyl-2-(5-oxovaleroyl)-*sn*-glycero-3-phosphocholine (POVPC) und 1-palmitoyl-2-glutaroyl-*sn*-glycero-3-phosphocholine (PGPC) are generated from 1-palmitoyl-2-arachidonoyl-*sn*-glycero-3-phosphocholine (PAPC) under conditions of oxidative stress. They are biologically active components of oxidized low-density lipoprotein (oxLDL) and significantly contribute to the toxicity of this particle in vascular cells (Berliner *et al*., 2001, Watson *et al.*, 1997; Subbanagounder *et al.*, 2000; Loidl *et al*., 2003). We have previously shown that PGPC and POVPC induce apoptotic cell death in cultured vascular smooth muscle cells (Loidl *et al.*, 2003; Fruhwirth *et al.*, 2006), in RAW 264.7 macrophages and in murine bone marrow-derived macrophages (Stemmer *et al.*, 2012). In vascular smooth muscle cells, apoptotic signaling was associated with activation of acid sphingomyelinase (aSMase), phosphorylation of p38 MAPK and JNK and activation of caspase-3. In macrophages, activation of ceramide synthases (CerS), mainly CerS 2, catalyzing a specific subset of ceramides, was identified as a late response to the oxPL (Halasiddappa *et al.*, 2013). All these features of oxPL-induced cell death can also be observed when vascular cells are exposed to oxLDL (Halasiddappa *et al.*, 2013; Salvayre *et al.*, 2002) and therefore is was concluded that POVPC and PGPC are main toxic components of this particle in the vascular wall.

Acid sphingomyelinase (aSMase) is a key upstream signaling component of oxPL and causally related to apoptotic cell death induced by PGPC or POVPC. Inhibition of this enzyme abolishes activation of downstream signaling enzymes such as p38, JNK and caspase-3. As a consequence apoptotic cell death is decreased. (Loidl *et al*., 2003; Stemmer *et al.*, 2012) The activation of aSMase by different stimuli in general, and by PKCδ in particular, is still subject to proof. However, here several models are being discussed that could contribute to this phenomenon. First of all, PGPC and POVPC are single-chain amphiphiles and as such easily incorporate into the surface monolayer of the cell plasma membrane (Moumtzi *et al.*, 2007; Rhode *et al.*, 2009). In the membrane they can unspecifically alter lateral membrane lipid organization and

dynamics and, in the end, membrane protein function. Unlike PGPC, POVPC contains a chemically reactive aldehyde function at the ω-position of its *sn*-2 acyl chain. Therefore it can form covalent Schiff bases with amino groups of aminophospholipids (Hermetter *et al*., 2013) or proteins (Stemmer *et al*., 2012; Stemmer and Hermetter, 2012). The resultant lipid-lipid adducts contain three hydrophobic chains with only a relatively small head group (Hermetter *et al*., 2013). They are very likely to modify or even destabilize the lipid phase and as a consequence modulate enzyme structures in biomembranes. Alkylation by POVPC would increase the hydrophobic contacts of a surface-bound membrane protein with the lipid phase of a membrane. Kinnunen and coworkers have shown that the presence of Poxno-PC, a longer chain homolog of POVPC, stimulated the activity of a snake venom phospholipase A2 on the components of artificial bilayers (Code *et al.*, 2010).

Finally, the group of Hannun has identified a very specific mechanism for the activation of an aSMase in cancer cells if stimulated with phorbol ester (Zeidan and Hannun, 2007). It is based on the primary activation of PKCδ, which is recruited by the stimulus to the cytoplasmic side of the plasma membrane. After autophosphorylation, it intracellularly moves to the lysosomes where it phosphorylates aSMase, which - in phosphorylated form - moves to the plasma membrane where it generates the intracellular mediator ceramide.

Larroque-Cardoso *et al.* (2013) have already published information that supports the assumption of a key signaling role of PKCδ in vascular smooth muscle cells. They found that PKCδ was activated under the influence of oxLDL and represents an apoptotic enzyme in these cells, which is causally related to activation of stress-induced kinases and ER stress. In J774A.1 macrophage cells, it was shown that oxLDL induced p53-dependent apoptosis by activating p38 MAPK and PKCδ signaling pathways (Giovannini *et al.*, 2011).

We addressed ourselves to the question whether PKCδ could also become involved in apoptosis induced by oxPL which are components of ox LDL. PKCδ can participate in apoptotic cell signaling in different ways (Figure 2.10). It can phosphorylate aSMase (Zeidan and Hannun, 2007), thereby promoting ceramide formation. Activation of

caspase-3 by phosphorylation may also be catalyzed by this kinase (Voss *et al.*, 2005). In turn, caspase-3 can give rise to cleavage of PKCδ (Kato *et al*., 2009) leading to the formation of an enzyme fragment (SDK1) that promotes apoptosis via 14-3-3ζ monomerization (Hamaguchi *et al.*, 2003).

In this study, we made an attempt to search for a role of PKCδ in oxPL-induced apoptosis of cultured RAW 264.7 macrophages. We found that silencing of this enzyme greatly reduced the capacity of the cells to undergo caspase-3-associated apoptosis. In oxPL-treated cells, PGPC and POVPC gave rise to phosphorylation of PKCδ. Fluorescence microscopy experiments using RFP-tagged PKCδ and fluorescently labeled oxPL provided evidence that the lipids recruited the enzyme from the cytosol to the plasma membrane. In addition, microscopic studies on the single molecule level revealed that lipid and protein motions in live cells are correlated. From all these observations, it was concluded that PKCδ not only mediates apoptotic signals of oxLDL (Larroque-Cardoso *et al.*, 2013), but also of its constituent oxPL PGPC and POVPC. Direct association of the enzyme with the toxic phospholipids is likely to be an important step in the early phase of apoptotic signaling.

2.3 Materials and Methods

Materials

Oxidized phospholipids (PGPC and POVPC) and their fluorescent analogs (BY-PGPE and BY-POVPE) were synthesized in our laboratory as previously described (Moumtzi *et al.*, 2007). Organic solvents and all other chemicals were purchased from Carl Roth (Karlsruhe, Germany), Sigma-Aldrich (Steinheim, Germany) or Merck (Darmstadt, Germany). Tissue culture materials were obtained from Sarstedt (Nürnbrecht, Germany) or Greiner (Kremsmünster, Austria). Dulbecco's modified Eagle medium (DMEM, 4,5 g/l glucose) with and without phenol red, heat-inactivated fetal bovine serum, PBS and cell culture supplements were obtained from PAA (Linz, Austria). Fluids for flow cytometry, FACS tubes and solutions were from BD Biosciences (Heidelberg, Germany). The Alexa Fluor® 488 Annexin V/Dead Cell Apoptosis Kit was purchased from Invitrogen (Eggenstein, Germany).

Cell culture

The macrophage cell line RAW 264.7 (ATCC No. TIB-71, American Type Culture Collection, Rockville, MD, USA) was a kind gift from Dagmar Kratky, Medical University of Graz, Austria. Cells were routinely grown in DMEM (4,5 g/l glucose, 25 mM HEPES, 4 mM L-glutamine, without sodium pyruvate) supplemented with 10 % (v/v) heat-inactivated FBS and 100 U/ml penicillin/streptomycin in humidified CO_2 (5 %) atmosphere at 37 °C. Cells were routinely spitted at 80 % confluency in DMEM supplemented with 10 % (v/v) heat-inactivated FBS.

Incubation of cells with lipids

Aqueous lipid dispersions containing the indicated concentrations of oxPL were prepared using the ethanol injection method (Batzri and Korn, 1973). Cells were incubated with lipid dispersions in culture media without phenol red containing 0,1 % (v/v) serum. The final ethanol concentration in the incubation mixtures did not exceed

1 % (v/v) of total volume. Culture media containing the same ethanol concentration were routinely used as controls.

Fluorescence microscopy of PKCδ-RFP and aSMase-GFP

Cells expressing the fusion proteins PKCδ-RFP and aSMase-GFP were observed with an Axiovert 35 inverted microscope (magnification: 320 x) equipped with a mercury-arc lamp and a CCD camera, driven by AxioVision software package (Carl Zeiss, Germany). GFP-fluorescence (Ex 395 nm, Em 478 nm) was detected using the following filter set: excitation filter BP 450–490 nm, beam splitter 510 nm and barrier filter LP 520 nm. RFP-fluorescence (Ex 555 nm, Em 584 nm) was observed using the following filter set: excitation filter LP 510 + KP 560, beam splitter 580 nm and emission filter LP 590.

Cloning of plasmid constructs

Template cDNA was synthesized from total RNA isolated from RAW 264.7 macrophages. The resultant cDNA was used to amplify the genes encoding for PKCδ (gi|118130235:14-2038) and for aSMase (gi|254750745:173-2056). The following primers were used: FW/PKCδ/SmaI 5′-tgc CCC GGG CCA CCA TGG CAC CCT TCC TGC GC-3′, REV/PKCδ/SmaI 5′-tgc CCC GGG CAA TGT CCA GGA ATT GCT CAA ACT TGG-3′, FW/aSMase/XBaI 5′-CTA GTC TAG ACT AGA TGC CCC ACC ACA GAG CAT C-3′ and REV/aSMase/NheI 5′- CAT CGC TAG CGC ACA ACA GGG GGC GTG AC -3′. The PCR products were purified using a GFX gel purification kit (GE Healthcare, Vienna, Austria) and ligated into the following vectors: pTagRFP-N1 (Evrogen, Moscow, Russia) and pcDNA3.1 (Invitrogen, Eggenstein, Germany). The ligated vectors were transformed into competent *E. coli* cells. Positive clones were identified using colony-PCR to check size and orientation of the insert. Finally, the integrity of the new plasmids was verified by DNA sequencing.

Transfection

For the transient overexpression of fusion proteins (PKCδ-RFP and aSMase-GFP) and for gene silencing experiments the Neon® Transfection system from Invitrogen (Eggenstein, Germany) was used. The voltage and pulse settings were fixed according to the manufacturer's recommendations for RAW 264.7 macrophages. FlexiTube siRNA for Prkcd (Gene ID 18753, Tube ID 2053907 and 2053906) and AllStars Negative Control siRNA were purchased from QIAGEN (Hilden, Germany). In a 10 µl Neon tip, 500000 cells were mixed with 0,5-2 µg plasmid DNA or with 20 pmol siRNA. Fluorescence micrographs of PKCδ-RFP and aSMase-GFP were taken 24 h after transfection.

Flow cytometry apoptosis assay

$6{,}5*10^5$ RAW 264.7 macrophages were initially seeded in a 24-well plate in culture media without phenol red. After incubation, cells were harvested by scraping and washed with cold PBS containing 2 mg/ml glucose. The harvested cells were resuspended in 100 µl Annexin V binding buffer and transferred into a FACS tube. 5 µl Alexa Fluor® 488 Annexin V and 5,5 µl propidium iodide (PI; 1 mg/ml stock solution) were added and samples were allowed to incubate at room temperature in the dark for 15 minutes. Prior to FACS measurement, samples were diluted in PBS containing 2 mg/ml glucose, gently mixed and kept on ice until analysis. Stained samples were then analyzed using a FACSCalibur flow cytometer (BD Biosciences, Heidelberg, Germany). The green and red emissions were measured at 530 nm and 575 nm, respectively (excitation: 488 nm laser). The [FSC, FL3H] diagram was performed to gate out the debris. The gated cells were analyzed in [FL1H, FL2H] log scale dot plots. Auto-fluorescence of the cells positioned in first decade, and compensation for Alexa Fluor® 488 fluorescence in FL2 channel was applied. The percentage of apoptotic cells (AnnexinV-positive), necrotic cells (PI-positive) and late apoptotic/early necrotic cell (double stained) were calculated using WinMDI 2.8 software package. The final ethanol concentrations in the incubation mixtures did not exceed 1 % (v/v) of the total volume.

Western blotting

RAW 264.7 macrophages were harvested for protein analysis by scraping. Subsequently the cell pellet was lysed using the mammalian cell lysis reagent CelLytic M containing protease and phosphatase inhibitor cocktails (Sigma-Aldrich, Steinheim, Germany) according to the manufacturer's instructions. Protein concentration of the cell lysates was determined using the method of Bradford (Bradford, 1976). Protein lysates were precipitated by addition of five volumes acetone overnight. On the next day, proteins were pelleted by centrifugation at 13000 rmp for 15 min at 4 °C. The pellets were dried and solubilized in sample buffer for gel electrophoresis. Aliquots containing 20 µg protein were subjected to SDS-PAGE on 10 % acrylamide gels. After electrophoresis, gels were blotted onto Immobilon-FL PVDF membranes (Merck Millipore, Darmstadt, Germany). Blots were routinely blocked with TBS buffer supplemented with 5 % (w/v) milk powder. Before the incubation with anti-phospho-antibodies started, blots were blocked with TBS buffer containing 1 % (w/v) BSA. After blocking, blots were washed and incubated with the respective antibodies overnight at 4 °C.

To quantify PKCδ silencing, "PKCdelta Mouse IgG2b Antibody" from BD BIOSciences (Heidelberg, Germany) was diluted 1:150 in TBST buffer containing 1 % (w/v) milk powder and 0,2 % (v/v) Tween. "Anti-Mouse IgG (H+L), F(ab')2 Fragment (Alexa®555)" from NEB Cell Signaling Technology (Frankfurt am Main, Germany) was used as secondary antibody, diluted 1:4000 in TBST buffer containing 5 % (w/v) milk powder and 0,1 % (v/v) Tween. Primary antibodies against GAPDH served as loading controls.

To detect PKCδ phosphorylation at Tyr-311, "Phospho-PKC-delta (Tyr311) Antibody" from NEB Cell Signaling Technology (Frankfurt am Main, Germany) was diluted 1:500 in TBST buffer containing 0,1 % (v/v) Tween and 5 % (w/v) BSA. Bands were detected with an anti-HRP antibody diluted 1:1000 in TBST buffer containing 5 % (w/v) milk powder and 0,1 % (v/v) TBST.

Caspase-3/7 assay

RAW 264.7 macrophages were seeded into flat clear bottom black TC treated 96-well microplates employing a cell number of 15000 cells per well. Cells were grown in 200 µl DMEM high glucose media supplemented with 10 % FBS overnight. Subsequently, the medium was removed and cells were gently rinsed with prewarmed PBS and incubated with 100 µl suspensions of either 50 µM POVPC or PGPC for different times. Caspase-3/7 activity was quantified using the Apo-ONE® Homogeneous Caspase-3/7 Assay (Promega, Mannheim, Germany) according to the manufactures protocol. Fluorescence in the wells was measured (excitation wavelength 499 nm, emission wavelength 521 nm) using a fluorescence plate reader (POLARstar Galaxy from MTX Lab Systems, Virginia, USA). The following filter sets were selected: 485P as excitation filter and 520P as emission filter.

Caspase activities were determined from the time-dependent increase in fluorescence intensity. For cells transfected with PKCδ-specific siRNA or with negative control siRNA, data obtained for cells preincubated with oxPL were normalized relative to data obtained for cells preincubated with 1 % ethanol. Next, caspase activities measured for cells treated with random sequence control siRNA (neg. siRNA) were set to 100 % and data from cells exposed to PKCδ-specific siRNA were expressed as % of controls.

RT-qPCR

Total RNA was extracted from RAW 264.7 cells using the RNeasy mini kit (Qiagen, Crawley, UK), 24 and 48 hours post-transfection. One µg total RNA was used for cDNA synthesis using the GoScript™ Reverse Transcription System (Promega, Mannheim, Germany). RT-qPCR assays were performed in 18 µl reaction volume containing 4,5 ng cDNA, primers and SYBR green master mix (Invitrogen, Eggenstein, Germany). Measurements were performed on an ABI Prism 7000 real-time PCR machine. Results were normalized against HPRT expression. Data were analyzed using a real-time PCR management and analysis system [http://genome.tugraz.at/qpcr; (Pabinger *et al.*, 2009)].

Primers were designed using the NCBI Primer-BLAST web tool to span an exon-exon-junction. Primer sequences were screened using a BLAST search to confirm specificity. The PCR products were separated on an agarose gel to confirm that products of the expected size were detected.

Lipid extraction and HPLC-MS

Protocol according to the procedure described by Daniel Koller (Koller *et al.*, PhD thesis, TU Graz, 2013).

$9*10^6$ RAW 264.7 macrophages were seeded in 58 cm^2 cell culture dishes and left with 11 ml of DMEM-media with 10 % heat inactivated FBS (FBShi) for 16 h. Afterwards, media was removed, cultures were washed with DMEM-media without FBShi and incubated with oxPL incubation media as described above. Control samples were incubated with DMEM-media without FBShi and with 1 % (v/v) ethanol under the same conditions. Cells were harvested by scraping after 2 h, 4 h or 8 h incubation time. Cell suspensions were transferred into 15 ml Falcon tubes on ice, followed by centrifugation at 453 g for 7 minutes at 4 °C. After the cell harvest, all working steps were carried out on ice. The supernatant was discarded, cells were washed with 5 ml ice cold PBS. A 0,5 ml aliquot was used to determine protein concentration. Cells were pelletized for protein determination, resuspended in 1 ml lysis buffer (Tris/HCl 50 µM; pH 7,4) and lysed by ultrasonication. Protein concentration was determined using a plate assay according to the method of Bradford (Bradford, 1976). Samples for lipid extraction were transferred in a glass vial, pelletized again at 453 g for 7 minutes. The supernatant was discarded and 3 ml $CHCl_3$/MeOH (2:1, v/v) were added. The sample was shaken at 1500 rpm for 1 h at 4 °C. After addition of 700 µl $MgCl_2$-solution (0,036 %) to improve phase separation, shaking of the sample was continued for additional 10 minutes. For phase separation, the samples were centrifuged at 300 g for 5 minutes. The lower organic phase was transferred with a syringe to a fresh glass vial and the organic solvent was removed under a stream of nitrogen. For mild alkaline hydrolysis, 400 µl of $CHCl_3$/MeOH/H_2O (16/16/5 per vol.) were added to the solvent-free lipid extracts and the solution was shaken vigorously. After addition of 400 µl 0,2

M NaOH in methanol, the samples were incubated at RT for 45 minutes. Following addition of 400 µl 0,5 M EDTA and 150 µl acetic acid and vigorous shaking, 1 ml $CHCl_3$ was added to extract the lipids. Extracts were shaken for 5 minutes and centrifuged at 300 g for 3 minutes to facilitate phase separation. The chloroform phase was transferred to a new vial and the solvent was removed under a nitrogen stream. Solvent-free lipid extracts were dissolved in 100 µl $CHCl_3$/MeOH (1:1 v/v) containing 100 pmol CER 12:0 (N-acyl), CER 25:0 (N-acyl) and SM 12:0 (N-acyl) as internal standards. Sphingolipid species were determined by reversed phase HPLC coupled to a TSQ Quantum Ultra (Thermo Scientific) triple quadrupole mass spectrometer as described by Fauland (Fauland *et al.,* 2011) and Radner (Radner *et al.*, 2010). The individual peak areas were calculated by QuanBrowser for all lipid species and lipids were quantified with reference to internal standards. Data were normalized relative to protein content. Data for test samples were determined relative to controls.

Single molecule microscopy and two-color cross-correlation number and brightness (ccN&B) analysis

Cell culture

The macrophage cell line RAW 264.7 (ATCC No.TIB-71, LGC Standards, Poland) was grown in DMEM (4,5 g/L D-glucose, L-glutamine, 110 mg/L sodium pyruvate) supplemented with 10 % FBS at 37 ºC in humidified CO_2 (5 %) atmosphere.

Cell transfection

Cells were transfected using the Neon® Transfection system from Invitrogen (Eggenstein, Germany) and transferred from the Neon™ Tip into culture plates containing microscopy coverslips and pre-warmed medium without antibiotics. Cells were cultured for approximately 18 h. For macroscopic imaging, the slide covered with the cells was rinsed three times with PBS and mounted onto a Chamlide chamber (Live Cell Instrument, Korea) with HEPES-buffered DMEM imaging medium.

Delivery of fluorescently labeled oxPL

Aqueous dispersions of 1 µM labeled oxPL in PBS buffer (1 mM Ca^{2+} and Mg^{2+}) were prepared using the ethanol injection method (Batzri and Korn, 1973). Final ethanol

concentrations did not exceed 1 % (v/v). For incubation with oxidized phospholipids, the cultured cells on the slides were rinsed three times with PBS. Next, the cells were incubated with an aqueous dispersion of labeled oxPL in humidified CO_2 (5 %) atmosphere for 5 minutes at 37 ºC. After incubation, the slide covered with the cells was rinsed again three times with PBS and mounted onto a Chamlide chamber with HEPES-buffered DMEM imaging medium.

Fluorescence microscopy

Confocal images for the Number and Brightness (N&B) analysis were acquired on an Olympus Fluoview 1000 microscope (Olympus, Tokyo, Japan) equipped with a water immersion objective (1.2 NA, 60 ×). For excitation, a 488 nm laser (Coherent, Santa Clara, CA) and a 543 nm He-Ne laser were used. The laser intensity measured at the back aperture of the objective was ~ 7 μW for both lasers. 490-525 nm band pass filter and 560 nm long pass filter were used in front of the detectors.

For every experiment, 100 frames consisting of 256 × 256 pixels were collected. The scanner speed along the fast and slow scanning axes were 10 μs/pixel and 3,68 ms/line, respectively. The scanner step corresponding to one pixel was 50 nm.

Spatial distributions of Bodipy- and RFP-brightness (B_1 and B_2, respectively) and cross-brightness (B_{cc}) were calculated using a homemade script in Matlab (MathWorks, Natick, MA) as described elsewhere (Digman *et al.*, 2009).

Briefly, for each pixel $B_{1,2}$ and B_{cc} were evaluated according to the following formulas:

$$B_{1,2} = \frac{\sigma_{1,2}^2}{\langle I_{1,2}\rangle}, B_{cc} = \frac{\sigma_{cc}^2}{\sqrt{\langle I_1\rangle\langle I_2\rangle}}, \quad (1)$$

where I_1 and I_2 stand for the mean fluorescence signal in the green and red channel, respectively. The variances σ^2 were calculated as follows:

$$\sigma_{1,2}^2 = \frac{\sum(I_{1.2}-\langle I_{1.2}\rangle)^2}{K}, \sigma_{cc}^2 = \frac{\sum(I_1-\langle I_1\rangle)(I_2-\langle I_2\rangle)}{K}. \quad (2)$$

K is the number of frames taken for the analysis.

Since the variance not only increases when diffusing molecules enter/ leave the examined region, but is also subject to overall cell movement and dye photobleaching, the undesired contributions have to be removed. Since both represent second-scale

trends in intensity, their removal is based on distinguishing random fluctuations (diffusion) from those trends. The intensity trace obtained for each pixel is cut into few-frame segments with suppressed manifestation of the trends. Within each segment, the mean segmental intensity is subtracted from each intensity value. Thus, random intensity fluctuations at each pixel for every frame are obtained. To reconstruct the trend-free intensities, Poisson-distributed random numbers for each pixel in each frame are generated. They are centered at the original intensity (unaffected by photobleaching) of each pixel in the first frame. These values are added to the calculated fluctuations and the de-trended data are processed using Eqs. 1 and 2. The joint motion of Bodipy-labeled lipids and RFP-labeled proteins manifests itself in a non-symmetric distribution of the B_{cc} values (in signal-containing pixels) around zero. If the B_{cc} values are shifted to positive values, joint motion occurs.

Single molecule microscopy and two-color cross-correlation number and brightness (ccN&B) analysis were performed in the laboratory of Martin Hof (Heyrovský Institute of Physical Chemistry, Academy of Sciences of the Czech Republic, Prague, Czech Republic).

Statistical analysis

Results are expressed as means +/− standard deviation (SD). Two-tailed unpaired Student's t-test was used to determine the significance of the differences. p-Values ≤ 0,05 were considered significant.

2.4 Results

It is known from different studies that oxidized LDL and its constituent oxPL PGPC and POVPC are toxic in macrophages (Steinbrecher *et al.*, 2004; Stemmer *et al.*, 2012). Here, we report on a detailed analysis of the mode of cell death that is induced by the respective phospholipid oxidation products in the cells. Figure 2.1 shows the fractions of viable, apoptotic and necrotic cells that were detected by FACS analysis in RAW 264.7 macrophages after treatment with 50 µM oxPL. PGPC and POVPC induced very similar apoptotic effects relative to controls. In addition, PGPC led to a much higher increase of necrotic cells. Obviously, PGPC is much more toxic to the cells and, as a consequence, much more detrimental to the cellular environment due to its strong necrotic effect.

Microscopic observations of cell morphology support the notion that PGPC and POVPC are detrimental to the integrity of RAW 264.7 macrophages (Figure 2.2). Signs of programmed cell death can be seen, including cell shrinking and membrane blebbing. After several hours, cell rounding and eventually massive release of the cells from the substratum becomes evident.

The time-dependent activation of caspase-3 and -7 was determined as a biochemical marker for apoptotic cell death induced by PGPC and POVPC. Both oxPL stimulated this enzyme already after 15 min incubation time, but after longer incubation times the activity profiles became different (Figure 2.3). Caspase activation by PGPC increased steadily during a period of four hours. In contrast, The POVPC effect on the enzyme was faster and caspase activity reached a maximum after two hours followed by a slow decrease. This data matches with the time-dependent formation of the apoptotic messenger ceramide which is generated under the influence of oxPL in RAW 264.7 macrophages (Figure 2.3 B and C). POVPC leads to a transient increase of ceramide concentration and reaches basal levels after 8 h. In contrast, the ceramide response to PGPC is slower. The ceramide concentration increases after 4 h. It is more pronounced compared with POVPC still increasing after 8 h. It has already been shown that ceramide formation by acid sphingomyelinase is causally related to apoptosis and

caspase activation in vascular cells (Loidl *et. al.*, 2003; Stemmer *et al.*, 2012). Recent studies showed that ceramide formation under the influence of both oxPL is also due to activation of ceramide synthases (Halasiddappa, *et al.*, 2013), but the relationship to caspase activation is still less clear.

Several reports have already emphasized a key role of PKCδ in apoptotic signaling in different cells. This enzyme may either activate the apoptotic caspase-3 directly by phosphorylation (Voss *et al.*, 2005) or indirectly via activation of acid sphingomyelinase (Zeidan and Hannun, 2007), followed by ceramide formation (Figure 2.10). In turn, PKCδ can be activated by caspase-3-induced cleavage (Kato *et al.*, 2009). Other mechanisms independent of caspase-3, involving SDK1 and 14-3-3ζ may also participate (Hamaguchi *et al.*, 2003).

To test the hypothesis that PKCδ is also activated in oxPL-induced macrophage cell death, we determined the phosphorylation of this enzyme at Tyr-311 under the influence of PGPC or POVPC. According to results from Western blot analysis, both oxPL have the capacity to phosphorylate the enzyme (Figure 2.4).

To identify the role of PKCδ and its relationship with caspase-3 and -7 activities in apoptotic signaling, the enzyme was knocked down in RAW 264.7 macrophages using siRNA technology. First of all, the silencing efficiency was checked with RT-qPCR on the transcription level and with Western blotting on the protein level. Cells transfected with scrambled sequence siRNA (negative siRNA) served as controls. Figure 2.5 shows a time-dependent decrease and an almost complete loss of protein expression after 48 h incubation (Figure 2.5 A and B). The RT-qPCR data also support the silencing effect (Figure 2.5 C). Silencing of PKCδ in RAW 264.7 macrophages led to a decrease in caspase-3/7 activation by oxPL in these cells (Figure 2.6). This effect was significantly more pronounced in the case of POVPC. From this result, it can be concluded that PKCδ is a proapoptotic kinase in macrophages under oxidative phospholipid stress. It is causally related to caspase-mediated cell death and required for full oxPL toxicity in these cells. The apoptotic activity of POVPC seems to depend on PKCδ to a larger extent as compared to PGPC.

Reports from the literature provide evidence that exogenous stimuli may initially recruit PKCδ to the plasma membrane (Zeidan and Hannun, 2007) before the kinase activates downstream components of intracellular signaling (e.g. sphingomyelinase). Thus, we addressed ourselves to the question whether and to what extent PKCδ can directly interact with oxPL in the cell surface or in the cytoplasm after oxPL incorporation. A fluorescent POVPC analog has been used in a previous study to identify covalent Schiff base formation of the aldehydo-phospholipid with a large number of membrane and cytosolic proteins in RAW 264.7 macrophages (Stemmer *et al.*, 2012). This biochemical approach is based on isolation and mass spectrometry identification of the lipid-protein adducts and does not allow direct monitoring of lipid-protein interactions in live cells. In addition, it is not suitable for the detection of PGPC-protein association, that is only mediated by physical interactions. To investigate the interactions of fluorescent POVPC and PGPC analogs with PKCδ, we expressed RFP-tagged enzyme constructs in RAW 264.7 macrophages. In these cells, we measured the codiffusion of the labeled protein with fluorescent oxPL on the single molecule level. In the absence of oxPL, RFP-PKCδ fluorescence mainly localizes to the cytosol and some „hot spots“ in the perinuclear region (Figure 2.7 A). In contrast, RFP alone is homogeneously expressed in the cytosol. Upon addition of a fluorescent PGPC analog (BY-PGPE), PKCδ fluorescence rapidly concentrates on the plasma membrane, where it initially colocalizes with the labeled oxPL (Figure 2.7 B). The same behaviour of PKCδ has already been observed when cultured cancer cells were stimulated with phorbol esters (Zeidan and Hannun, 2007). Localization of RFP alone was not affected by the oxPL. A fluorescent POVPC analog (BY-POVPE) also led to enrichment of labeled PKCδ on the cell surface, but the extent of protein recruitment to the cell suface was cell-dependent. More detailed inspection of fluorescence patterns of single cells showed that the cell population was heterogeneous with respect to lipid uptake. Efficient plasma membrane labeling by fluorescent POVPC (Figure 2.7 C, I) was associated with efficient membrane recruitment of fluorescent PKCδ. In single cells that showed less intense labeling by BY-POVPE, much less fluorescent protein was observed at the membrane (Figure 2.7 C, II). Such differences were not

seen, when the cells were exposed to fluorescent PGPC, probably because the latter lipid shows a higher amphiphilicity due to its negatively charged *sn*-2 acyl residue and thus more easily inserts into the plasma membrane. Localization of the „pure“ RFP was hardly affected by the oxPL.

Quantitative analysis of protein and lipid dynamics on the single molecule level provided a more detailed picture of lipid-protein interactions and showed that binding probabilities may differ considerably in a lipid- and protein-specific manner. For this purpose, fluorescently tagged PKCδ was expressed in RAW 264.7 macrophages followed by addition of fluorescent oxPL under the same experimental conditions as described above. Then, the motions of single protein and oxPL molecules in the cells were simultaneously observed by acquiring a two-color movie of selected cells. The data obtained for protein/ BY-POVPE and protein/ BY-PGPE pairs were subjected to two-color cross-correlation number and brightness (ccN&B) analysis to detect codiffusion of the individual components in a lipid-protein complex.

The meanings of ccN&B are as follows: From ccN&B values around zero, it can be inferred that two different fluorescent components do not move together. ccN&B shifts to positive values are indicative for codiffusion of two fluorescent molecules, e.g. lipid and protein. However, absolute ccN&B values of fluorophore pairs bound to larger protein scaffolds or membranes have to be interpreted with caution. The motion of the supramolecular (membrane) system itself may give rise to synchronous movements of the attached fluorophores that lead to an increase in ccN&B, independent of bimolecular fluorophore (lipid-protein) interaction. The ccN&B data presented in this work have already been corrected for second, but not for sub second scale movements, which could be due to membrane undulations (Brown, 2003). We do not show the quantitative contribution of these supramolecular motions to our ccN&B data. We guess that the order of magnitude for such motions is similar in cell membranes either preincubated with BY-PGPE or BY-POVPE. If this hypothesis is true, the observed differences in ccN&B will be largely a consequence of different codiffusions of these lipids with RFP(-tagged) proteins. Therefore, we only quantitatively compare ccN&Bs of fluorescent PGPC and POVPC analogs as a consequence of complexation with

fluorescent proteins, thus simply stating whether the lipid-protein pair shows a positive shift relative to zero, or not. In Figure 2.8 typical ccN&B distributions are shown for fluorescent PGPE (PGPC analog) and POVPE (POVPC analog) in plasma membranes of cells expressing PKCδ-RFP or RFP alone. Figure 2.8 shows that significant shifts relative to zero can be induced by both lipids. More detailed results are presented in Table 2.1 from pixel analysis in whole cells, the plasma membrane and the cytosol (see below). Obviously, there are differences between ccN&B values between the latter two compartments, but they are difficult to interpret. ccN&Bs also depend on local (lipid) fluorophore concentrations which in turn would increase their probability of protein binding. This is one more reason to avoid quantitative consequences of the individual lipids and to find out whether a positive ccN&B shift relative to zero is detectable.

The ccN&B values were determined for all pixels of the fluorescence images. Table 2.1 shows the most frequent maximum values of ccN&B in the whole cell (corresponding pixels), and specifically in the membrane region and in the cytosol. Both phospholipids shifted ccN&B to positive values relative to zero (zero signifies no correlation) when correlated to PKCδ-RFP fluorescence, indicating joint motion of a lipid and protein inside the cell (Figure 2.8, Table 2.1). In reference experiments, we also performed ccN&B analysis for fluorescent analogs of POVPC and PGPC in whole cells expressing solely RFP. Whereas BY-POVPE showed a significant extent of interaction, PGPC association with this protein was less pronounced.

Comparison of ccN&B values obtained at a „subcellular level“ provides a more detailed picture for lipid-protein affinities and the capacity of an exogenously added fluorescent oxidized phospholipid to recruit fluorescent PKCδ or RFP to the plasma membrane (Figure 2.8, Table 2.1). From the positive ccN&B values, it can be concluded that at least small tendencies of lipid-protein association are detectable for all pairs of fluorescent oxidized phospholipids and PKCδ or RFP in the plama membrane and the „cytosol“. However, the probability of such interactions in either compartment depends on the protein and the phospholipid. In agreement with the fluorescence micrographs, ccN&Bs show a pronounced activity of BY-PGPE in

recruiting PKCδ to the surface membrane (ccN&Bmax 0,08/ membrane). The same effect is observed with the fluorescent POVPC analog (see I. BY-POVPE: ccN&Bmax 0,08/ membrane). The ccN&B value measured for the aldehydo-phospholipid BY-POVPE in the cytosol is also positively shifted. This may be taken as a hint, that covalent complex formation may also be responsible for lipid-protein interactions in the cell interior. Single cells containing less fluorescent POVPC (see II. BY-POVPE) hardly show association with PKCδ in the cell surface (ccN&Bmax 0,02) (see also Figure 2.8). Binding of RFP to the plasma membrane can be observed in cells labeled with BY-PGPE or BY-POVPC (ccN&Bmax 0,03/ membrane, ccN&Bmax 0,07/ membrane, respectively). One is tempted to say that chemically reactive aldehydo-lipid shows a higher tendency to form protein conjugates as compared to its carboxylate counterpart, provided whole membrane movement and lipid concentration are comparable (see above). But ccN&Bmax values are higher for BY-POVPE both in the plasma membrane as well as in the „cytosol“ compared to BY-PGPE.
In summary, the cross-correlation and brightness analysis of lipid and protein motion provides evidence that fluorescent PGPC and POVPC analogs recruit PKCδ to the plasma membrane. This effect is influenced by phospholipid uptake which is more efficient in the case of PGPC. If lipid uptake into cells is limited, the amount of incorporated lipid may be too low for attracting the enzyme. For instance, POVPC is less polar than PGPC and uptake may differ on the single cell level. In addition, a certain fraction of this phospholipid may be masked by Schiff base formation with aminophospholipids and proteins. It is not clear if the chemically bound form of POVPC loses its PKCδ affinity. Finally, in agreement with previous proteomic analyses (Stemmer *et al.*, 2012), it can be inferred from the „cytosolic“ ccN&B values that the aldehyde increases the ability of BY-POVPE to form lipid-protein complexes.

Activation of an aSMase generating the apoptotic mediator ceramide can be stimulated after phosphorylation by PKCδ (Zeidan and Hannun, 2007). ASMase activitiy is causally related to oxPL-induced cell death in RAW 264.7 macrophages (Loidl *et. al.*, 2003; Stemmer *et al.*, 2012). To identify spatial proximity of PKCδ and aSMase, which is a prerequisite for their functional interdependence, we coexpressed

fluorescently tagged PKCδ-RFP and aSMase-GFP in cultured RAW 264.7 macrophages. Figure 2.9 shows the fluorescence patterns of both enzymes in the same cells. Superimposition of both fluorescence images reveals a „perfect“ colocalization of the labeled proteins. Interestingly, both enzymes also colocalized in COS-7 cells. Thus, it is likely that the close enzyme association is not a specific phenomenon, but may be utilized for an efficient cellular stress response to external stimuli in many cells. The colocalization is a prerequisite for a functional relationship of PKCδ and aSMase. The latter of course is still subject to proof.

2.5 Discussion

Chronic exposure to the truncated oxidized phospholipids PGPC and POVPC induces apoptosis in vascular cells. This phospholipid toxicity is associated with very early activation of acid sphingomyelinase, generating the apoptotic mediator ceramide, activation of the stress kinases p38 MAPK and JNK, and finally, activation of the executor caspases-3 and -7. (Loidl *et. al.*, 2003; Stemmer *et al.*, 2012) Synthesis of ceramide catalyzed by ceramide synthases during prolonged interaction of the oxPL with the cells may also play a role, perhaps in the execution phase of apoptosis (Halasiddappa *et al.*, 2013). The present study provides evidence for the contribution of another important component to the toxic signaling of oxPL, namely protein kinase C-delta (PKCδ). We found that silencing of this enzyme compromises oxPL-induced activation of caspase-3 and -7 and thus protects the cells from apoptotic cell death. Thus, next to aSMase (Stemmer *et al.*, 2012), PKCδ is a signaling enzyme that is causally related to oxPL toxicity in RAW 264.7 macrophages.

In vascular cells as well as in cancer cells, PKCδ is an important apoptotic signaling component which is connected to the formation of ceramide. In malignant cells, PKCδ acts as a proapoptotic tumor suppressor. Its function is lost in human squamous cell carcinoma (D'Costa *et al.*, 2006) and in melanoma (Halder *et al.*, 2014). In mammary carcinoma (Zeidan and Hannun, 2007) and prostate cancer cells (Sumitomo *et al.*, 2002), PKCδ is involved in sphingomyelinase activation and ceramide formation (see below). A direct relationship between increased ceramide concentrations and membrane recruitment of a PKC isoform has been found in rat aortic vascular smooth muscle cells (A7r5). It was shown that treatment of these cells with exogenous ceramide led to phosphorylation and membrane recruitment of PKCζ, within caveolin-enriched lipid microdomains. (Fox *et al.*, 2007)

PKCδ activation is also relevant for cell death involved at various stages of arteriosclerosis. It has been shown that oxLDL, which contains PGPC and POVPC, induces apoptosis in the human macrophage cell line J774A.1 and also activates p38 MAPK and PKCδ signaling pathways (Giovannini *et al.*, 2011). Obviously, PKCδ is

one more component in an apoptotic signaling network that is triggered both by oxPL and oxLDL. Our findings support the assumption that oxPL largely determine the toxicity of the lipoprotein particle in vascular cells. The group of Hannun (Zeidan and Hannun, 2007) demonstrated that PKCδ is directly involved in aSMase activation and ceramide formation: In mammary carcinoma cells stimulated with phorbol esters, PKCδ is recruited to the plasma membrane where it undergoes autophosphorylation. The phosphorylated enzyme translocates to the endolysosomes where it phosphorylates aSMase. By this means activated aSMase moves to the plasma membrane to generate ceramide. This model is in agreement with an independent study showing that lysosomal ceramide does not participate in apoptotic signaling (Segui *et al.*, 2000). Several features described for the apoptotic activity PKCδ were also found by our group in RAW 264.7 macrophages under the influence of oxidized phospholipid stress. From fluorescence correlation microscopy experiments, it can be inferred that fluorescent analogs of PGPC and POVPC give rise to fast recruitment of RFP-tagged PKCδ to the plasma membrane of RAW 264.7 macrophages (Figure 2.7, Figure 2.8).

The perfect colocalization of fluorescently tagged PKCδ with aSMase (Figure 2.9) may be regarded as a further hint for spatial and perhaps functional interaction of both enzymes. Finally, PGPC and POVPC lead to phosphorylation of PKCδ (Figure 2.5) which has been suggested to represent a very early initial step of apoptotic signaling by this enzyme.

In this study, evidence was found that PKCδ is causally related to oxPL-induced cell death. Silencing of the former enzyme by siRNA led to significant reduction of caspase-3/7 activity in response to PGPC or POVPC (Figure 2.6). According to reports from the literature, at least three mechanisms can be responsible for (or coordinately lead to) this effect (Figure 2.10). Firstly, membrane-associated oxPL activate PKCδ which in turn phosphorylates aSMase followed by ceramide formation in the plasma membrane. After several additional steps, this finally results in caspase-3 activation (see above, Zeidan and Hannun, 2007). Phosphorylation of PKCδ by the oxPL (Figure 2.4), recruitment of the enzyme to the plasma membrane (Figure 2.7) and the close

vicinity of PKCδ to aSMase (Figure 2.9) would be in line with this model. Secondly, caspase-3 can enhance PKCδ-mediated apoptosis, since it catalyzes the cleavage of this protein (Kato *et al*., 2009). It has been shown in vascular smooth muscle cells under oxidative stress, that the PKCδ fragment, namely SDK1, phosphorylates the antiapoptotic 14-3-3ζ leading to the formation of the apoptotic 14-3-3ζ monomer (Hamaguchi *et al.*, 2003). Thirdly, PKCδ can in turn further increase the activity of caspase-3 by phosphorylation of the latter enzyme. It has been shown in monocytes that PKCδ associates with caspase-3, thus facilitating the phosphorylation of the protease. Overexpression of PKCδ resulted in an increase of monocyte apoptosis, whereas its inhibition blocked activation of caspase-3 resulting in decreased apoptosis (Voss *et al.*, 2005).

Recruitment of PKCδ to the plasma membrane followed by autophosphorylation and activation of aSMase seems to be a particular process contributing to apoptotic signaling of oxPL in cells (see above and Zeidan and Hannun, 2007). Our data show that both PGPC and POVPC give rise to this phenomenon (Figure 2.7, Table 2.1). However, the respective underlying molecular mechanisms are probably quite different for the following reasons. Both oxPL can modify biophysical membrane properties, e.g. lateral membrane distribution, local membrane curvature, as well as electrostatic charges, leading to binding of PKCδ to the cytoplasmic side of the plasma membrane. PGPC directly enhances the net negative charge of the lipid bilayer due to its *sn*-2 carboxy function. POVPC indirectly induces the same result by decreasing the number of positive charges due to chemical Schiff base formation with aminophospholipids and proteins. We suppose that most of the membrane-bound POVPC exists in the form of covalently but loosely associated conjugates. Therefore, the effect of free POVPC only plays a minor role in modulation of biophysical membrane properties. Obviously, the enrichment of the membrane with single chain amphiphiles, and the increase of the net negative charge, seem to be minimum requirements for the recruitment of PKCδ. The chemically reactive POVPC could also improve membrane binding of this enzyme via an entirely independent mechanism. Direct modification of PKCδ via the *sn*-2 aldehyde group of POVPC would lead to

enzyme alkylation and as a consequence anchor the protein to the membrane. A typical example for such a mechanism has been reported by the Kinnunen group. They found that Poxno-PC, a longer chain homolog of POVPC, enhanced the activity of a water-soluble phospholipase. Poxno-PC reduced the lag times of enzyme-catalyzed phospholipid degradation, probably because of protein lipidation, resulting in more intimate binding of the protein to its supramolecular substrate. (Code *et al.*, 2010) Whether or not this phenomenon contributes to the enrichment of PKCδ at the plasma membrane must be left open. However, it has to be emphasized again that membrane recruitment is specific for PKCδ, since POVPC does not recruit RFP to the surface membrane, despite the fact that it forms conjugates with the protein in the membrane and the "cytosol" (Figure 2.7, Table 2.1).

Covalent POVPC-protein association is not restricted to the plasma membrane. We found that this lipid also binds to a protein fraction in the cell interior (Stemmer *et al.*, 2012). Protein modification by reactive lipids could also trigger enzyme activation. Of course, this hypothesis is subject to proof. To date, modification of proteins by lipid aldehydes and its consequences for protein function have extensively been studied for malondialdehyde and hydroxyalkenals, but to a lesser extent for aldehydo-phospholipids. In most cases, lipidation of enzymes decreased their activities (Grimsrud *et al.*, 2008), e.g. Hsp90 or protein disulfide isomerase (Carbone *et al.*, 2005). However, alkylation of a soluble phospholipase by an aldehydo-oxPL, improved enzyme activity, but due to a supramolecular effect (Code *et al.*, 2010). The lipid chain firmly attached the protein to the membrane interface and brought the enzyme in closer contact with its substrate.

Both PGPC and POVPC activate caspase-3/7 in RAW 264.7 macrophages in a lipid-specific and time-dependent manner. The maximum enzyme response to POVPC is observed earlier as compared to PGPC (maximum activities after 2 h and 4 h incubation, respectively). These differences in caspase activation correlate with the respective time-dependent ceramide profiles induced by PGPC and POVPC. Ceramide formation is due to the activation of aSMase at short incubation times and due to the activities of a subset of ceramide synthases after longer incubation with oxPL.

Ceramide formation due to aSMase is mandatory for oxPL-induced cell death and is likely to be involved in the initiation of apoptosis (Loidl *et al.*, 2003). PKCδ could play a role in this early signaling phase if it is activated and interacts with aSMase. This enzyme has already shown to be indispensable for caspase activation. The contribution of ceramide generated by the action of ceramide synthases in this szenario is less clear at the moment. It could be involved in the execution phase of apoptosis leading to membrane stress and organelle dysfunction. Thus, we are still far from a detailed understanding of how and to what extent ceramide, ceramide synthesizing enzymes and PKCδ coordinately mediate apoptosis in macrophages under influence of oxidized phospholipids.

Acknowledgments

This work was supported by the Austrian Science Fund FWF (project title "OxPL-protein targets and apoptotic signaling of oxidized phospholipids", project number I308-B12).

We would like to acknowledge Verena Kohler for her contribution to the experimental work in the laboratory during her internship in the group of Prof. Albin Hermetter.

2.6 Tables

Table 2.1 Codiffusion of PKCδ-RFP and fluorescent oxPL molecules in RAW 264.7 macrophages.

PKCδ-RFP or RFP were expressed in RAW 264.7 macrophages followed by incubation with fluorescent oxPL as described in the legend to Figure 2.7. To detect codiffusion of fluorescent lipid and protein in whole cells and cellular compartments (cytosol or membrane), two-color cross-correlation number and brightness (ccN&B) analysis was performed as described under Materials and Methods. CcN&B shifted to positive values indicates joint motion of protein and lipid. Lipids: BY-PGPE; I. BY-POVPE: in cells with efficient lipid uptake; II. BY-POVPE: in cells with low lipid uptake.

		ccN&Bmax values:			
	Lipid	**Whole cell**	**Cytosol**	**Membrane**	**n**
PKCδ-RFP	BY-PGPE	0,02 +/-0,01	0,03 +/-0,02	0,08+/-0,03	14
	I. BY-POVPE	0,03 +/-0,01	0,05 +/-0,02	0,08 +/-0,05	3
	II. BY-POVPE	0,02 +/-0,02	0,04 +/-0,03	0,02 +/-0,02	5
RFP	BY-PGPE	0,02 +/-0,01	0,03 +/-0,02	0,03 +/-0,02	8
	BY-POVPE	0,07 +/-0,03	0,09 +/-0,02	0,07 +/-0,02	5

2.7 Figures

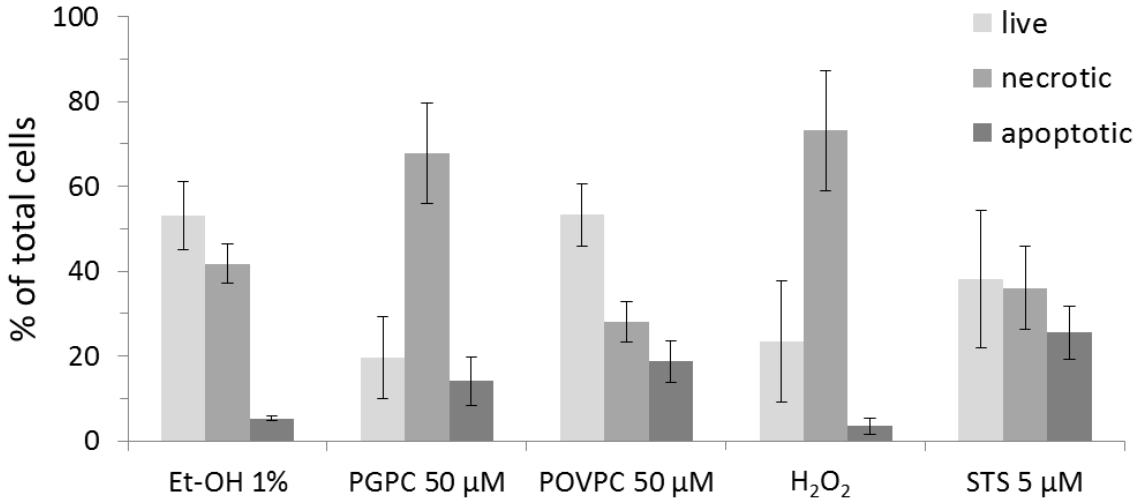

Figure 2.1 Cytotoxicity of oxPL in RAW 264.7 macrophages.

Cells were incubated with 50 µM PGPC or POVPC in low serum medium (0,1 % FBS) for 4 h. Control cells were incubated with medium containing 1 % (v/v) ethanol. Cells incubated with 5 µM Staurosporine (STS) or 30 mM H_2O_2 served as positive controls for apoptosis and necrosis, respectively. After stimulation, cells were harvested, stained with propidium iodide (PI) and Annexin V, and analyzed by flow cytometry. Intact cells were unstained. Cells stained by PI or both dyes were considered necrotic. Cells stained by Annexin V were considered apoptotic. Results are expressed as means ± SD ($n \geq 4$).

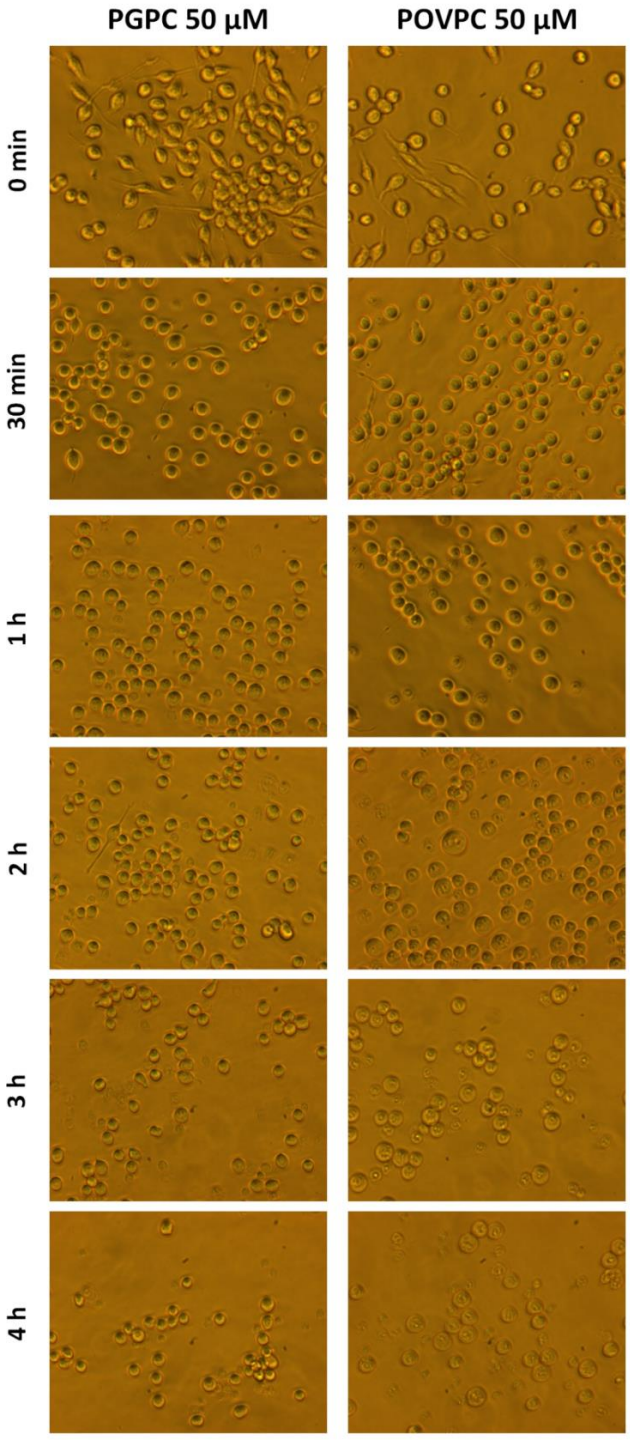

Figure 2.2 Effects of oxPL on RAW 264.7 macrophages morphology.

RAW 264.7 cells were incubated with 50 µM POVPC or PGPC in DMEM containing 0,1 % FBS for the indicated times. Photomicrographs of the cells (magnification: 320x) were taken using an Axiovert 35 inverted microscope equipped with a CCD camera. Observed changes in cell morphology were rounding of the cells, shrinkage, cell lysis and detachment.

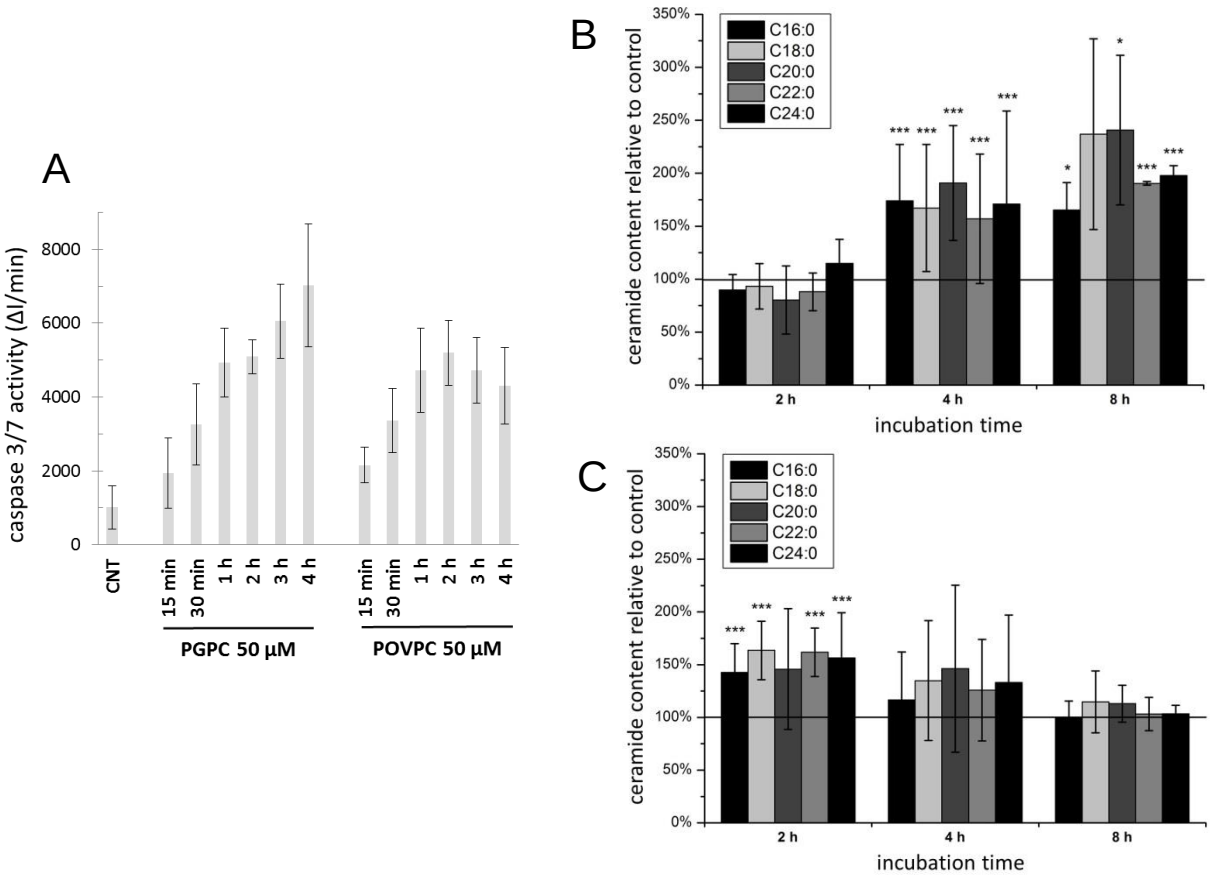

Figure 2.3 Time-dependent activation of caspase-3/7 and ceramide generation by oxPL in RAW 264.7 macrophages.

Panel A: *Cells grown in 96-well plates were treated with dispersions of 50 µM PGPC or POVPC in DMEM under low serum concentrations (0,1 % FBS) or media supplemented with 1 % ethanol as a control for the indicated times. The incubation was stopped by the addition of lysis buffer containing a pro-fluorescent caspase-3/7 substrate. Caspase-3/7 activation was assessed using a homogeneous fluorescence caspase-3/7 assay. Data are expressed as means ± S.D. (n ≥ 5).*

Panel B and C: *Effects of oxPL on ceramide levels. RAW 264.7 macrophages were incubated with 50 µM PGPC (panel B) or 50 µM POVPC (panel C) in DMEM media for various times. Lipid extracts were prepared and ceramide species were determined by MS as described in Materials and Methods. N-acyl chains of the individual ceramide species are specified in the insert. Data are expressed as means ± SD (n = 5). * $p \leq 0,05$, *** $p \leq 0,005$. Panel B and C were taken from the doctoral thesis of Daniel Koller (Koller et al., PhD thesis, TU Graz, 2013).*

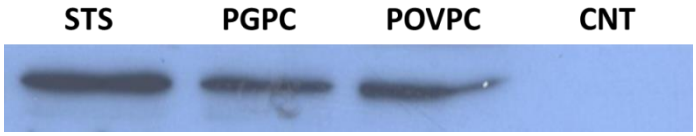

Figure 2.4 Western blot analysis of PKCδ phosphorylation at Tyr-311.

RAW 264.7 macrophages were incubated with DMEM high glucose media containing 100 µM POVPC or PGPC, or 5 µM staurosporine (STS) for 4 h. Media containing only 1 % (v/v) ethanol served as a control (CNT). After incubation, the cells were harvested and lysed. Sample aliquots (20 µg protein) were analyzed for phosho-PKCδ levels by Western blotting using an anti phospho-Tyr-311 antibody. In oxPL-treated as well as in staurosporine-treated cells, phosphorylation of PKCδ was detected.

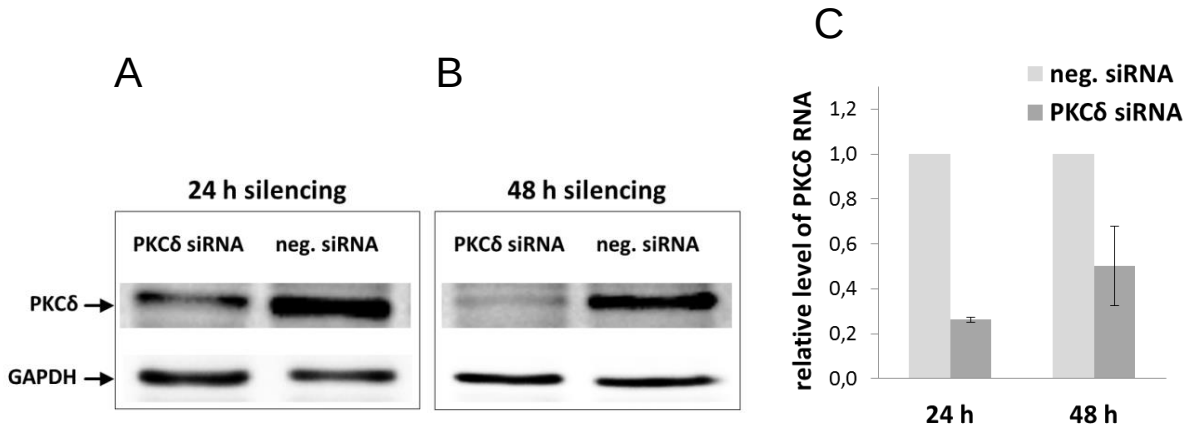

Figure 2.5 PKCδ knockdown in RAW 264.7 cells by RNA interference.

RAW 264.7 macrophages were seeded in 24-well plates and transfected with 20 pmol siRNA specific for PKCδ per well. Control siRNA with scrambled sequences (neg. SiRNA) served as control. 24 h or 48 h after transfection, cells were harvested to isolate protein and RNA. ***Panel A and B:*** *Detection of PKCδ silencing by Western blotting. 20 µg protein lysate per lane were loaded and separated on 12,5 % SDS gels. Proteins were transferred to membranes and incubated with antibodies specific for PKCδ and GAPDH. PKCδ was recognized at 78 kDa and GAPDH, serving as loading control, at 37 kDa.* ***Panel C:*** *Detection of PKCδ silencing by quantitative real time PCR (RT-qPCR). 24 h and 48 h after transfection, the amount of PKCδ mRNA transcript was analyzed by RT-qPCR using primers specific for PKCδ. Results were normalized against GAPDH-expression ($n \geq 3$, mean ± S.D.).*

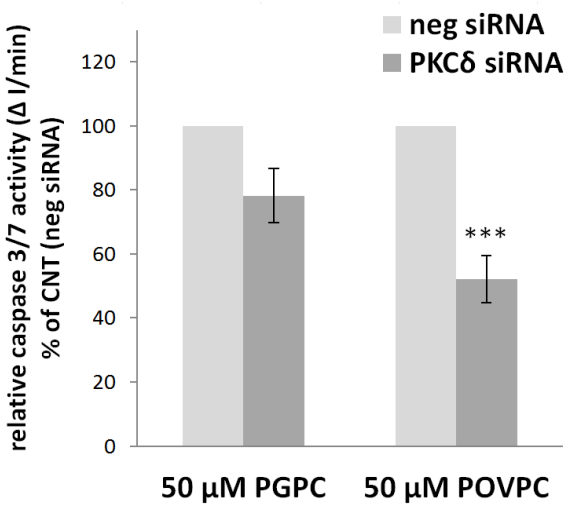

Figure 2.6 Effect of PKCδ knockdown on oxPL-induced caspase-3/7 activation.

*RAW 264.7 cells were transfected with scrambled siRNA (negative siRNA) or siRNA specific for PKCδ for 48 h followed by incubation with 50 µM PGPC or POVPC in DMEM under low serum concentrations (0,1 % FBS) for 1 h. Caspase-3/7 activity is expressed as percent of control (neg. siRNA). It was determined using a homogeneous fluorescence activity assay (for details see Materials and Methods). PKCδ knock down was associated with decreased caspase-3/7 activities in cells that had been exposed to PGPC or POVPC. Data are expressed as means ± SD (n ≥ 3). Significances were determined by Student's t-test (two tailed, unpaired). *** P ≤ 0,001, compared with control.*

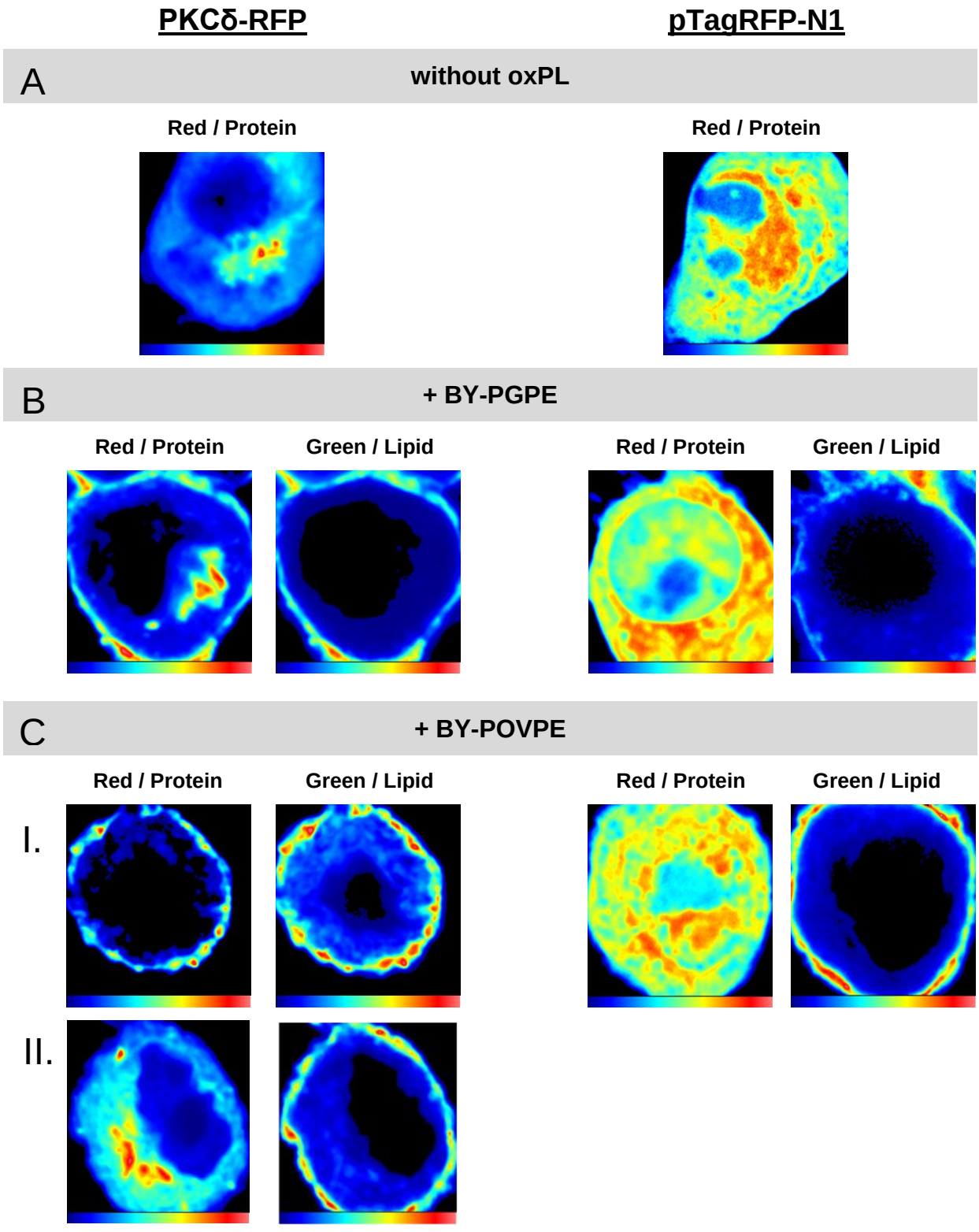

Figure 2.7 Colocalization of PKCδ-RFP and fluorescent oxPL in RAW 264.7 macrophages.

Continued on the following page

RAW 264.7 macrophages were transfected with an expression vector encoding for the fusion protein PKCδ-RFP or with the "empty" vector encoding for RPF (pTagRFP-N1) on the day prior to the measurements and cultured on slides in DMEM. 24 h after transfection, the cells on the slides were rinsed three times with PBS and then incubated with dispersions of 1 µM BY-PGPE or BY-POVPE in PBS buffer for 5 min at 37 °C. After incubation, the cells were again rinsed three times with PBS and mounted onto a Chamlide chamber containing DMEM imaging medium with 20 mM HEPES. Fluorescence was imaged as described under Materials and Methods. In the experiment with cells expressing PKCδ-RFP, two cell fractions were observed after incubation with BY-POVPE, showing high (I) and low (II) lipid uptake, respectively.

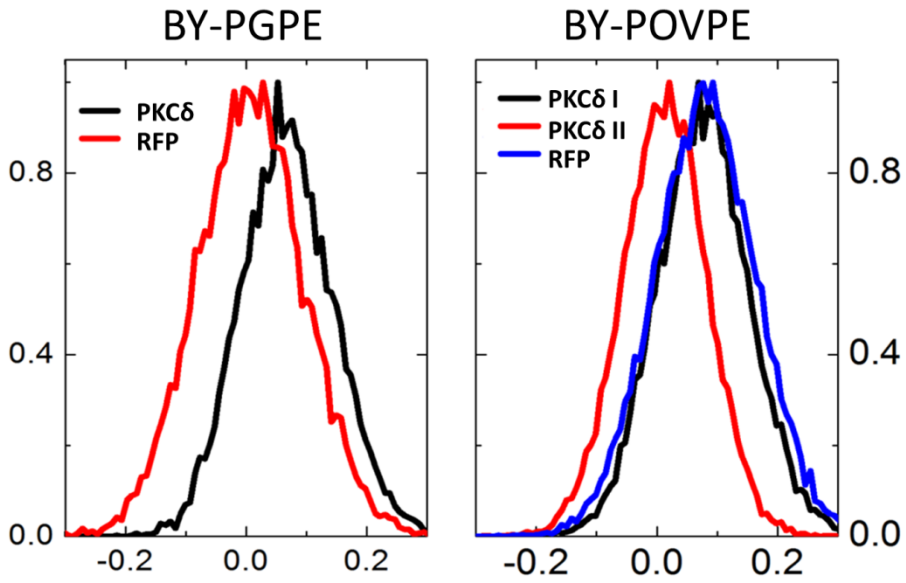

Figure 2.8 Codiffusion of PKCδ-RFP and fluorescent oxPL molecules in plasma membranes of RAW 264.7 macrophages.

PKCδ-RFP or RFP were expressed in RAW 264.7 macrophages followed by incubation with fluorescent oxPL as described in the legend to Figure 2.7. To detect codiffusion of fluorescent lipid and protein, two-color cross-correlation number and brightness (ccN&B) analysis was performed as described under Materials and Methods. A shift of ccN&B to positive values indicates joint motion of protein and lipid. After addition of either of both oxPL, BY-PGPE or BY-POVPE (only PKCδ I), to macrophages expressing PKCδ-RFP, ccN&B shifted to positive values. Lipids: BY-PGPE; BY-POVPE: "PKCδ I" in cells with efficient uptake of BY-POVPE; "PKCδ II" in cells with low uptake of BY-POVPE.

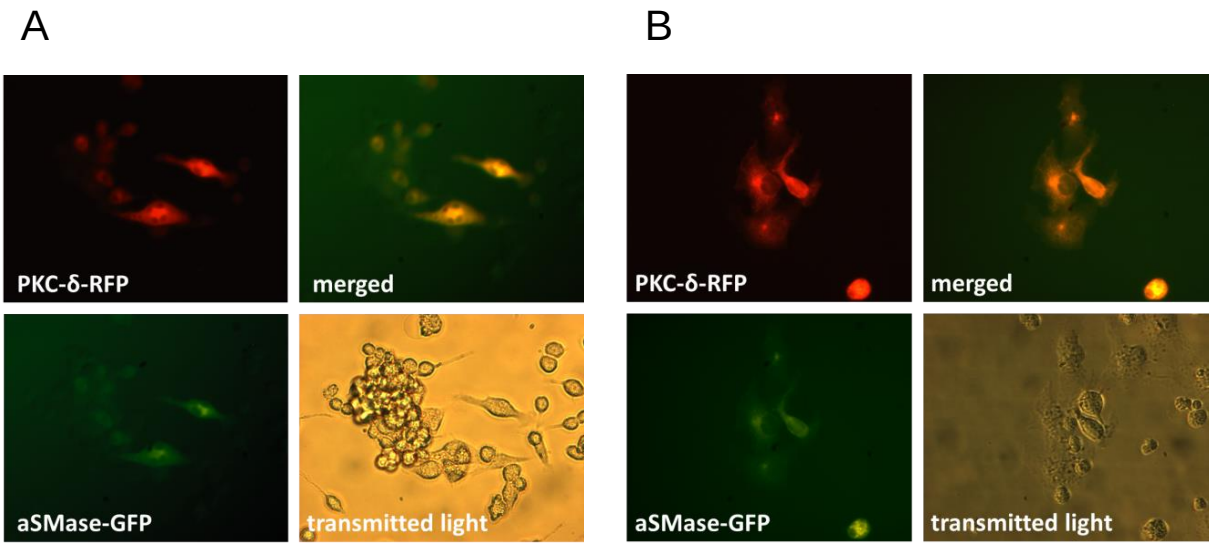

Figure 2.9 Colocalization of PKCδ-RFP and aSMase-GFP in RAW 264.7 macrophages and Cos-7 cells.

RAW 264.7 macrophages (A) and Cos-7 cells (B), were cotransfected with expression vectors encoding for PKCδ-RFP and aSMase-GPF. After 24 h, expression of the fluorescent proteins was observed. Transmission and fluorescence images of the same sections were collected at the same time. For both cell lines, merged images of PKCδ-RFP and aSMase-GPF fluorescence reveal seamless colocalization of the two proteins.

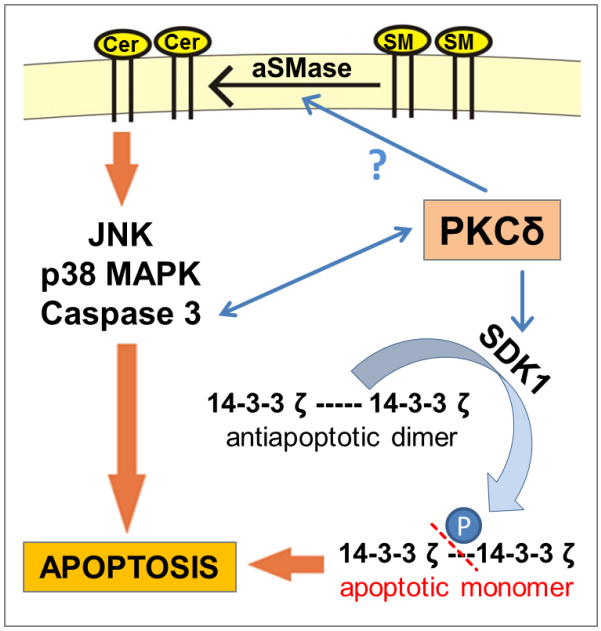

Figure 2.10 Tentative model of oxPL-induced cell death involving PKCδ, 14-3-3ζ and caspase-3.

Caspase-3, JNK, p38 MAPK and aSMase have previously been identified as components of oxPL-induced apoptotic cell death in vascular cells (Loidl et al., 2003; Stemmer et al., 2012).

Acid sphingomyelinase (aSMase) catalyzes the formation of the lipid mediator ceramide (Cer) from sphingomyelin (SM) in the plasma membrane. Ceramide propagates the apoptotic oxPL signal. In this work, evidence is provided that protein kinase C-delta (PKCδ) also plays a causal role in this scenario. It is mandatory for caspase-3 activation, which might at least be in part due to its capacity to stimulate aSMase (Zeidan and Hannun, 2007). This assumption is further supported by our findings showing that oxidized phospholipids directly interact with PKCδ (Figure 2.8), which in turn colocalizes with aSMase (Figure 2.9).

2.8 References Chapter 2

Batzri, S. & Korn, E.D. 1973, "Single bilayer liposomes prepared without sonication", *Biochimica et biophysica acta*, vol. 298, no. 4, pp. 1015-1019.

Berliner, J.A., Subbanagounder, G., Leitinger, N., Watson, A.D. & Vora, D. 2001, "Evidence for a role of phospholipid oxidation products in atherogenesis", *Trends in cardiovascular medicine*, vol. 11, no. 3-4, pp. 142-147.

Bradford, M.M. 1976, "A rapid and sensitive method for the quantitation of microgram quantities of protein utilizing the principle of protein-dye binding", *Analytical Biochemistry*, vol. 72, pp. 248-254.

Brown, F.L. 2003, "Regulation of protein mobility via thermal membrane undulations", *Biophysical journal*, vol. 84, no. 2 Pt 1, pp. 842-853.

Carbone, D.L., Doorn, J.A., Kiebler, Z., Ickes, B.R. & Petersen, D.R. 2005, "Modification of heat shock protein 90 by 4-hydroxynonenal in a rat model of chronic alcoholic liver disease", *The Journal of pharmacology and experimental therapeutics*, vol. 315, no. 1, pp. 8-15.

Carbone, D.L., Doorn, J.A., Kiebler, Z. & Petersen, D.R. 2005, "Cysteine modification by lipid peroxidation products inhibits protein disulfide isomerase", *Chemical research in toxicology*, vol. 18, no. 8, pp. 1324-1331.

Code, C., Mahalka, A.K., Bry, K. & Kinnunen, P.K. 2010, "Activation of phospholipase A2 by 1-palmitoyl-2-(9'-oxo-nonanoyl)-sn-glycero-3-phosphocholine in vitro", *Biochimica et biophysica acta*, vol. 1798, no. 8, pp. 1593-1600.

D'Costa, A.M., Robinson, J.K., Maududi, T., Chaturvedi, V., Nickoloff, B.J. & Denning, M.F. 2006, "The proapoptotic tumor suppressor protein kinase C-delta is lost in human squamous cell carcinomas", *Oncogene*, vol. 25, no. 3, pp. 378-386.

Digman, M.A., Wiseman, P.W., Choi, C., Horwitz, A.R. & Gratton, E. 2009, "Stoichiometry of molecular complexes at adhesions in living cells", *Proceedings of the National Academy of Sciences of the United States of America*, vol. 106, no. 7, pp. 2170-2175.

Fauland, A., Kofeler, H., Trotzmuller, M., Knopf, A., Hartler, J., Eberl, A., Chitraju, C., Lankmayr, E. & Spener, F. 2011, "A comprehensive method for lipid profiling by liquid chromatography-ion cyclotron resonance mass spectrometry", *Journal of lipid research*, vol. 52, no. 12, pp. 2314-2322.

Fox, T.E., Houck, K.L., O'Neill, S.M., Nagarajan, M., Stover, T.C., Pomianowski, P.T., Unal, O., Yun, J.K., Naides, S.J. & Kester, M. 2007, "Ceramide recruits and activates protein kinase C zeta (PKC zeta) within structured membrane microdomains", *The Journal of biological chemistry*, vol. 282, no. 17, pp. 12450-12457.

Fruhwirth, G.O., Moumtzi, A., Loidl, A., Ingolic, E. & Hermetter, A. 2006, "The oxidized phospholipids POVPC and PGPC inhibit growth and induce apoptosis in vascular smooth muscle cells", *Biochimica et biophysica acta,* vol. 1761, no. 9, pp. 1060-1069.

Giovannini, C., Vari, R., Scazzocchio, B., Sanchez, M., Santangelo, C., Filesi, C., D'Archivio, M. & Masella, R. 2011, "OxLDL induced p53-dependent apoptosis by activating p38MAPK and PKCdelta signaling pathways in J774A.1 macrophage cells", *Journal of molecular cell biology,* vol. 3, no. 5, pp. 316-318.

Grimsrud, P.A., Xie, H., Griffin, T.J. & Bernlohr, D.A. 2008, "Oxidative stress and covalent modification of protein with bioactive aldehydes", *The Journal of biological chemistry,* vol. 283, no. 32, pp. 21837-21841.

Halasiddappa, L.M., Koefeler, H., Futerman, A.H. & Hermetter, A. 2013, "Oxidized phospholipids induce ceramide accumulation in RAW 264.7 macrophages: role of ceramide synthases", *PloS one,* vol. 8, no. 7, pp. e70002.

Halder, K., Banerjee, S., Bose, A., Majumder, S. & Majumdar, S. 2014, "Overexpressed PKCdelta downregulates the expression of PKCalpha in B16F10 melanoma: induction of apoptosis by PKCdelta via ceramide generation", *PloS one,* vol. 9, no. 3, pp. e91656.

Hamaguchi, A., Suzuki, E., Murayama, K., Fujimura, T., Hikita, T., Iwabuchi, K., Handa, K., Withers, D.A., Masters, S.C., Fu, H. & Hakomori, S. 2003, "Sphingosine-dependent protein kinase-1, directed to 14-3-3, is identified as the kinase domain of protein kinase C delta", *The Journal of biological chemistry,* vol. 278, no. 42, pp. 41557-41565.

Hermetter, A., Kopec, W. & Khandelia, H. 2013, "Conformations of double-headed, triple-tailed phospholipid oxidation lipid products in model membranes", *Biochimica et biophysica acta,* vol. 1828, no. 8, pp. 1700-1706.

Kato, K., Yamanouchi, D., Esbona, K., Kamiya, K., Zhang, F., Kent, K.C. & Liu, B. 2009, "Caspase-mediated protein kinase C-delta cleavage is necessary for apoptosis of vascular smooth muscle cells", *American journal of physiology.Heart and circulatory physiology,* vol. 297, no. 6, pp. H2253-61.

Koller, D. 2013, *Effects of Oxidized Phospholipids on Gene Expression and Sphingolipid Metabolism in RAW 264.7 macrophages*, Technical University of Graz.

Larroque-Cardoso, P., Swiader, A., Ingueneau, C., Negre-Salvayre, A., Elbaz, M., Reyland, M.E., Salvayre, R. & Vindis, C. 2013, "Role of protein kinase C delta in ER stress and apoptosis induced by oxidized LDL in human vascular smooth muscle cells", *Cell death & disease,* vol. 4, pp. e520.

Loidl, A., Sevcsik, E., Riesenhuber, G., Deigner, H.P. & Hermetter, A. 2003, "Oxidized phospholipids in minimally modified low density lipoprotein induce apoptotic signaling via activation of acid sphingomyelinase in arterial smooth muscle cells", *The Journal of biological chemistry,* vol. 278, no. 35, pp. 32921-32928.

Moumtzi, A., Trenker, M., Flicker, K., Zenzmaier, E., Saf, R. & Hermetter, A. 2007, "Import and fate of fluorescent analogs of oxidized phospholipids in vascular smooth muscle cells", *Journal of lipid research,* vol. 48, no. 3, pp. 565-582.

Pabinger, S., Thallinger, G.G., Snajder, R., Eichhorn, H., Rader, R. & Trajanoski, Z. 2009, "QPCR: Application for real-time PCR data management and analysis", *BMC bioinformatics,* vol. 10, pp. 268-2105-10-268.

Radner, F.P., Streith, I.E., Schoiswohl, G., Schweiger, M., Kumari, M., Eichmann, T.O., Rechberger, G., Koefeler, H.C., Eder, S., Schauer, S., Theussl, H.C., Preiss-Landl, K., Lass, A., Zimmermann, R., Hoefler, G., Zechner, R. & Haemmerle, G. 2010, "Growth retardation, impaired triacylglycerol catabolism, hepatic steatosis, and lethal skin barrier defect in mice lacking comparative gene identification-58 (CGI-58)", *The Journal of biological chemistry,* vol. 285, no. 10, pp. 7300-7311.

Rhode, S., Grurl, R., Brameshuber, M., Hermetter, A. & Schutz, G.J. 2009, "Plasma membrane fluidity affects transient immobilization of oxidized phospholipids in endocytotic sites for subsequent uptake", *The Journal of biological chemistry,* vol. 284, no. 4, pp. 2258-2265.

Salvayre, R., Auge, N., Benoist, H. & Negre-Salvayre, A. 2002, "Oxidized low-density lipoprotein-induced apoptosis", *Biochimica et biophysica acta,* vol. 1585, no. 2-3, pp. 213-221.

Segui, B., Bezombes, C., Uro-Coste, E., Medin, J.A., Andrieu-Abadie, N., Auge, N., Brouchet, A., Laurent, G., Salvayre, R., Jaffrezou, J.P. & Levade, T. 2000, "Stress-induced apoptosis is not mediated by endolysosomal ceramide", *FASEB journal : official publication of the Federation of American Societies for Experimental Biology,* vol. 14, no. 1, pp. 36-47.

Steinbrecher, U.P., Gomez-Munoz, A. & Duronio, V. 2004, "Acid sphingomyelinase in macrophage apoptosis", *Current opinion in lipidology,* vol. 15, no. 5, pp. 531-537.

Stemmer, U., Dunai, Z.A., Koller, D., Purstinger, G., Zenzmaier, E., Deigner, H.P., Aflaki, E., Kratky, D. & Hermetter, A. 2012, "Toxicity of oxidized phospholipids in cultured macrophages", *Lipids in health and disease,* vol. 11, pp. 110-511X-11-110.

Stemmer, U. & Hermetter, A. 2012, "Protein modification by aldehydophospholipids and its functional consequences", *Biochimica et biophysica acta,* vol. 1818, no. 10, pp. 2436-2445.

Stemmer, U., Ramprecht, C., Zenzmaier, E., Stojcic, B., Rechberger, G., Kollroser, M. & Hermetter, A. 2012, "Uptake and protein targeting of fluorescent oxidized phospholipids in cultured RAW 264.7 macrophages", *Biochimica et biophysica acta,* vol. 1821, no. 4, pp. 706-718.

Subbanagounder, G., Watson, A.D. & Berliner, J.A. 2000, "Bioactive products of phospholipid oxidation: isolation, identification, measurement and activities", *Free radical biology & medicine,* vol. 28, no. 12, pp. 1751-1761.

Sumitomo, M., Ohba, M., Asakuma, J., Asano, T., Kuroki, T., Asano, T. & Hayakawa, M. 2002, "Protein kinase Cdelta amplifies ceramide formation via mitochondrial signaling in prostate cancer cells", *The Journal of clinical investigation,* vol. 109, no. 6, pp. 827-836.

Voss, O.H., Kim, S., Wewers, M.D. & Doseff, A.I. 2005, "Regulation of monocyte apoptosis by the protein kinase Cdelta-dependent phosphorylation of caspase-3", *The Journal of biological chemistry,* vol. 280, no. 17, pp. 17371-17379.

Watson, A.D., Leitinger, N., Navab, M., Faull, K.F., Horkko, S., Witztum, J.L., Palinski, W., Schwenke, D., Salomon, R.G., Sha, W., Subbanagounder, G., Fogelman, A.M. & Berliner, J.A. 1997, "Structural identification by mass spectrometry of oxidized phospholipids in minimally oxidized low density lipoprotein that induce monocyte/endothelial interactions and evidence for their presence in vivo", *The Journal of biological chemistry,* vol. 272, no. 21, pp. 13597-13607.

Zeidan, Y.H. & Hannun, Y.A. 2007, "Activation of acid sphingomyelinase by protein kinase Cdelta-mediated phosphorylation", *The Journal of biological chemistry,* vol. 282, no. 15, pp. 11549-11561.

Chapter 3

OxPL modulate enzyme activities of chaperones and protein disulfide isomerase *in vitro* and in cultured skin cancer cells

Vogl F[a], Ramprecht C[a], Zenzmaier E[a], Schaider H[b], Hermetter A[a].

a Institute of Biochemistry, Graz University of Technology, Graz, Austria

b Dermatology Research Centre, The University of Queensland, School of Medicine, Translational Research Institute, Brisbane, Australia

3.1 Abstract

The short-chain oxidized phospholipids (oxPL) 1-palmitoyl-2-glutaroyl-*sn*-glycero-3-phosphocholine (PGPC) and 1-palmitoyl-2-(5-oxovaleroyl)-*sn*-glycero-3-phosphocholine (POVPC) are cytotoxic in melanoma and non-melanoma skin cancer cells. In these cells, oxPL efficiently induce apoptosis, which is associated, in most cases, with aSMase activity and changes in cellular ceramide levels.

It was the aim of this study to identify functions of the cellular proteins that are directly targeted by oxPL in SCC-13 cells and to elucidate their specific roles in oxPL-induced cell death. We found that a fluorescent analog of POVPC forms Schiff base adducts with proteins in these cells. This covalent adduct formation is due to the fact that POVPC contains an aldehydo group at the ω-position of the *sn*-2 acyl chain, which can covalently react with (amino) nucleophiles. Among the identified protein-lipid adducts are several proteins from the heat shock protein family (Hsps) and the protein disulfide isomerase family (PDIs). We found that PGPC and POVPC altered the enzymatic activities of Hsps and PDI *in vitro*. In line with modification and dysfunction of Hsps and PDIs, the expression levels of the ER-stress markers GADD34 and IRE-1 were upregulated in oxPL-treated cells. Finally, oxPL affect the expression of ceramide synthase 4, which is an enzyme of *de novo* ceramide synthesis, and also localizes to the ER. Ceramides are mediators of apoptotic cell death elicited by PGPC and POVPC.

In summary, our findings indicate that cytotoxic oxPL interfere with ER enzymes on the expression level, as well as on the protein level, thereby affecting protein structure and function. These ER-specific effects could be part of the molecular mechanisms by which oxPL mediate apoptotic signals in skin cancer cells.

3.2 Introduction

The oxidized phospholipids 1-palmitoyl-2-(5-oxovaleroyl)-*sn*-glycero-3-phosphocholine (POVPC) and 1-palmitoyl-2-glutaroyl-*sn*-glycero-3-phosphocholine (PGPC) are generated from (poly)unsaturated diacyl- and alk(en)ylacyl glycerophospholipids under conditions of oxidative stress. They are components of mmLDL (Berliner *et al*., 2001; Watson *et al.*, 1997) and contribute to the toxic effects of the particle in vascular cells (Subbanagounder *et al.*, 2000; Loidl *et al*., 2003) and to its role in atherogenesis.

It was shown in our laboratory, that PGPC and POVPC induce apoptosis in vascular smooth muscle cells (Fruhwirth *et al.*, 2006; Loidl *et al.*, 2003) as well as in primary and cultured macrophages (Stemmer *et al.*, 2012). Therefore, it was concluded that the oxPL-induced cell death contributes to the progression of arteriosclerosis. Recently, we found that oxPL are also toxic in cultured cancer cells. They induce apoptosis in several human melanoma cell lines as well as in squamous carcinoma cell lines. In healthy melanocytes and in HaCat keratinocytes, the toxicity of the oxPL is significantly lower compared to the cancer cell lines. In most investigated cell lines the oxPL-mediated cell death is associated with ceramide formation. Depending on the cell line, activation of sphingomyelinases (nSMase, aSMase) and/ or increased ceramide levels have been found. (Ramprecht *et al.*, PhD thesis, TU Graz, 2013) Various studies have been devoted to the role of ceramide in cancer. It has been shown that many chemotherapeutic drugs as well as gamma-irradiation induce cell death via the generation of ceramide. The proapoptotic messenger ceramide can be produced by several enzymes of sphingolipid metabolism including shingomyelinases and the enzymes of *de novo* spingolipid synthesis. Conversely, defects in sphingolipid metabolism lead to cancer therapy resistance. (Henry *et al*., 2013; Huang *et al*., 2011)

OxPL may interfere with lipids and proteins in the plasma membrane as well as with intracellular biomolecules. These interactions depend on the functional group in the *sn*-2 position of the oxPL. The truncated *sn*-2 acyl chain differs between POVPC and PGPC, resulting in different modes of action: POVPC contains an aldehyde group

which can form covalent Schiff bases with free amino groups of proteins and aminophospholipids (Stemmer *et al.*, 2012). In contrast, PGPC carries a carboxy group and therefore only physically interacts with other biomolecules. Lipid-modification might affect the structure as well as the function of the targeted biomolecules. To identify the proteins that are prone to covalent adduct formation with oxPL, we previously identified the primary protein targets of BY-POVPE, a fluorescent analog of POVPC, in cultured RAW 264.7 macrophages (Stemmer *et al.*, 2012). It was found that targeting of cellular proteins is a selective process. Only a defined subset of the total proteome was labeled. The respective polypeptides may be considered potential platforms for the toxic signaling of the oxidized phospholipids. The identified target proteins are functionally involved in cell proliferation, apoptosis, transport and stress response. In this study, we screened SCC-13 tumor cells for the primary protein targets of BY-POVPE that could contribute to oxPL-induced apoptosis and oxPL toxicity in skin cancer cells.

Protein modification by lipids affects protein structure, and as a consequence protein function. The functional impact of protein modification by lipid aldehydes (e.g. malondialdehyde and hydroxyalkenals) has been subject to investigation by several groups. Saturated aldehydes can form Schiff bases with amino groups of phospholipids and/ or proteins. Thereby they affect polarity, structure and function of their target molecules. POVPC contains an ω-aldehydo acyl residue in position *sn*-2 of glycerol and therefore possesses the capacity of modifying nucleophilic biomolecules.

Reactive lipid aldehydes and their protein adducts accumulate in cells under conditions of oxidative stress. Alkenals can undergo Michael addition with lysine, histidine and cysteine residues, resulting in either gain or loss of function of the modified enzymes. Since Lys, His, and Cys residues are frequently located in the active center of enzymes, protein modification by lipid electrophiles such as hydroxynonenals leads to inactivation of many proteins including membrane transporters as well as enzymes e.g. isocitrate dehydrogenase, thioredoxin or glutathione peroxidase. (Grimsrud *et al.*, 2008) According to recent reports, Hsp90 and protein disulfide isomerase (PDI) are also inactivated by modification with reactive aldehydes (Carbone *et al.*, 2005).

Furthermore, PDI modification with 4-HNE has been detected in HMEC-1 cells after treatment with oxLDL. These cells showed elevated levels of ER stress markers and inhibition of PDI activity, resulting in apoptotic cell death. Inhibition of PDI potentiated ER stress and apoptosis by oxLDL. (Muller *et al.*, 2013)

Molecular chaperones are stress-inducible proteins responding to heat shock, oxidative stress or infection. It has been shown that expression levels of molecular chaperones are elevated in various human tumors. In cancer cells, their high expression levels often correlate with resistance to apoptosis and chemotherapy (Calderwood *et al.*, 2006; Jolly and Morimoto, 2000). Therefore, Hsp inhibitors promise a high therapeutical potential as anti-cancer agents. Meanwhile, the inhibition of several Hsps, e.g. Hsp90, Hsp70 and Hsp27 is subject of investigation in cancer therapy. Some of these inhibitors have already been studied in clinical trials. (Jego *et al.*, 2013) In this work, we investigated the effect of oxPL on chaperone function and expression in cultured skin cancer cells.

In addition to specific chaperones belonging to the Hsp70 and Hsp90 families, PDI is another important chaperone in the ER. PDI is a thiol oxidoreductase, catalyzing the formation, breakdown and rearrangement of disulfide bonds between cysteine residues of proteins (Wilkinson and Gilbert, 2004). The formation of correct disulfide bonds is of great importance during protein synthesis and folding. In a variety of human cancer cells, increased levels of PDI have been detected. Inhibition of PDI in such cells increases the apoptotic effect of ER stress-inducing chemotherapeutic drugs. For example, the PDI inhibitor bacitracin enhances the apoptotic effect of the ER stress-inducing chemotherapeutic drugs Fenretinide and Velcade in melanoma (Lovat *et al.*, 2008). The same PDI-dependent effect could be induced by RNA interference. The apoptotic response of human melanoma cells to Fenretinide was enhanced if PDI was knocked down (Corazzari *et al.*, 2007).

The studies described above above suggest a link between ER stress and apoptosis. The ER is an important organelle for the regulation of calcium homeostasis, protein synthesis and folding. As a consequence, “ER stress” leads to the accumulation of misfolded proteins in the ER and impairment of ER function induces a stress response.

ER stress activates the so-called unfolded protein response (UPR) to restore ER homeostasis. At least three signaling proteins are involved in the UPR: IRE-1, PERK and ATF6 (Sano and Reed, 2013). If the regulatory mechanisms of UPR fail to reduce ER stress, or if the cells are subjected to constant stress levels (e.g. persistent oxidative stress), apoptotic pathways are activated. Apoptosis triggered by ER stress is induced by mitochondria-dependent and –independent cell death pathways. In this case, the apoptotic signals are generated directly in the ER membrane involving IRE-1. This membrane spanning protein functions as a sensor of misfolded proteins in the ER lumen. The presence of unfolded proteins leads to autophosphorylation of IRE-1. (Malhotra and Kaufman, 2007; Rao *et al.*, 2004; Sano and Reed, 2013) The phosphorylated, active, form of IRE-1 has an RNase activity, catalyzing the alternative splicing of XBP-1 mRNA, which results in translation of the XBP-1 protein (Uemura *et al.*, 2009). This protein is a transcription factor involved in the regulation of several genes during the UPR.

Here, we report on the impact of oxPL on the enzymatic activities of molecular chaperones and protein disulfide isomerase. In addition, we determined the effect of oxPL on the expression of ER stress markers (GADD34, IRE-1) and one of its consequences, the unconventional splicing of XBP-1, in SCC-13 cells. We found that all these components/ reactions are activated by oxPL and therefore may be considered toxic signaling components of PGPC and POVPC in skin cancer cells.

3.3 Materials and Methods

Materials

Oxidized phospholipids (PGPC and POVPC) and their fluorescent analogs (BY-PGPE and BY-POVPE) were synthesized in our laboratory as previously described (Moumtzi *et al.*, 2007). Organic solvents and all other chemicals were purchased from Carl Roth (Karlsruhe, Germany), Sigma-Aldrich (Steinheim, Germany) or Merck (Darmstadt, Germany). RPMI-1640 media with or without phenol red, fetal calf serum (FCS) and trypsin were purchased from Gibco (Carlsbad, CA). Phosphate buffered saline (PBS) and all other supplements for cell culture were from PAA Laboratories (Linz, Austria), unless otherwise indicated. Tissue culture dishes and flasks were obtained from Sarstedt (Nürmbrecht, Germany) or Greiner (Kremsmünster, Austria).

Cell culture

SCC-13 cells were provided by Dr. James G. Rheinwald (Department of Dermatology, Brigham and Women's Hospital, Harvard Medical School, Boston, Massachusetts) (Rheinwald and Beckett, 1981). SCC-13 cells were grown in RPMI-1640 medium (supplemented with 10 % FCS, 10 units/ml penicillin/streptomycin, 4 mM L-glutamine). The cells were routinely grown at 37 °C in humidified CO_2 (5 %) atmosphere. All experiments were carried out in RPMI-1640 medium without phenol red (see above) supplemented with 0,1 % FCS to minimize degradation of the oxidized phospholipids by lipases under high serum conditions (Fruhwirth *et al.*, 2006).

Incubation of cells with lipids

Aqueous lipid dispersions containing the indicated concentrations of oxPL were prepared using the ethanol injection method (Batzri and Korn, 1973). Cells were incubated with lipid dispersions in culture media without phenol red containing 0,1 % (v/v) FCS. The final ethanol concentration in the incubation mixtures did not exceed

1 % (v/v) of total volume. Culture media containing the same ethanol concentration were routinely used as controls.

Determination of protein targets of BY-POVPE in SCC-13 cells

Protocol according to the procedure described by Claudia Ramprecht (Ramprecht *et al.*, PhD thesis, TU Graz, 2013).

Labeling of cell proteins with BY-POVPE

SCC-13 cells were grown to 80 % confluency in 21 cm tissue culture dishes overnight in full growth medium. Cells were washed once with serum free media and subsequently incubated with 3,5 ml BY-POVPE dispersion (1 µM to 10 µM concentration range) in incubation medium or 3,5 ml serum free medium containing 1 % (v/v) ethanol as a negative control. Following incubation, cells were washed once with ice-cold PBS, scraped into 3 ml PBS (containing 10 mM $NaCNBH_3$ for stabilization and reduction of formed Schiff bases) and harvested by centrifugation (4 °C, 5 min, 300xg). The supernatant was discarded, cells were suspended in 1 ml ice-cold PBS containing 10 mM $NaCNBH_3$ and sonicated for 5 sec using a Bronson sonifier equipped with a 4 mm sonitip. Cell debris were removed by centrifugation (4 °C, 10 min, 1000xg). $NaCNBH_3$ was added to the supernatant (final concentration 20 mM) and the solution was incubated under stirring at room temperature for 30 min. Following the reduction of formed Schiff bases with $NaCNBH_3$, the protein concentration of the sample was determined using the method of Bradford (Bradford, 1976). For gel electrophoresis, proteins were precipitated from defined sample aliquots using acetone. For this purpose, ten volumes of ice-cold acetone were added to the aqueous samples. Samples were kept overnight at -20 °C. After centrifugation (4 °C, 30 min, 20000xg), the supernatant was removed, the pellet was dried under a stream of air, solubilized in sample buffer for gel electrophoresis and stored at -20 °C.

Separation of proteins by 1-D gel electrophoresis

SDS-PAGE was performed according to the method of Fling and Gregerson (Fling and Gregerson, 1986) in a Tris/glycine buffer system. Samples containing 100 µg protein per lane were dissolved in 50 µl loading buffer and applied onto a 20x20 cm SDS gel.

SDS gels were prepared and separated according to the PROTEAN II xi cell protocol provided by BioRad (4,5 % stacking gel, 10 % resolving gel). Gels were fixed overnight in aqueous solutions containing 7 vol.% acetic acid and 10 vol.% ethanol. BY-fluorescence was detected using a BioRad laser scanner (Ex 488 nm, Em 530/30 BP). For visualization of the total proteome, gels were stained with SYPRO Ruby™ according to the manufacturer's instructions (Molecular Probes) and scanned at 605 nm upon excitation at 488 nm.

2-D gel electrophoresis

For 2-D gel electrophoresis, samples containing 70 µg protein per gel were precipitated as described above. The protein pellet was solubilized in 135 µl rehydration buffer, containing 7 M urea, 2 M thiourea, 4 % Chaps, 0,002 % bromphenol blue and 2 % Pharmalyte™3-10, at 37 °C for 30 min. Isoelectric focusing and subsequent SDS-PAGE were performed according to the method of Görg *et al.* (Görg *et al.*, 1988). In detail, proteins were separated in the first dimension by isoelectric focusing in 7 cm immobilized nonlinear pH 3-10 gradients (Immobiline™Dry Strip Gel strips; GE Healthcare, Germany) using Multiphor II (GE Healthcare). A discontinuous voltage gradient was used starting at 0 V and increasing to 200 V within the first minute. Subsequently, the voltage was further increased to 3500 V during the following 1,5 h and held at this level for another 1,5 h. In the second dimension, proteins were separated by 10 % SDS-PAGE on 7 cm gels at 20 mA constant current. Fluorescence of formed BY-POVPE-protein complexes and SYPRO Ruby™ fluorescence representing the full proteome were visualized as described above.

Tryptic digest and LC-MS/MS analysis

Fluorescent bands containing BY-POVPE-protein complexes of 1-D and 2-D gels were cut out from the acrylamide gels and tryptically digested according to the method of Shevchenko *et al.* (Shevchenko *et al.*, 1996). Peptide extracts were dissolved in formic acid (0,1 %) and separated by a nano-HPLC-system (ULTIMATE™3000 nanoLC system, Dionex, Amsterdam, The Netherlands) as described (Birner-Gruenberger and Hermetter, 2007), except for the following gradient: solvent A:

water, 0,3 % formic acid; solvent B: acetonitrile/water 80/20 (v/v), 0,3 % formic acid; 0-5 min: 4 % B, after 40 min 55 % B, then for 5 min 90 % B, and 47 min reequilibration at 4 % B. The peptides were ionized in a Finnigan nano-ESI source equipped with Nanospray tips (PicoTip™Emitter; New Objective, Woburn, MA) and analyzed in a Thermo-Finnigan LTQ linear iontrap mass spectrometer (Thermo, San Jose, CA). MS analysis was performed by Manfred Kollroser, Medical University of Graz and by Gerhard Rechberger, University of Graz.

The MS/MS data were analyzed by searching the NCBI nonredundant public database with SpektrumMill Rev.03.03.084 (Agilent, Darmstadt, Germany) software. Acceptance parameters were two or more identified distinct peptides according to Carr *et al.* (Carr *et al.*, 2004). Identified protein sequences were subjected to identification by SwissProt database to search for protein target candidates.

In vitro chaperone activity assay

The chaperone activity assay used in this work was adapted from the high-throughput assay published by Galam *et al*. (Galam *et al.*, 2007) and the method of Thulasiraman and Matts (Thulasiraman and Matts, 1998). The basic principle of the assay is described in Figure 3.1.

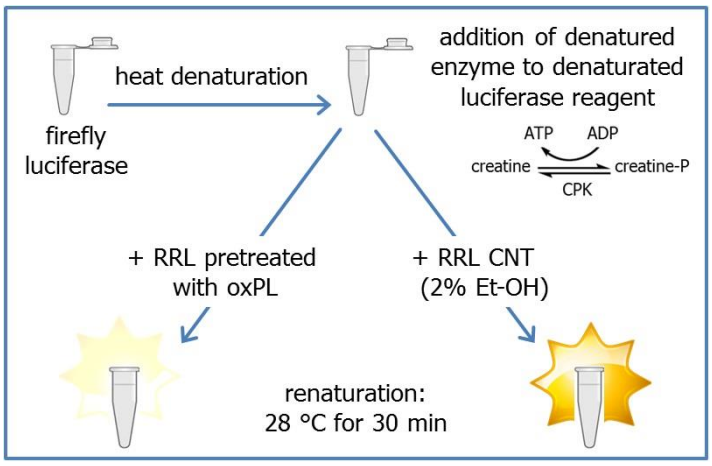

Figure 3.1 Principle of the in vitro chaperone assay.

This chaperone assay is based on the renaturation of thermally denatured firefly luciferase in rabbit reticulocyte lysate (RRL). Firefly luciferase is reversibly denaturated, resulting in a decrease of its enzymatic activity. RRL contains a plethora

of chaperones and co-chaperones and therefore provides ideal conditions for refolding of misfolded proteins. The chaperoning activity of RRL involves a cooperative action of Hsp70 and Hsp90 (Schumacher et al., 1994). Native RRL has the capacity to efficiently refold luciferase, whereas pretreatment of RRL with oxPL diminishes this effect. The renaturation capacity of RRL results in recovery of luciferase enzymatic activity and is quantified by luminescence. For the luciferase reaction, the substrate luciferin and ATP are required. Therefore the buffer contains an ATP regenerating system (creatine phosphate and creatine phosphokinase (CPK)).

A recombinant firefly luciferase, untreated rabbit reticulocyte lysate (RRL) and the Bright-Glo™ Luciferase Assay System were purchased from Promega (Promega, Mannheim, Germany). Acetylated BSA, adenosine 5'-triphosphate, creatine phosphate and creatine phosphokinase were from Sigma-Aldrich (Steinheim, Germany). The following buffer solutions were used in the assay:

Stability Buffer (SB): 25 mM Tricine-NaOH pH 7,8, 8 mM $MgS0_4$, 0,1 mM EDTA, 10 mg/ml acetylated BSA, 10 % (v/v) glycerol and 1 % (v/v) Triton X-100. SB was stored at -70 °C. Luciferase lyophilisate was dissolved in SB without Triton X-100 and Glycerol. The two latter chemicals were added after luciferase lyophilisate was completely dissolved.

Cold mix (CM): 100 mM Tris-HCl, pH 7,7, 10 mM $Mg(OAc)_2$, 375 mM KCl, 15 mM ATP and 25 mM creatine phosphate. CM was stored at -70 °C.

Denatured luciferase reagent: 1 ml contains 800 µl cold mix, 80 µl of creatine phosphokinase stock (stock concentration was 10 mg/ml in 50 % (v/v) glycerol), 108 µl deionized water and 12,5 µl of firefly luciferase stock (stock concentration was 0,5 mg/ml in SB). Before addition to the reaction mix, firefly luciferase was heat denatured at 41 °C for 10 min.

The renaturation reaction was performed at 28 °C. The assay mixture contained one volume of denatured luciferase reagent and one volume of modified RRL or untreated RRL. RRL modification was performed for 20 min at room temperature in the presence of 2 % (v/v) ethanol (CNT) or the lipids POPC, PGPC or POVPC. Lipid concentrations were 100 and 200 µM.

To exclude the possibility that the lipids directly interfere with firefly luciferase during the renaturation reaction, a pretest was performed: Firefly luciferase was treated with 100 µM PGPC or POVPC. Control samples (CNT) contained luciferase in buffer containing 2 % (v/v) ethanol. After incubation at 28 °C for 30 min, luminescence (counts/ sec) was measured.

For luminescence measurements the Bright-Glo™ Luciferase Assay System was used according to the manufacturer's recommendations. Data were expressed as percent of the ethanol control. Data are means of three independent experiments.

In vitro PDI activity assay

PDI activity was determined using the non-fluorescent dimer dieosin glutathione disulfide (Di-E-GSSG) as a substrate according to the PDI reductase activity assay published by Raturi and Mutus (Raturi and Mutus, 2007). Di-E-GSSG was a generous gift from Dr. Bulent Mutus (University of Windsor, Canada). PDI catalyzes the reduction of Di-E-GSSG to the fluorescent monomer E-GSH. PDI enzyme from bovine liver (Sigma Aldrich) was diluted into PDI assay buffer (0,1 M potassium phosphate buffer, pH 7,0, 2 mM EDTA) containing 5 µM DTT. Each reaction mixture contained 0,25 Units of PDI. Ethanolic solutions of the oxPL PGPC and POVPC or the control lipid POPC were injected into the assay mixture. Final lipid concentrations were 25, 50 and 100 µM. A solution of PDI containing ethanol served as reference for PDI activity. PDI assay buffer containing 5 µM DTT was used as negative control. Assay buffer supplemented with 10 mM DTT served as positive control for substrate cleavage. After 5 min of equilibration, the PDI-reaction was started by addition of 150 nM Di-E-GSSG. Immediately after substrate addition, the time-dependent increase in fluorescence intensity was measured using a fluorescence spectrometer from Shimadzu (λ_{Ex}=568 nm, λ_{Em}=602 nm).

PDI activity in SCC-13 cells

PDI reductase activity of SCC-13 cells was determined using the same assay as described for the *in vitro* experiments (see above). $4*10^5$ SCC-13 cells were seeded in

6-well plates a day before the experiments to obtain 80 % confluency. Cells were harvested by scraping, washed with PBS buffer and pelleted by centrifugation. The cell pellet was then diluted in PDI assay buffer containing 5 µM DTT. For each reaction, an aliquot of 100 µl containing one fourth of the cells grown in a 6-well were used. To each sample 100 µl lipid dispersions in PDI assay buffer containing 5 µM DTT were added. The final lipid concentrations were 200, 100 and 50 µM. After 15 min of incubation at room temperature, the PDI reaction was started by addition of 150 nM Di-E-GSSG. Immediately after substrate addition, the time-dependent increase in fluorescence intensity was measured using a fluorescence plate reader (POLARstar Galaxy from MTX Lab Systems, Virginia, USA). The following filter sets were used: 485-P excitation filter and 520-P emission filter. The increase of fluorescence intensity during a 15 min reaction period was determined as a measure for enzyme activity.

RT-qPCR

SCC-13 cells were incubated with lipid dispersions containing 50 µM PGPC or POVPC in RPMI-1640 medium under low serum conditions (0,1 % FBS) for 6 h to determine expression levels of ceramide synthase 4 (CerS4) and the ER stress markers IRE-1 and GADD34. Control cells were incubated with medium supplemented with 1 % (v/v) ethanol. SCC-13 cells grown in media containing 10 % FBS were used to determine the basal mRNA levels of all six CerS isoforms.

After incubation, total RNA was extracted from the cells using the RNeasy mini kit (Qiagen, Crawley, UK). One µg total RNA was used for cDNA synthesis using the GoScript™ Reverse Transcription System (Promega, Mannheim, Germany). Subsequently, expression levels of GADD34, IRE-1 and CerS1-6 were analyzed by RT-qPCR. For this purpose, RT-qPCR assays were performed in 18 µl reaction volume containing 4,5 ng cDNA, primers and SYBR green master mix (Invitrogen, Eggenstein, Germany). The RT-qPCR reaction was performed on an ABI Prism 7000 real-time PCR machine. Results were normalized against L34 expression. Data were analyzed using a real-time PCR management and analysis system [http://genome.tugraz.at/qpcr; (Pabinger *et al.*, 2009)].

Primers were designed using the NCBI Primer-BLAST web tool to span an exon-exon-junction. Primer sequences were screened using a BLAST search to confirm specificity. The PCR products were separated on an agarose gel to confirm that products of the expected size were detected.

PCR detection of alternative splicing of XBP-1

SCC-13 cells were treated with lipid dispersions containing 50 µM PGPC or POVPC in RPMI-1640 medium under low serum conditions (0,1 % FBS) for 6 h. Control cells (CNT) were incubated with media supplemented with 1 % (v/v) ethanol. After cell harvesting, RNA was isolated and reverse transcribed into cDNA (see above). Alternative spliced forms of XBP-1 were detected by PCR amplification of cDNA. The two alternative transcript variants of the XBP-1 gene differ by a 26 nt region that is missing in transcript variant 2. The used primers bind upstream (XBP-1-F 5′- GGG AAT GAA GTG AGG CCA GT -3′) and downstream (XBP-1-R 5′- CCT TCT GGG TAG ACC TCT GGG AG -3′) of the 26-nucleotides spliced sequence. This results in a 230 bp PCR product for the spliced XBP-1 mRNA and a 256 bp PCR product for the unspliced form. The following conditions were used for the PCR reaction: 94 °C for 7 min, 40 cycles at 94 °C for 15 s, 55 °C for 25 s and 68 °C for 15 s, and a final step at 68 °C for 7 min. PCR products were separated on agarose gels. A 50-bp DNA ladder (Thermo Scientific) was included on the gels as a size standard.

Statistical analysis

Data are expressed as means ± standard deviation (SD). Two-tailed unpaired Student's t-test was used to determine the significance of the differences. A p-value ≤0,05 was considered significant.

3.4 Results

It has previously been shown that the oxidized phospholipids PGPC and POVPC efficiently induce apoptosis in SCC-13 skin cancer cells, whereas a reference cell line (HaCaT) was almost unaffected (Ramprecht *et al.*, PhD thesis, TU Graz, 2013). To obtain information on the molecular mechanisms of lipid-induced cell death, the primary protein targets of the fluorescently labeled POVPC analog BY-POVPE, were identified in SCC-13 cells. To verify the influence of the oxPL on individual "target" protein function, we studied the effect of POVPC on candidate proteins. Our initial studies focused on proteins relevant to heat shock and stress response. We determined the inhibition of chaperoning activity by oxPL and measured the effect of PGPC and POVPC on the activity of isolated PDI *in vitro*. In addition, we found that PGPC and POVPC activate elements of the ER stress response and decrease the expression of a specific CerS isoform involved in the synthesis of the lipid mediator ceramide.

3.4.1 Identification of the primary protein targets of BY-POVPE in SCC-13 squamous carcinoma cells

To visualize adduct formation between cellular proteins and oxPL, we used BY-POVPE as a fluorescently labeled analog of POVPC. This aldehydo-phospholipid can undergo Schiff base formation with $-NH_2$ groups of proteins, thus forming covalent lipid-protein adducts. Schiff bases are labile and therefore, it is necessary to stabilize these adducts by reduction with $NaCNBH_3$ to form stable amines which represent the final analytes.

Specifically, SCC-13 cells were incubated with fluorescently labeled BY-POVPE, followed by chemical reduction of the formed Schiff bases, protein isolation and protein separation by 1-D or 2-D gel electrophoresis (Figure 3.2). For protein analysis on 1-D gels, the cells were incubated with various concentrations (1, 5, 10 µM) of BY-POVPE. For protein separation on 2-D gels, the cells were incubated with 10 µM BY-POVPE. Figure 3.2 shows fluorescently labeled lipid-protein adducts (panel A) and the

full proteome (panel B) stained with Sypro Ruby of the same 1-D gel. Panels D and E show lipid fluorescence and total protein stains in an 2-D gel, respectively. The number of lipid-stained bands and spots are much smaller as compared to the corresponding total proteome stains, indicating that only a limited subset of the total proteome was targeted by BY-POVPE. Moreover, the patterns of the lipid-stained proteins do not depend on BY-POVPE concentration. Thus, we conclude that protein targeting by BY-POVPE in SCC-13 cells is a rather selective than a random process. The chemically stabilized lipid-protein complexes were identified by MS/MS. For this purpose, 60 bands were excised from 1-D gels (Figure 3.2, panel C) and 60 spots were isolated from 2-D gels (Figure 3.2, panel D). The individual protein bands and spots were tryptically digested, followed by MS/MS analysis of the peptides as described in Materials and Methods. Database search (SwissProt) revealed 167 proteins isolated from 1-D gels and 106 proteins from 2-D gels. Remarkably, ten percent of the identified proteins are related to protein folding and stress response. These respective candidates comprise 15 and 11 proteins detected in the 1-D and 2-D gels, respectively. They are listed in Table 3.1. The identified polypeptides are members of the major protein families involved in the cellular heat shock response: the Hsp70 family, the Hsp90 family, the chaperone family and the chaperonin family. A complete list of the identified proteins and a detailed analysis of their functions (functional annotation clustering) can be found in the doctoral thesis of Claudia Ramprecht (Ramprecht *et al.*, PhD thesis, TU Graz, 2013).

3.4.2 Effect of PGPC and POVPC on chaperone and PDI enzyme activities

The primary protein targets of BY-POVPE include several members of the Hsp90 and Hsp70 families as well as three isoforms of protein disulfide isomerase (PDI A3, PDI A4 and PDI A6) (Table 3.1). To investigate the effect of protein modification by the aldehydo-phospholipid POVPC on the enzymatic activity of Hsps and PDI we used established enzymatic assays.

The effect of oxPL on chaperone activity was determined using an indirect assay based on renaturation of firefly luciferase in rabbit reticulocyte lysate (RRL) (Galam *et al.*,

2007). For this purpose, the renaturation of thermally denatured firefly luciferase in RRL was determined in the presence and in the absence of oxPL. Since oxPL can modify many different proteins and in particular affect protein function in the assay mixture, it is mandatory that these lipids do not influence the enzymatic activity of firefly luciferase which is just a reporter enzyme in the Hsp assay. To exclude such unwanted side effects, firefly luciferase was incubated with oxPL for 30 min at 28 °C (in the absence of RRL), followed by luminometric measurement of enzymatic activity. Under relevant assay conditions, PGPC and POVPC did not affect the enzymatic activity of firefly luciferase. Subsequently, we measured the renaturation capacity of RRL to reactivate heat-denatured firefly luciferase in RRL in the presence of PGPC, POVPC or POPC or 2 % (v/v) ethanol (control). In RRL preincubated with oxPL, the renaturation of denatured firefly luciferase was diminished in comparison to control RRL pretreated with 2 % (v/v) ethanol (CNT; 2 % (v/v) ethanol was regularly used for the preparation of lipid solutions). Pretreatment of RRL with the reference lipid POPC did not have any significant impact on its capacity to reactivate denatured luciferase compared to control RRL. 200 µM PGPC showed more efficient inhibition of firefly renaturation than 100 µM PGPC. 200 µM POVPC or POPC showed similar effects compared with 100 µM lipid. In summary, oxPL inhibit the chaperoning function of RRL, which is partly due to its content in Hsps. The common membrane phospholipid (POPC), containing two long acyl chains, leaves Hsp function unaffected.

The second enzyme of interest in this study was PDI. This enzyme catalyzes the reduction / oxidation of -S-S- / -SH groups in proteins depending on the redox state of the cells. As a consequence, PDI is essential for proper protein folding and function.
To investigate the influence of PGPC and POVPC on PDI reductase activity *in vitro* (Figure 3.4) and in SCC-13 cells (Figure 3.5), we used the fluorogenic substrate Di-E-GSSG (for details see Materials and Methods). Enzyme activity was determined from the increase in fluorescence intensity due to reductive cleavage of the disulfide bond and separation of the fluorophores. In the *in vitro* experiment, PDI reductase activity appeared to be reduced in the presence of PGPC independent of lipid concentration in

the range between 25 to 100 µM. In contrast, POVPC increased PDI reductase activity in a concentration-dependent manner. In SCC-13 cells the situation was different compared to the *in vitro* experiment. After addition of lipids to a cell suspension in assay buffer (for experimental details see Materials and Methods), PDI activity of SCC-13 cells was determined. Both oxPL PGPC and POVPC enhanced PDI activity of cells compared to ethanol treated control cells (Figure 3.5).

The control lipid POPC showed only minor effects on PDI reductase activity in both the *in vitro* and the cell experiment. To maintain PDI in its fully active reduced state, the PDI assay buffer contained 5 µM DTT. Therefore, this buffer system was used as a negative control to warrant the stability of the substrate Di-E-GSSG under the experimental conditions used. A sample containing 10 mM DTT served as a positive control, because the high DTT concentration leads to fast and quantitative reduction of the substrate. Since ethanolic solutions of oxPL were used in all experiments, the PDI reference samples for PDI activity were supplemented with 2 % (v/v) ethanol, but did not contain oxPL.

3.4.3 PGPC and POVPC activate elements of ER stress in SCC-13 cancer cells

It was previously shown by our group that fluorescently labeled analogs of oxPL partially localize to the endoplasmic reticulum of human melanoma cells (Ramprecht *et al.*, PhD thesis, TU Graz, 2013). Thus, we addressed ourselves to the question, whether oxPL might interfere with protein function in this cellular compartment and induce ER stress. Specifically, we measured the expression of ER stress markers in SCC-13 cells. For this purpose, RNA was isolated from SCC-13 cells that had been preincubated with 50 µM oxPL for 6 h. After reverse transcription, cDNA was analyzed by RT-qPCR analysis for the expression of ER stress markers. In addition, alternative splicing of XBP-1 mRNA was determined as a marker of ER stress. We found that the ER stress markers GADD34 and IRE-1 were 1,5-fold upregulated in SCC-13 cells under the influence of 50 µM PGPC or POVPC (Figure 3.6, panel B). Under the same conditions, alternative splicing of XBP-1 was also detected in oxPL-treated cells (Figure 3.6, panel A). This data is in line with work by Sanson *et al.*

showing that oxLDL, which contains PGPC and POVPC, also induced ER stress in vascular cells (Sanson *et al.*, 2009). Furthermore, it was shown in the latter study that ER stress was causally related to apoptosis. However, a relationship between apoptosis induced by oxidized phospholipids and ER-stress is still subject to proof.

The ER is the site of *de novo* ceramide synthesis. Important enzymes of this pathway are ceramide synthases that utilize sphinganine (from the *de novo* pathway) or sphingosine (from the sphingolipid recycling pathway) for the formation of dihydroceramide and ceramide, respectively (Levy and Futerman, 2010). It has already been shown that PGPC and POVPC enhance the synthesis of C16-, C22-, and C24:0-Cer species and activate CerS2 on the transcriptome and activity level in RAW 264.7 macrophages (Halasiddappa *et al.*, 2013). In SCC-13 cells, oxPL also influence CerS expression, but in a totally different manner. From mRNA expression profiles of the six CerS isoforms in SCC-13 cells, it can be inferred that CerS2 is the predominant isoform in these cells, too. In contrast, the expression of CerS3, CerS4, CerS5 and CerS6 is much lower. CerS1 mRNA level was below the detection limit (Figure 3.7, panel A). PGPC and POVPC treatment led to a 50 % reduction of CerS4 mRNA expression in SCC-13 cells (Figure 3.7, panel B). CerS4 preferentially catalyzes the formation of ceramides containing C18-C20 N-acyl chains (Levy and Futerman, 2010). To date CerS4 is a poorly studied isoform with low expression levels in many tissues. Thus, further experiments are needed to understand the consequences of this downregulation. This information could be very helpful, since ceramide synthases are important targets of chemotherapeutic drugs. They catalyze the formation of ceramides that are mediators of apoptotic cell death.

3.5 Discussion

It has previously been shown that the oxidized phospholipids PGPC and POVPC efficiently induce apoptosis in SCC-13 skin cancer cells. The oxPL-induced cell death in SCC-13 cells is associated with activation of acid sphingomyelinase and the formation of the second messenger ceramide. (Ramprecht *et al.*, PhD thesis, TU Graz, 2013) In the present study, we identified the primary protein targets of oxPL in SCC-13 cells to reveal the components that are likely to be involved in oxPL-induced apoptotic signaling. In addition, we performed functional studies on selected protein target candidates to further clarify their specific roles in oxPL-induced cell death.

The identified target proteins form covalent Schiff bases with the fluorescently labeled oxPL BY-POVPE. A comparison to earlier findings in RAW 264.7 macrophages (Stemmer *et al.*, 2012) confirms that covalent protein modification by BY-POVPE is a selective process in both cell types, affecting only a defined subset of the cellular proteome (Figure 3.2). Similar results were obtained using biotin-tagged probes for lipid target identification in endothelial cells (Gugiu *et al.*, 2008). The number of protein targets identified in SCC-13 cells is much higher compared to the earlier results obtained with vascular cells. The target proteins found in SCC-13 cells are involved in different cellular processes. In this work, we mainly focused on the proteins functionally related to heat shock response and oxidative stress response (Table 3.1), since these protein families are involved to a large extent in oncogenesis and resistance to chemotherapy.

Physiological pH conditions are favorable for Schiff base formation of aldehydo-phospholipids with $-NH_2$ groups of lysines, since at this pH a small but sufficient fraction of this amino acid is deprotonated. The reaction of lysines with lipid aldehydes on the LDL surface and its physiological consequences have been extensively studied with respect to apoB modification (Gillotte *et al.*, 2000) and modification of cellular proteins (Zarkovic *et al.*, 2013). Most of these studies have been devoted to protein modification by hydroxynonenal (HNE) and malondialdehyde (MDA).

Our study is the first one reporting on protein modification by phospholipid aldehydes in cancer cells. The results are remarkable insofar as many of the identified oxPL targets are also subject to modification by other electrophiles e.g. with carbonyls of acyl residues. In a global proteomic study, Kim *et al.* (2006) identified the polypeptides that are acetylated at lysine residues. Interestingly, there is a huge overlap between the identified proteins in the latter study and the protein targets of BY-POVPE in RAW 264.7 macrophages, on the one hand, and in SCC-13 cells, on the other hand. Therefore, we speculate that the hydrophilic lysine residues that are available for acetylation are prone to modification by phospholipid aldehydes, too. Lysine acetylation of cellular proteins regulates their function in several cellular processes including stress response. For example, acetylation and deacetylation of lysine residues regulate Hsp90 activity (Kovacs *et al.*, 2005). In agreement with the above hypothesis, Hsp90 is also modified by BY-POVPE.

To elucidate the effect of oxPL on molecular chaperoning activity, we performed gain and loss of function experiments with molecular chaperones and with PDI. It has already been shown that Hsp90 and PDI are inactivated by modification with reactive aldehydes (Carbone *et al*., 2005). In this work, POVPC was used as a lipid aldehyde. In the chaperone activity assay PGPC and POVPC reduced the renaturation capacity of RRL (Figure 3.3). RRL contains a mixture of various chaperones and cochaperones, but for its chaperoning activity a cooperative action of Hsp70 and Hsp90 is substantial (Schumacher *et al.*, 1994). Therefore, it could be possible that the inhibitory effect of the oxPL on the chaperoning activity of RRL is due to inhibition of the two major families involved, namely Hsp90 and Hsp70. These chaperone families are particularly important in tumorigenesis and cancer therapy, because they are invaluable for cell survival (see below). To find out, which chaperones are predominantly affected by oxPL inhibition, further experiments with defined chaperone – cochaperone pairs are required.

In contrast to chaperoning activities, the disulfide reductase activity of PDI was significantly enhanced by POVPC (< 2-fold), whereas treatment of PDI with PGPC led to a 50 % reduction in activity *in vitro* (Figure 3.4). In SCC-13 cells both PGPC

and POVPC led to an increase in PDI activity (Figure 3.5). This data is at variance with the results obtained with isolated PDI *in vitro*. We have currently no explanation for this effect. Further experiments will be needed to find out what components are involved in the cellular effects of oxPL. In addition, it has to be clarified how and to what extent PDI activity is modulated by lower oxPL concentrations than 50 µM. Finally, we do not know the stoichiometry of PDI modification, nor the sites of amino acid modification. Such information has already been provided for Hsp72 modification by 4-HNE (Carbone *et al*., 2004). From the latter study it could be inferred that 4-HNE modified Hsp72 at Cys267 in the ATPase domain of the chaperone and as consequence inhibited protein function. The binding sites of PDI and Hsps for oxPL still await identification.

Since PDI is invaluable for proper protein folding and activity, we speculate that an inhibitory effect of oxPL on PDI function may contribute to apoptosis, whereas a stimulatory effect would rather be protective. It has been shown that oxLDL inhibits PDI reductase activity in HMEC-1 cells (Muller *et al.*, 2013). It appears that the single compounds PGPC and POVPC differentially influence PDI activity *in vitro* compared to oxLDL that contains a plethora of lipid oxidation products.

In addition to posttranslational modification, chaperone activities can be modulated by alterations in their expression levels. We found that cellular oxPL stress leads to upregulation of several chaperones in the ER (see unfolded protein response) on the transcriptional level in SCC-13 cells. In addition, we studied the expression of CerS. These enzymes catalyze the formation of ceramides in the ER, which contribute to membrane stress in these organelles.

We found that PGPC and POVPC enhance the transcription of IRE-1 and GADD34. In addition, they induce unconventional splicing of XBP-1 mRNA (Figure 3.6). This data is in line with the observation that the activation of IRE-1 during the unfolded protein response results in alternative splicing of XBP-1 (Uemura *et al.*, 2009). We conclude that oxPL-induced apoptosis in SCC-13 cells is linked to ER stress and to the unfolded protein response. Since similar effects have already been reported for oxLDL, it is tempting to say that truncated oxPL contribute to the ER activity of the oxidized

lipoproteins. In pancreatic cancer, the alkyl-lysophospholipid analog Edelfosine also induces apoptosis via induction of ER stress (Gajate *et al.*, 2012). Edelfosine is structurally similar to PGPC and POVPC. Both lipids are highly amphipathic molecules and contain only one long hydrophobic hydrocarbon chain bound to the *sn*-1 position of the glycerol backbone. Thus, it can be speculated that both compounds induce similar (membrane) effects that may contribute to their cytotoxicity.

Chaperone activities are modulated by protein levels and posttranslational modifications, on the one hand, and by transcriptional regulation, on the other hand. In several classes of tumors, alterations of Hsp expression have been found. In breast tumors, lung cancer, leukemias and Hodgkin's disease, elevated levels of Hsp90a, Hsp90b and Hsp60 have been documented. Hsp70 overexpression in breast tumors is associated with poor prognosis and high metastatic potential. This can be explained by the fact that Hsp70 is an antiapoptiotic protein that reduces caspase activation. (Schmitt *et al.*, 2007; Moenner *et al.*, 2007; Calderwood *et al.*, 2006; Jolly and Morimoto, 2000)

Thus, Hsps have become interesting targets in the development of new anti-cancer drugs. There are numerous attempts to sentisize cancer cells towards chemotherapy by inhibiting molecular chaperones with specific inhibitors. For example, inhibitors of Hsp90 have already been tested in clinical trials for anticancer activity. Different molecular mechanisms of inhibitor toxicity have been reported - e.g. by inhibition of ATP binding to the nucleotide-binding pocket of Hsp90. (Sidera and Patsavoudi, 2014)

The cellular upregulation of ER-proteins under stress conditions seems to be a delicate balance between restoration of ER function, on the one hand, and induction of apoptosis, on the other hand. Some cancer cells make use of UPR-induced survival mechanisms by upregulation of certain chaperones to promote cell survival and to gain a growth advantage. In this study, we demonstrate that oxPL interfere with chaperones on a functional and transcriptional level: They alter the function of Hsps and PDI on the protein level and induce upregulation of the ER stress markers IRE-1 and GADD34. From these results, it can be inferred that the oxPL may induce a shift in the

cellular signaling pathways towards apoptotic signaling not only in vascular cells but also in skin cancer cells.

PGPC and POVPC decrease the mRNA expression levels of ceramide synthase 4 (CerS4) which belongs to the family of ceramide synthases. These enzymes catalyze the N-acylation step at ceramide synthesis and localize to the ER. In untreated SCC-13 cells, the expression pattern of all six CerS isoforms was very similar to the expression pattern previously identified in RAW 264.7 macrophages with CerS2 being the predominant isoform (Halasiddappa *et al.*, 2013). The relative expression levels of CerS3, CerS4, CerS5 and CerS6 were much lower. CerS1 mRNA levels were below the detection limit. Exposure to oxPL led to a 50 % decrease in CerS4 expression in SCC-13 cells. CerS4 is expressed at high levels in the skin, leucocytes, heart and liver. It catalyzes the formation of ceramide derivatives containing C18-22 fatty acids (Levy and Futerman, 2010). Unlike other CerS isoforms, CerS4 does not affect the sensitivity of cancer cells to established chemotherapeutic drugs (Min *et al.*, 2007). Thus, we must leave it open, whether or to what extent, downregulation of this enzyme by oxPL contributes to lipid toxicity in SCC-13 cells. Our studies have only been performed on the transcriptome level so far. Thus, further studies will be required to investigate whether or to what extent oxPL modify the enzymatic activity of CerS4 and the other isoforms. Modulation of ceramide formation is a hallmark of oxPL activity in cultured vascular and some cancer cells. In SCC-13 cells, the situation is less clear. PGPC activates acid sphingomyelinase, but does not increase ceramide formation. POVPC shows the opposite effects (Ramprecht *et al.*, PhD thesis, TU Graz, 2013). However, it is unclear at present which enzymes/ pathways are responsible for the formation of apoptotic ceramides. Such information would be very useful since several chemotherapeutic drugs induce cell death via the generation of ceramide (Henry *et al.*, 2013; Huang *et al.*, 2011).

Ceramide formation, induction of ER stress and modulation of chaperone activity may not be the only mechanisms by which oxPL mediate their apoptotic effect in SCC-13 cells. The toxicity of oxPL seems to be mediated by interacting with several cellular components. First of all, the effective cellular uptake of oxPL in the plasma membrane

is a prerequisite of their toxicities. It is accompanied by an increase in membrane fluidity (Rhode *et al*., 2009). OxPL easily insert in cell surfaces and accumulate in clusters, thereby perturbing membrane organization. Van Blitterswijk showed that biophysical disturbance of cell membranes is the basis for understanding the apoptotic effect of alkylphospholipids on cells (van Blitterswijk and Verheij, 2013). In various skin cancer cell lines, the oxPL elicit their toxic effects by ceramide generation via activation of aSMase (Ramprecht *et al.*, PhD thesis, TU Graz, 2013). The apoptotic messenger ceramide subsequently leads to activation of MAPK and finally, to the activation of the effector caspases caspase-3 and 7 (Loidl *et al.*, 2003). In macrophages, it was additionally shown that PGPC triggers the upregulation of many genes (Koller *et al.*, PhD thesis, TU Graz, 2013). These observations are in line with results obtained with living HaCat cells under the influence of alkylphospholipids. These compounds also showed strong effects on the gene expression profiles (Semini *et al.*, 2011).

OxPL share similar structural features with alkyl-lysophospholipids including a long hydrophobic hydrocarbon chain and a large head group. As a consequence, they show a high degree of amphiphilicity. Thus, it seems to be likely that both phospholipid classes may induce similar membrane effects to activate their toxic signaling. In contrast to the targeted therapy approaches of many anti-cancer drugs, oxPL-induced cell death is not dependent on specific target molecules. Immediately after uptake into the cell plasma membrane, they induce supramolecular / membrane effects in cells. Stress associated pathways are leading to (apoptotic) cell death. The participation of these latter pathways in oxPL signaling in cancer cells is still subject to proof.

Synthetic alkyl-lysophospholipids also function as membrane-targeted anticancer agents that activate stress pathways (e.g. JNK) in cancer cells. They show promising preclinical and clinical results as chemotherapeutics. However, they also produce unwanted effects in cancer cells. Despite their multitargeted and relatively unspecific mode of action, resistance of cancer cells to alkyl-lysophospholipids has been reported. (van Blitterswijk and Verheij, 2013) In this context, it has to be noted that the metabolic stability of O-alkyl lysophospholipids is higher compared to their 1-O-acyl

oxPL counterparts because they cannot be hydrolytically degraded. As a consequence, the cells could get rid of the oxPL more easily by simple enzymatic hydrolysis without the need of oxidative cleavage or expressing multiple drug resistance proteins. Of course, this hypothesis needs to be verified and must be subject to further investigation.

3.6 Tables

Table 3.1 Heat shock proteins and protein disulfide isomerases are primary protein targets of BY-POVPE in SCC-13 cells.

Cells were incubated with BY-POVPE (10 µM) in serum free medium for 30 min followed by protein isolation and 1-D or 2-D gel electrophoresis of the labeled proteins (see Figure 3.2). Fluorescent protein bands (1-D gels) and spots (2-D gels) were excised and tryptically digested. Subsequently, peptides were analyzed by MS/MS and targets were identified by database search (SwissProt). Here all proteins relevant to heat shock response and oxidative stress from 1-D- and 2-D gels are listed. They are categorized by chaperone families. Abbreviations used for subcellular localizations: cyt (cytoplasmic), mt (mitochondrial), nuc (nuclear), ER (endoplasmic reticulum). Blue lettering indicates protein targets identified in 1-D- as well as in 2-D gels. Black lettering indicates that the target was either found in 1-D- or in 2-D gel.

Family	Short Name		Full Name	Database ID	Gene Name
Hsp70	HSC70 (Hsp73)	cyt, nuc	Heat shock cognate 71 kDa protein (Heat shock 70 kDa protein 8)	P11142	HSPA8, HSC70, HSP73, HSPA10
	BiP / Grp78	ER, cyt	78 kDa glucose-regulated protein (BiP)	P11021	HSPA5, GRP78
Hsp90	Cdc37	cyt	Hsp90 co-chaperone Cdc37 (p50Cdc37)	Q16543	CDC37, CDC37A
	Hsp90a	cyt	Heat shock protein Hsp 90-alpha (Hsp86)	P07900	HSP90AA1, HSP90A, HSPC1, HSPCA
	Hsp90b	ER	Heat shock protein 90 kDa beta member 1 (Endoplasmin, GRP-94)	P14625	HSP90B1, GRP94, TRA1
Chaperonins	TCP-1-delta	cyt	T-complex protein 1 subunit delta (CCT-delta)	P50991	CCT4, CCTD, SRB
	Hsp60	mt	60 kDa heat shock protein, mitochondrial (Chaperonin 60 (CPN60))	P10809	HSP60, HSPD1
Chaperones	PDI A3	ER	Protein disulfide-isomerase A3 (ERp57, ERp60, p58)	P30101	PDIA3, ERP57, ERP60, GRP58
	PDI A6	ER	Protein disulfide-isomerase A6 (ERp5, Thioredoxin domain-containing protein)	Q15084	PDIA6
	PDI A4	ER	Protein disulfide-isomerase A4 (ERp70, ERp72)	P13667	PDIA4, ERP70, ERP72
	Calreticulin	ER, cyt	Calreticulin (CRP55, CRP55, ERp60, grp60)	P27797	CALR, CRTC
	ERp46	ER	Thioredoxin domain-containing protein 5 (ERp46)	Q8NBS9	TXNDC5, TLP46
	ERp29	ER	Endoplasmic reticulum resident protein 29 (ERp28, ERp31)	P30040	ERP29, C12orf8, ERP28
Oxidative stress related		mt	Superoxide dismutase [Mn], mitochondrial	P04179	SOD2

3.7 Figures

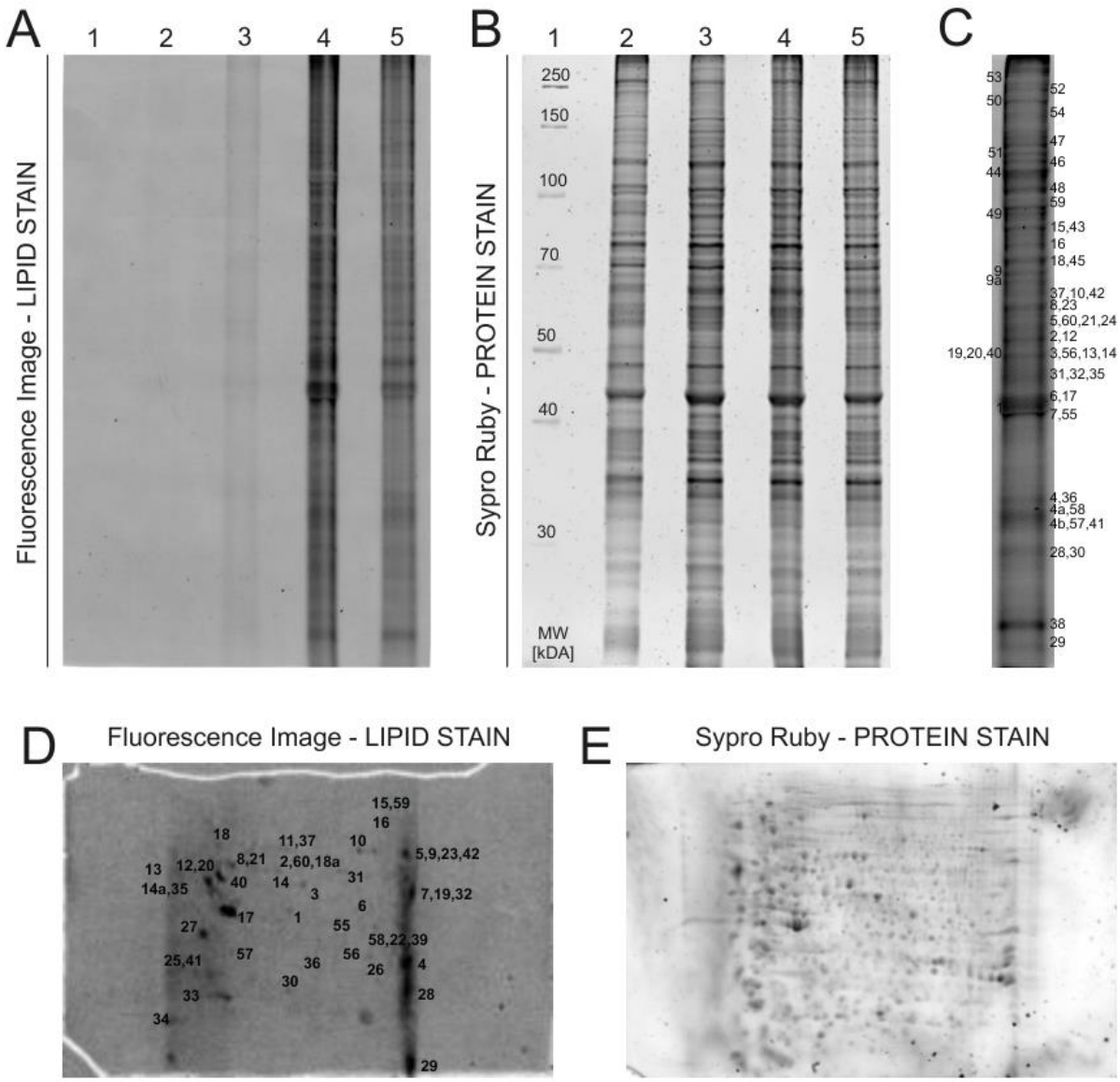

Figure 3.2 Protein targets of fluorescent BY-POVPE in SCC-13 cells.

Panels A and B: *Cells were incubated with different concentrations of fluorescent BY-POVPE for 30 minutes. The formed Schiff bases were stabilized by reduction with $NaCNBH_3$. After lysis of the cells, proteins were precipitated with acetone. 100 µg sample protein per lane were separated by 1-D gel electrophoresis as described in Materials and Methods. Fluorescent protein bands were imaged using a fluorescence laser scanner (BioRad). The lipid stain (A) represents proteins that are covalently*

bound to BY-POVPE. The Sypro Ruby protein stain (B) represents the "full proteome" of the same gel. 1: protein standard; 2: negative control (incubation with 1 % (v/v) ethanol in incubation medium for 30 min); 3-5: incubation of cells with 1 µM / 10 µM / 5 µM BY-POVPE for 30 min respectively. The staining of the proteins by BY-POVPE is a selective process. The absolute amount of BY-POVPE does not influence the selectivity of the lipid-protein interaction thus leading to the same fluorescence patterns irrespective of lipid concentration.

Panel C: *BY-labeled protein bands identified by MS/MS analysis. The labeled bands were excised, proteins were tryptically digested and identified by MS/MS analysis. The data are summarized in the doctoral thesis of Claudia Ramprecht (Ramprecht et al., PhD thesis, TU Graz, 2013).* ***Panels D and E:*** *Two-dimensional gel electrophoresis of fluorescent lipid-protein adducts after incubation of cells with 10 µM BY-POVPE (D) and total protein stain of the same gel with Sypro ruby (E). Spots were excised and proteins were tryptically digested and identified by MS/MS analysis. The results are summarized in the doctoral thesis of Claudia Ramprecht (Ramprecht et al., PhD thesis, TU Graz, 2013).*

This figure was taken from the doctoral thesis of Claudia Ramprecht (Ramprecht et al., PhD thesis, TU Graz, 2013).

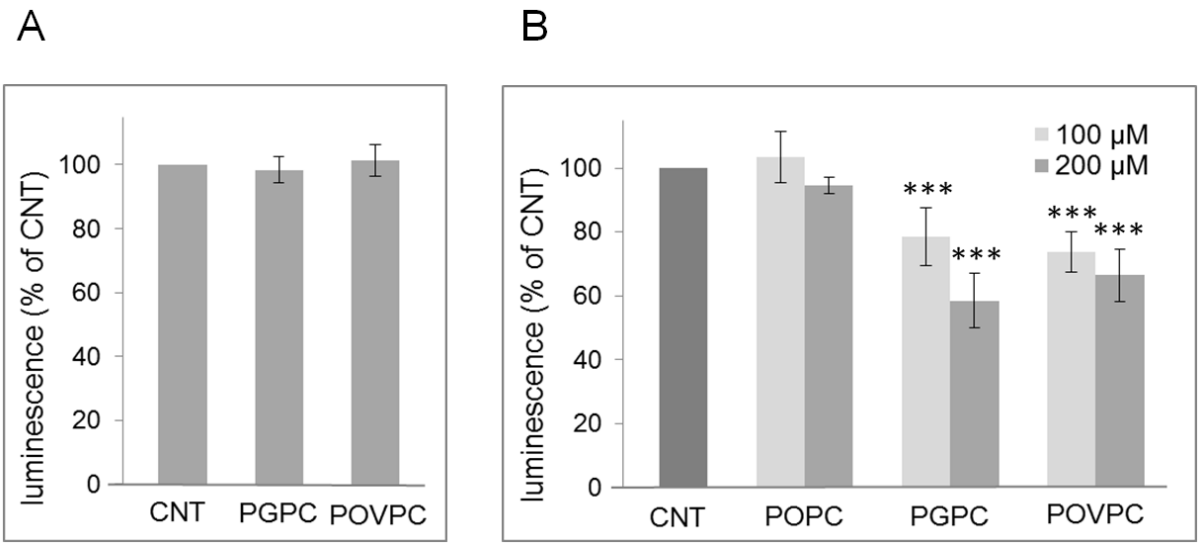

Figure 3.3 Effect of PGPC and POVPC on luciferase activity and renaturation in rabbit reticulocyte lysate.

Panel A: *Effect of PGPC or POVPC on enzymatic activity of luciferase. Firefly luciferase was incubated with 100 µM PGPC or POVPC. The control sample (CNT) contained luciferase in buffer containing 2 % (v/v) ethanol. After incubation at 28 °C for 30 min, luminescence was measured. Data are expressed as percent of the ethanol control. For experimental details, see Materials and Methods. Data are shown as means ± SD (n ≥ 3).* ***Panel B:*** *Effect of PGPC and POVPC on renaturation of firefly luciferase in rabbit reticulocyte lysate. RRL was incubated with 2 % (v/v) ethanol (CNT) or with phospholipids (POPC, PGPC or POVPC) as described in Materials and Methods. Each lipid was applied at two concentrations (100 and 200 µM). Heat-denatured firefly luciferase was added to the lipid-treated and the control RRL (CNT). Luciferase renaturation was performed at 28 °C for 30 min and was followed by luminescence measurement. Values are presented as percent of the ethanol control (CNT). Data are expressed as means ± SD (n ≥ 4). Significances were determined by Student's t-test (two tailed, unpaired).* *** *P ≤ 0,001, compared with control.*

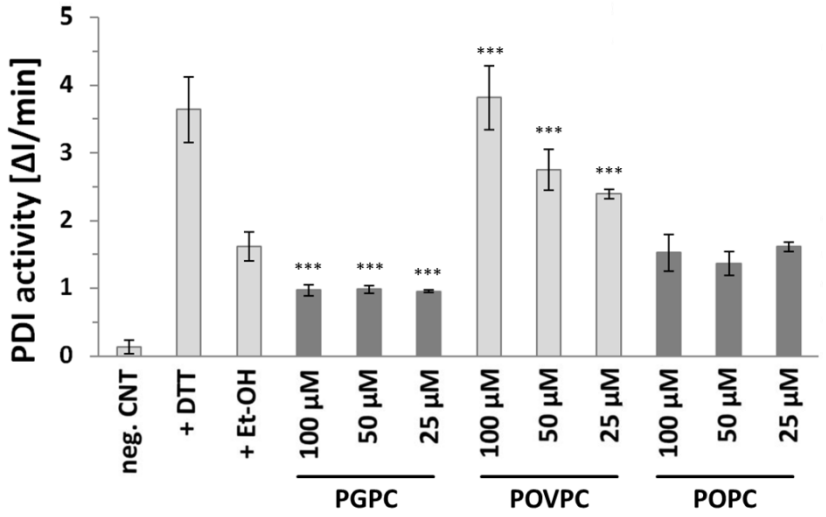

Figure 3.4 Influence of PGPC and POVPC on enzymatic activity of protein disulfide isomerase in vitro.

*PDI reductase activity was determined in vitro using the non-fluorescent dimer dieosin glutathione disulfide (Di-E-GSSG) as a substrate. PDI catalyzes the reduction of Di-E-GSSG to the fluorescent monomer E-GSH. PDI enzyme was diluted into PDI assay buffer (see Materials and Methods) containing 5 µM DTT. Ethanolic solutions of the oxPL PGPC and POVPC or the control lipid POPC were injected into the assay mixture. The final lipid concentrations were 25, 50 and 100 µM. PDI in the presence of the solvent ethanol served as a reference for PDI activity (+Et-OH). PDI assay buffer containing 5 µM DTT was used as negative control (low DTT concentration keeps the enzyme in the reduced state; neg. CNT). Assay buffer supplemented with 10 mM DTT served as positive control for substrate cleavage (fast reduction of the substrate; "PDI activity"+DTT). After 5 min of equilibration, the PDI-reaction was started by addition of 150 nM Di-E-GSSG. Immediately after substrate addition, the time-dependent increase in fluorescence intensity was measured using a fluorescence spectrometer (λ_{Ex}=568 nm, λ_{Em}=602 nm). For a detailed description, see Materials and Methods. Data are expressed as means ± SD (n ≥ 3). Significances were determined by Student's t-test (two tailed, unpaired). *** P ≤ 0,001, compared with ethanol control.*

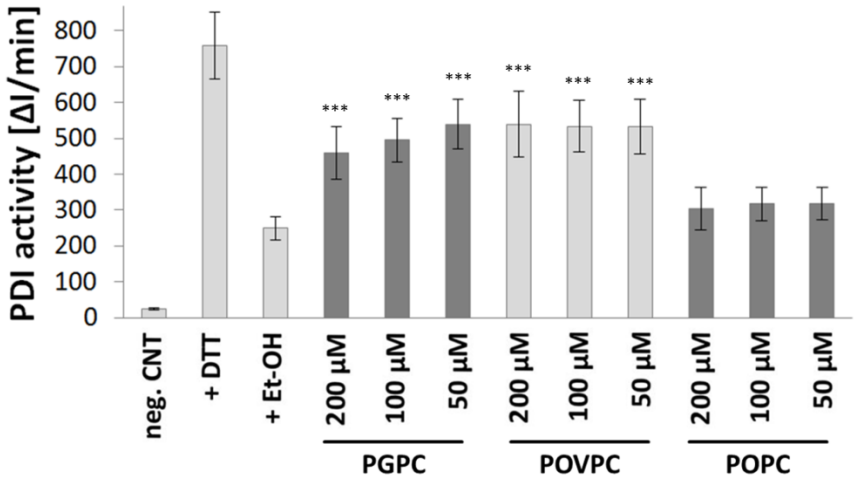

Figure 3.5 Influence of PGPC and POVPC on the enzymatic activity of protein disulfide isomerase in SCC-13 cells.

*SCC-13 cells were cultured as described under Materials and Methods. The cells were harvested and suspended in PDI assay buffer. The cell suspensions were then incubated with PGPC, POVPC or POPC for 15 min after injection of ethanolic phospholipid solutions. Cell suspensions treated with ethanol alone served as a reference for basal PDI activity in SCC13 cells (+Et-OH). The enzymatic reaction was started by addition of 150 nM Di-E-GSSG. Enzyme activity was determined from time-dependent increase in fluorescence intensity (ΔI/min). PDI assay buffer containing only 5 µM DTT was used as negative control (low DTT concentration keeps the enzyme in the reduced state; neg. CNT). Assay buffer supplemented with 10 mM DTT served as positive control for substrate cleavage (fast reduction of the substrate; "PDI activity"+DTT). Data are expressed as means ± SD (n ≥ 3). Significances were determined by Student's t-test (two tailed, unpaired). *** P ≤ 0,001, compared with ethanol control.*

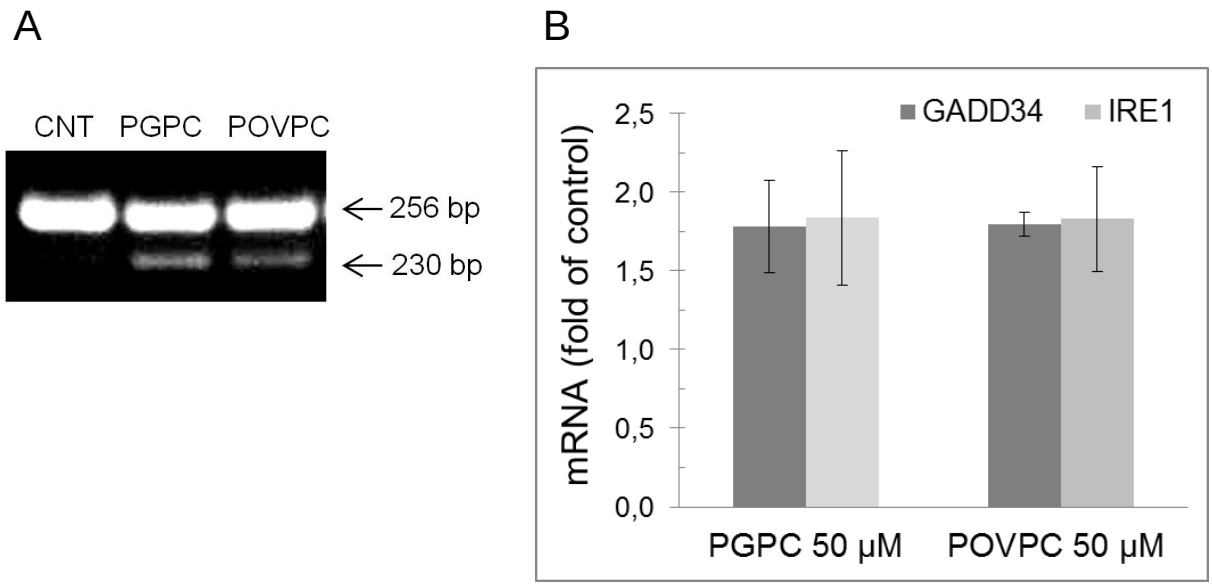

Figure 3.6 PGPC and POVPC induce alternative splicing of XBP-1 mRNA and expression of the ER stress response genes GADD34 and IRE-1 in SCC-13 cells.

SCC-13 cells were incubated with dispersions of 50 µM PGPC or POVPC in RPMI-1640 medium under low serum conditions (0,1 % FBS) for 6 h. Control cells (CNT) were incubated with media supplemented with 1 % (v/v) ethanol. After cell harvesting, RNA was isolated and reverse transcribed into cDNA. The resultant cDNA was analyzed by RT-qPCR for GADD34- and IRE-1-expression. Alternative spliced forms of XBP-1 were detected by conventional PCR. XBP-1 is a transcription factor involved in the unfolded protein response. Its expression is regulated by unconventional mRNA splicing. The endonuclease IRE-1 - together with a yet unknown RNA ligase - is involved in this process (Uemura et al., 2009).

Panel A: *XBP-1 mRNA splicing was analyzed using PCR. For details see Materials and Methods. The 256 bp and 230 bp bands correspond to the intact and the spliced products.* ***Panel B:*** *mRNA levels of the ER stress markers GADD34 and IRE-1 are shown as fold expression of control cells. Data are expressed as means ± SD ($n \geq 3$).*

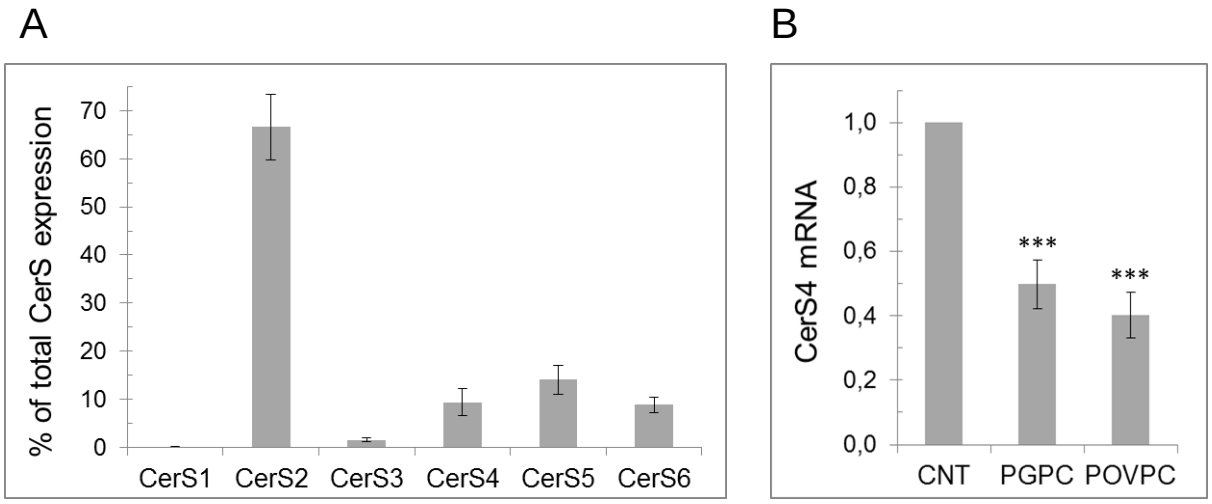

Figure 3.7 Expression profiles of ceramide synthase isoforms in SCC-13 cells. Effect of oxPL on ceramide synthase 4 expression.

Panel A: *SCC-13 cells grown in RPMI-1640 media (10 % FBS) were harvested and cDNA was synthesized. mRNA levels of all CerS isoforms were determined by RT-qPCR as described under Materials and Methods.* ***Panel B:*** *SCC-13 cells were incubated with 50 µM PGPC, 50 µM POVPC or 1 % (v/v) ethanol (CNT) in RPMI-1640 under low serum conditions (0,1 % FBS) for 6 h. RNA was isolated, reverse transcribed and CerS4 expression was determined by RT-qPCR. In the oxPL-treated cells, CerS4 mRNA levels were reduced. Data are expressed as means ± SD (n = 3). Significances were determined by Student's t-test (two tailed, unpaired). *** $P \leq 0{,}001$, compared with control.*

3.8 References Chapter 3

Batzri, S. & Korn, E.D. 1973, "Single bilayer liposomes prepared without sonication", *Biochimica et biophysica acta,* vol. 298, no. 4, pp. 1015-1019.

Berliner, J.A., Subbanagounder, G., Leitinger, N., Watson, A.D. & Vora, D. 2001, "Evidence for a role of phospholipid oxidation products in atherogenesis", *Trends in cardiovascular medicine,* vol. 11, no. 3-4, pp. 142-147.

Birner-Gruenberger, R. & Hermetter, A. 2007, "Activity-based proteomics of lipolytic enzymes", *Current drug discovery technologies,* vol. 4, no. 1, pp. 1-11.

Bradford, M.M. 1976, "A rapid and sensitive method for the quantitation of microgram quantities of protein utilizing the principle of protein-dye binding", *Analytical Biochemistry,* vol. 72, pp. 248-254.

Calderwood, S.K., Khaleque, M.A., Sawyer, D.B. & Ciocca, D.R. 2006, "Heat shock proteins in cancer: chaperones of tumorigenesis", *Trends in biochemical sciences,* vol. 31, no. 3, pp. 164-172.

Carbone, D.L., Doorn, J.A., Kiebler, Z., Ickes, B.R. & Petersen, D.R. 2005, "Modification of heat shock protein 90 by 4-hydroxynonenal in a rat model of chronic alcoholic liver disease", *The Journal of pharmacology and experimental therapeutics,* vol. 315, no. 1, pp. 8-15.

Carbone, D.L., Doorn, J.A., Kiebler, Z. & Petersen, D.R. 2005, "Cysteine modification by lipid peroxidation products inhibits protein disulfide isomerase", *Chemical research in toxicology,* vol. 18, no. 8, pp. 1324-1331.

Carbone, D.L., Doorn, J.A., Kiebler, Z., Sampey, B.P. & Petersen, D.R. 2004, "Inhibition of Hsp72-mediated protein refolding by 4-hydroxy-2-nonenal", *Chemical research in toxicology,* vol. 17, no. 11, pp. 1459-1467.

Carr, S., Aebersold, R., Baldwin, M., Burlingame, A., Clauser, K., Nesvizhskii, A. & Working Group on Publication Guidelines for Peptide and Protein Identification Data 2004, "The need for guidelines in publication of peptide and protein identification data: Working Group on Publication Guidelines for Peptide and Protein Identification Data", *Molecular & cellular proteomics : MCP,* vol. 3, no. 6, pp. 531-533.

Corazzari, M., Lovat, P.E., Armstrong, J.L., Fimia, G.M., Hill, D.S., Birch-Machin, M., Redfern, C.P. & Piacentini, M. 2007, "Targeting homeostatic mechanisms of endoplasmic reticulum stress to increase susceptibility of cancer cells to fenretinide-induced apoptosis: the role of stress proteins ERdj5 and ERp57", *British journal of cancer,* vol. 96, no. 7, pp. 1062-1071.

Fling, S.P. & Gregerson, D.S. 1986, "Peptide and protein molecular weight determination by electrophoresis using a high-molarity tris buffer system without urea", *Analytical Biochemistry,* vol. 155, no. 1, pp. 83-88.

Fruhwirth, G.O., Moumtzi, A., Loidl, A., Ingolic, E. & Hermetter, A. 2006, "The oxidized phospholipids POVPC and PGPC inhibit growth and induce apoptosis in vascular smooth muscle cells", *Biochimica et biophysica acta,* vol. 1761, no. 9, pp. 1060-1069.

Gajate, C., Matos-da-Silva, M., Dakir, e., Fonteriz, R.I., Alvarez, J. & Mollinedo, F. 2012, "Antitumor alkyl-lysophospholipid analog edelfosine induces apoptosis in pancreatic cancer by targeting endoplasmic reticulum", *Oncogene,* vol. 31, no. 21, pp. 2627-2639.

Galam, L., Hadden, M.K., Ma, Z., Ye, Q.Z., Yun, B.G., Blagg, B.S. & Matts, R.L. 2007, "High-throughput assay for the identification of Hsp90 inhibitors based on Hsp90-dependent refolding of firefly luciferase", *Bioorganic & medicinal chemistry,* vol. 15, no. 5, pp. 1939-1946.

Gillotte, K.L., Horkko, S., Witztum, J.L. & Steinberg, D. 2000, "Oxidized phospholipids, linked to apolipoprotein B of oxidized LDL, are ligands for macrophage scavenger receptors", *Journal of lipid research,* vol. 41, no. 5, pp. 824-833.

Gorg, A., Postel, W. & Gunther, S. 1988, "The current state of two-dimensional electrophoresis with immobilized pH gradients", *Electrophoresis,* vol. 9, no. 9, pp. 531-546.

Grimsrud, P.A., Xie, H., Griffin, T.J. & Bernlohr, D.A. 2008, "Oxidative stress and covalent modification of protein with bioactive aldehydes", *The Journal of biological chemistry,* vol. 283, no. 32, pp. 21837-21841.

Gugiu, B.G., Mouillesseaux, K., Duong, V., Herzog, T., Hekimian, A., Koroniak, L., Vondriska, T.M. & Watson, A.D. 2008, "Protein targets of oxidized phospholipids in endothelial cells", *Journal of lipid research,* vol. 49, no. 3, pp. 510-520.

Halasiddappa, L.M., Koefeler, H., Futerman, A.H. & Hermetter, A. 2013, "Oxidized phospholipids induce ceramide accumulation in RAW 264.7 macrophages: role of ceramide synthases", *PloS one,* vol. 8, no. 7, pp. e70002.

Henry, B., Moller, C., Dimanche-Boitrel, M.T., Gulbins, E. & Becker, K.A. 2013, "Targeting the ceramide system in cancer", *Cancer letters,* vol. 332, no. 2, pp. 286-294.

Huang, W.C., Chen, C.L., Lin, Y.S. & Lin, C.F. 2011, "Apoptotic sphingolipid ceramide in cancer therapy", *Journal of lipids,* vol. 2011, pp. 565316.

Jego, G., Hazoume, A., Seigneuric, R. & Garrido, C. 2013, "Targeting heat shock proteins in cancer", *Cancer letters,* vol. 332, no. 2, pp. 275-285.

Jolly, C. & Morimoto, R.I. 2000, "Role of the heat shock response and molecular chaperones in oncogenesis and cell death", *Journal of the National Cancer Institute,* vol. 92, no. 19, pp. 1564-1572.

Kim, S.C., Sprung, R., Chen, Y., Xu, Y., Ball, H., Pei, J., Cheng, T., Kho, Y., Xiao, H., Xiao, L., Grishin, N.V., White, M., Yang, X.J. & Zhao, Y. 2006, "Substrate and functional diversity of lysine acetylation revealed by a proteomics survey", *Molecular cell,* vol. 23, no. 4, pp. 607-618.

Koller, D. 2013, *Effects of Oxidized Phospholipids on Gene Expression and Sphingolipid Metabolism in RAW 264.7 macrophages*, Technical University of Graz.

Kovacs, J.J., Murphy, P.J., Gaillard, S., Zhao, X., Wu, J.T., Nicchitta, C.V., Yoshida, M., Toft, D.O., Pratt, W.B. & Yao, T.P. 2005, "HDAC6 regulates Hsp90 acetylation and chaperone-dependent activation of glucocorticoid receptor", *Molecular cell,* vol. 18, no. 5, pp. 601-607.

Levy, M. & Futerman, A.H. 2010, "Mammalian ceramide synthases", *IUBMB life,* vol. 62, no. 5, pp. 347-356.

Loidl, A., Sevcsik, E., Riesenhuber, G., Deigner, H.P. & Hermetter, A. 2003, "Oxidized phospholipids in minimally modified low density lipoprotein induce apoptotic signaling via activation of acid sphingomyelinase in arterial smooth muscle cells", *The Journal of biological chemistry,* vol. 278, no. 35, pp. 32921-32928.

Lovat, P.E., Corazzari, M., Armstrong, J.L., Martin, S., Pagliarini, V., Hill, D., Brown, A.M., Piacentini, M., Birch-Machin, M.A. & Redfern, C.P. 2008, "Increasing melanoma cell death using inhibitors of protein disulfide isomerases to abrogate survival responses to endoplasmic reticulum stress", *Cancer research,* vol. 68, no. 13, pp. 5363-5369.

Malhotra, J.D. & Kaufman, R.J. 2007, "Endoplasmic reticulum stress and oxidative stress: a vicious cycle or a double-edged sword?", *Antioxidants & redox signaling,* vol. 9, no. 12, pp. 2277-2293.

Min, J., Mesika, A., Sivaguru, M., Van Veldhoven, P.P., Alexander, H., Futerman, A.H. & Alexander, S. 2007, "(Dihydro)ceramide synthase 1 regulated sensitivity to cisplatin is associated with the activation of p38 mitogen-activated protein kinase and is abrogated by sphingosine kinase 1", *Molecular cancer research : MCR,* vol. 5, no. 8, pp. 801-812.

Moenner, M., Pluquet, O., Bouchecareilh, M. & Chevet, E. 2007, "Integrated endoplasmic reticulum stress responses in cancer", *Cancer research,* vol. 67, no. 22, pp. 10631-10634.

Moumtzi, A., Trenker, M., Flicker, K., Zenzmaier, E., Saf, R. & Hermetter, A. 2007, "Import and fate of fluorescent analogs of oxidized phospholipids in vascular smooth muscle cells", *Journal of lipid research,* vol. 48, no. 3, pp. 565-582.

Muller, C., Bandemer, J., Vindis, C., Camare, C., Mucher, E., Gueraud, F., Larroque-Cardoso, P., Bernis, C., Auge, N., Salvayre, R. & Negre-Salvayre, A. 2013, "Protein disulfide isomerase modification and inhibition contribute to ER stress and apoptosis induced by oxidized low density lipoproteins", *Antioxidants & redox signaling,* vol. 18, no. 7, pp. 731-742.

Pabinger, S., Thallinger, G.G., Snajder, R., Eichhorn, H., Rader, R. & Trajanoski, Z. 2009, "QPCR: Application for real-time PCR data management and analysis", *BMC bioinformatics*, vol. 10, pp. 268-2105-10-268.

Ramprecht, C. 2013, *Toxicity of Oxidized Phospholipids in Cultured Skin Cancer Cell Lines*, Technical University of Graz.

Rao, R.V., Ellerby, H.M. & Bredesen, D.E. 2004, "Coupling endoplasmic reticulum stress to the cell death program", *Cell death and differentiation*, vol. 11, no. 4, pp. 372-380.

Raturi, A. & Mutus, B. 2007, "Characterization of redox state and reductase activity of protein disulfide isomerase under different redox environments using a sensitive fluorescent assay", *Free radical biology & medicine*, vol. 43, no. 1, pp. 62-70.

Rheinwald, J.G. & Beckett, M.A. 1981, "Tumorigenic keratinocyte lines requiring anchorage and fibroblast support cultured from human squamous cell carcinomas", *Cancer research*, vol. 41, no. 5, pp. 1657-1663.

Rhode, S., Grurl, R., Brameshuber, M., Hermetter, A. & Schutz, G.J. 2009, "Plasma membrane fluidity affects transient immobilization of oxidized phospholipids in endocytotic sites for subsequent uptake", *The Journal of biological chemistry*, vol. 284, no. 4, pp. 2258-2265.

Sano, R. & Reed, J.C. 2013, "ER stress-induced cell death mechanisms", *Biochimica et biophysica acta*, vol. 1833, no. 12, pp. 3460-3470.

Sanson, M., Auge, N., Vindis, C., Muller, C., Bando, Y., Thiers, J.C., Marachet, M.A., Zarkovic, K., Sawa, Y., Salvayre, R. & Negre-Salvayre, A. 2009, "Oxidized low-density lipoproteins trigger endoplasmic reticulum stress in vascular cells: prevention by oxygen-regulated protein 150 expression", *Circulation research*, vol. 104, no. 3, pp. 328-336.

Schmitt, E., Gehrmann, M., Brunet, M., Multhoff, G. & Garrido, C. 2007, "Intracellular and extracellular functions of heat shock proteins: repercussions in cancer therapy", *Journal of leukocyte biology*, vol. 81, no. 1, pp. 15-27.

Schumacher, R.J., Hurst, R., Sullivan, W.P., McMahon, N.J., Toft, D.O. & Matts, R.L. 1994, "ATP-dependent chaperoning activity of reticulocyte lysate", *The Journal of biological chemistry*, vol. 269, no. 13, pp. 9493-9499.

Semini, G., Klein, A. & Danker, K. 2011, "Impact of alkylphospholipids on the gene expression profile of HaCaT cells", *Pharmacogenetics and genomics*, vol. 21, no. 7, pp. 375-387.

Shevchenko, A., Wilm, M., Vorm, O. & Mann, M. 1996, "Mass spectrometric sequencing of proteins silver-stained polyacrylamide gels", *Analytical Chemistry*, vol. 68, no. 5, pp. 850-858.

Sidera, K. & Patsavoudi, E. 2014, "HSP90 inhibitors: current development and potential in cancer therapy", *Recent patents on anti-cancer drug discovery*, vol. 9, no. 1, pp. 1-20.

Stemmer, U., Dunai, Z.A., Koller, D., Purstinger, G., Zenzmaier, E., Deigner, H.P., Aflaki, E., Kratky, D. & Hermetter, A. 2012, "Toxicity of oxidized phospholipids in cultured macrophages", *Lipids in health and disease,* vol. 11, pp. 110-511X-11-110.

Stemmer, U., Ramprecht, C., Zenzmaier, E., Stojcic, B., Rechberger, G., Kollroser, M. & Hermetter, A. 2012, "Uptake and protein targeting of fluorescent oxidized phospholipids in cultured RAW 264.7 macrophages", *Biochimica et biophysica acta,* vol. 1821, no. 4, pp. 706-718.

Subbanagounder, G., Watson, A.D. & Berliner, J.A. 2000, "Bioactive products of phospholipid oxidation: isolation, identification, measurement and activities", *Free radical biology & medicine,* vol. 28, no. 12, pp. 1751-1761.

Thulasiraman, V. & Matts, R.L. 1998, "Luciferase renaturation assays of chaperones and chaperone antagonists", *Methods in molecular biology (Clifton, N.J.),* vol. 102, pp. 129-141.

Uemura, A., Oku, M., Mori, K. & Yoshida, H. 2009, "Unconventional splicing of XBP-1 mRNA occurs in the cytoplasm during the mammalian unfolded protein response", *Journal of cell science,* vol. 122, no. Pt 16, pp. 2877-2886.

van Blitterswijk, W.J. & Verheij, M. 2013, "Anticancer mechanisms and clinical application of alkylphospholipids", *Biochimica et biophysica acta,* vol. 1831, no. 3, pp. 663-674.

Watson, A.D., Leitinger, N., Navab, M., Faull, K.F., Horkko, S., Witztum, J.L., Palinski, W., Schwenke, D., Salomon, R.G., Sha, W., Subbanagounder, G., Fogelman, A.M. & Berliner, J.A. 1997, "Structural identification by mass spectrometry of oxidized phospholipids in minimally oxidized low density lipoprotein that induce monocyte/endothelial interactions and evidence for their presence in vivo", *The Journal of biological chemistry,* vol. 272, no. 21, pp. 13597-13607.

Wilkinson, B. & Gilbert, H.F. 2004, "Protein disulfide isomerase", *Biochimica et biophysica acta,* vol. 1699, no. 1-2, pp. 35-44.

Zarkovic, N., Cipak, A., Jaganjac, M., Borovic, S. & Zarkovic, K. 2013, "Pathophysiological relevance of aldehydic protein modifications", *Journal of proteomics,* vol. 92, pp. 239-247.

Appendix

Protein targets of BY-POVPE in cultured RAW 264.7 macrophages

4.1 Expression of RFP-constructs of selected target protein candidates in RAW 264.7 macrophages

To visualize adduct formation between cellular proteins and oxPL, RAW 264.7 macrophages were incubated with BY-POVPE as a fluorescently labeled analog of POVPC. This aldehydo-phospholipid can undergo Schiff base formation with -NH_2 groups of proteins, thus forming covalent lipid-protein adducts. Chemically stabilized lipid-protein conjugates were identified by MS/MS followed by database search. The study revealed that protein targeting by POVPC is a selective process, since only a limited subfraction of the total proteome is targeted by the fluorescent lipid. The proteins that were identified by this method are involved in apoptosis, stress response, lipid metabolism and transport. (Stemmer *et al.*, 2012)

Selected target protein candidates were cloned into a vector encoding for RFP (pTagRFP-N1). For experimental details see 2.3 Materials and Methods. The aim of this study was to identify potential interactions between specific target proteins and fluorescently labeled lipids in live cells. For this purpose, macrophages expressing fluorescent fusion proteins were incubated with fluorescently labeled oxPL (BY-POVPE or BY-PGPE). A typical experiment has already been performed with PKCδ-RFP in the laboratory of Martin Hof (Heyrovský Institute of Physical Chemistry, Academy of Sciences of the Czech Republic, Prague, Czech Republic). Codiffusion of fluorescent proteins and oxPL has been tracked using single molecule microscopy. The results of the two-color cross-correlation number and brightness (ccN&B) analysis are shown in Figure 2.8 and Table 2.1. The intracellular interaction of additional fluorescent target proteins and fluorescent oxPL is subject of ongoing work.

In Table 4.1, a complete list of the vector constructs encoding for RFP fusion proteins with the target proteins PKCδ, 14-3-3ζ, p21 activated kinase, SYK, Stomatin, Histone H4, Vdac-1, Hsp90, Hsp72, CathD and aSMase can be found. Additional information about the respective gene identification numbers (GI numbers) and the sizes of the sequences cloned into the vector pTagRFP-N1 is provided in Table 4.1. Information

about the expression levels of the fusion proteins in RAW 264.7 cells and the subcellular localizations in literature and in our experiments are listed in Table 4.1. The fluorescence pattern of cells expressing RFP-tagged fusion proteins of PKCδ, 14-3-3ζ, p21 activated kinase, SYK, Stomatin, Histone H4, Vdac-1 and Hsp90 are shown in Table 4.2.

Table 4.1 List of vector constructs.

Selected target protein candidates were cloned into a vector encoding for RFP (pTagRFP-N1). For experimental details see 2.3 Materials and Methods. For each protein cloned into the vector, information is provided about GI number, full protein name and size of the DNA sequence encoding for the respective protein. Additional information is provided about the cellular localizations and expression levels of the respective fusion proteins in RAW 264.7 cells.

	GI number, protein name	**Size**	**Cellular localization *in literature* *(in transfected cells)***	**Expression level**
Vector pTagRFP-N1	purchased from Evrogen	Vector: 4,7 kb	*Cytoplasm (Cytoplasm)*	+++
PKCδ	>gi|118130235, protein kinase C delta (Prkcd)	Insert: 2 kb	*Cytoplasm (Cytoplasm)*	+++
14-3-3ζ	>gi|274321230, tyrosine 3-monooxygenase	Insert: 0,7 kb	*Cytoplasm (Cytoplasm)*	+++
p21 activated kinase	>gi|56118303, p21 protein (Cdc42/Rac)-activated kinase 2	Insert: 1,6 kb	*Cytoplasm (Cytoplasm)*	+++

Continued on the following page

SYK	>gi|56550044, spleen tyrosine kinase (Sykb)	Insert: 1,9 kb	*Cytoplasm (Cytoplasm)*	+++
Stomatin	>gi|118129913 stomatin (Stom)	Insert: 0,85 kb	*PM (PM, nuclear membrane)*	++
Histone H4	>gi|339895742, histone cluster 4 H4 (Hist4h4)	Insert: 0,3 bp	*Nucleus (partly in nucleus)*	++
Vdac-1	>gi|158508670, voltage-dependent anion channel 1	Insert: 0,85 kb	*OMM, PM (PM)*	+
Hsp90	>gi|6755862, heat shock protein 90 beta (Grp94)	Insert: 2,4 kb	*ER lumen (Cytoplasm)*	+
Hsp72	>gi|74198977, heat shock protein 8 (Hsc70)	Insert: 1,9 kb	Cytoplasm (Cytoplasm)	~
CathD	>gi|21450788, cathepsin D (Ctsd)	Insert: 1,2 kb	Lysosome	~
aSMase	>gi|254750745, Acid sphingo-myelinase, lysosomal (Smpd1)	Insert: 1,9 kb	Lysosome (Cytoplasm)	~

+++ very good expression
++ good expression
+ weak expression
~ hardly expressed, cytotoxic

Table 4.2 Subcellular localization of RFP-tagged fusion proteins in RAW 264.7 macrophages and Cos-7 cells.

RAW 264.7 macrophages and Cos-7 cells (only Vdac-1) were transfected with vectors encoding for RFP fusion proteins with PKCδ, 14-3-3ζ, p21 activated kinase, SYK, Stomatin, Histone H4, Vdac-1 and Hsp90 (vectors are listed in Table 4.1). Cells transfected with the empty vector pTagRFP-N1 express RFP alone. After 24 h, expression of the fluorescent fusion proteins was observed under a fluorescence microscope. Transmission and fluorescence images of the same sections were collected at the same time.

	Fluorescence micrographs	Transmission micrographs
Vector pTagRFP-N1 (100x)	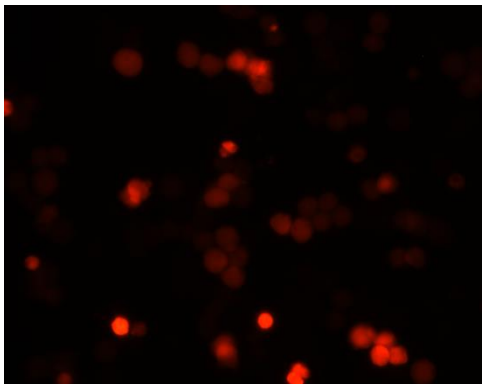	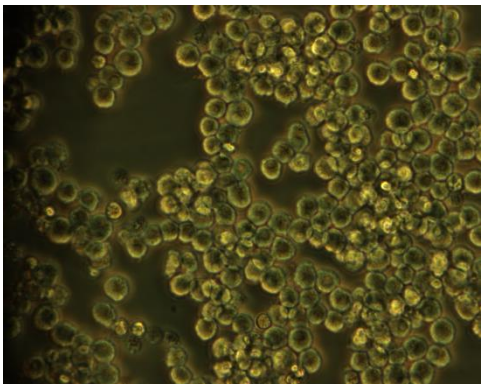
PKCδ (100x)	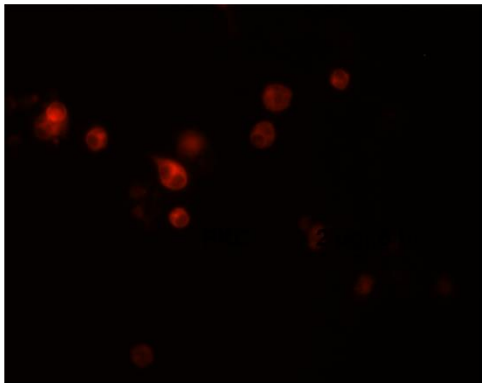	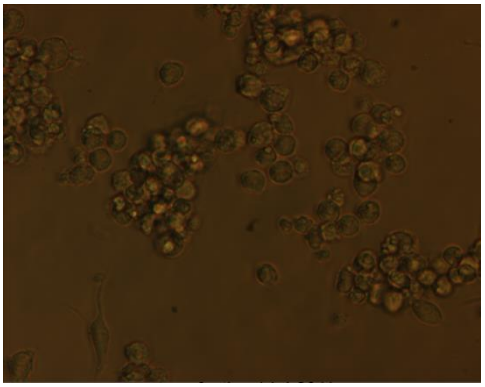

Continued on the following page

14-3-3ζ (400x)	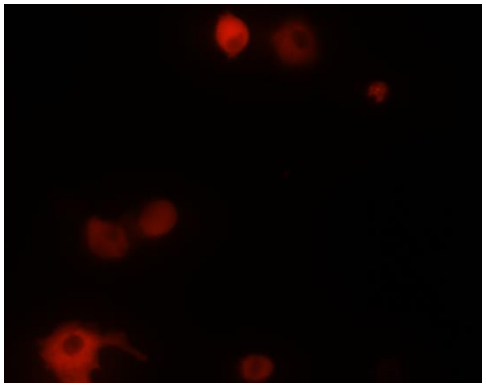	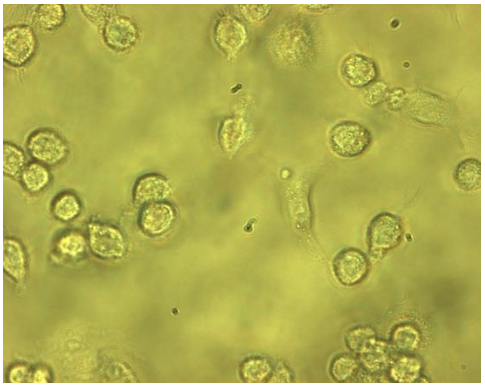
p21 activated kinase (400x)	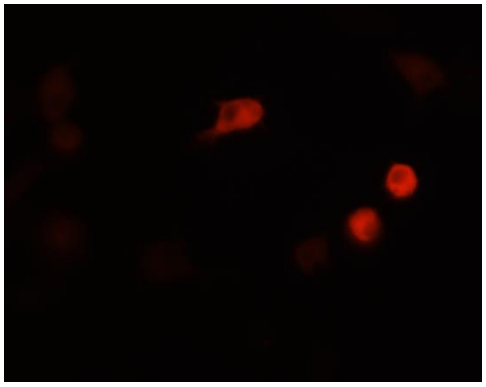	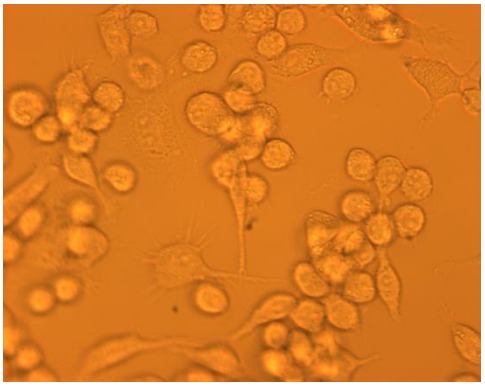
SYK (400x)	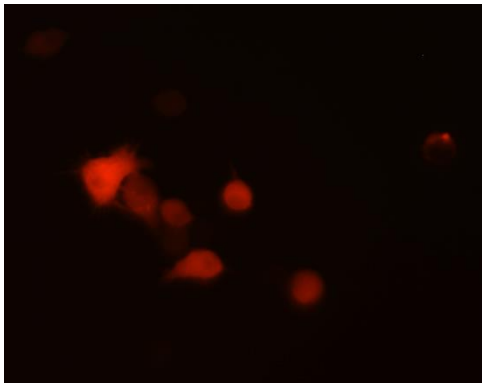	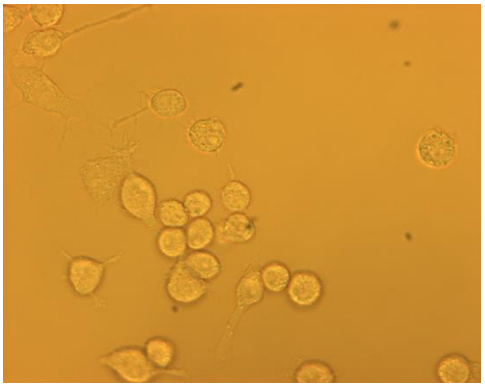
Stomatin (400x)	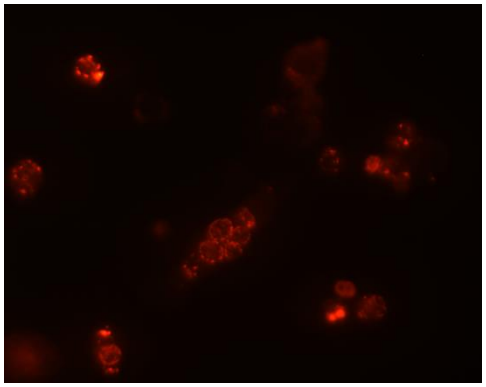	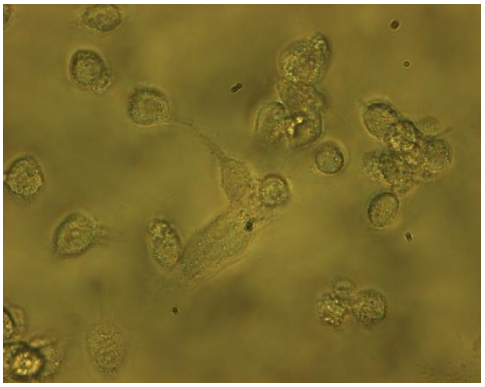

Continued on the following page

H4 (400x)	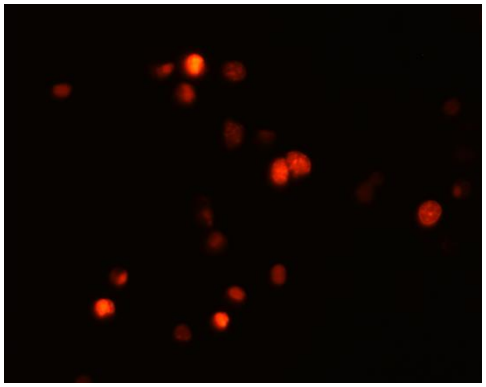	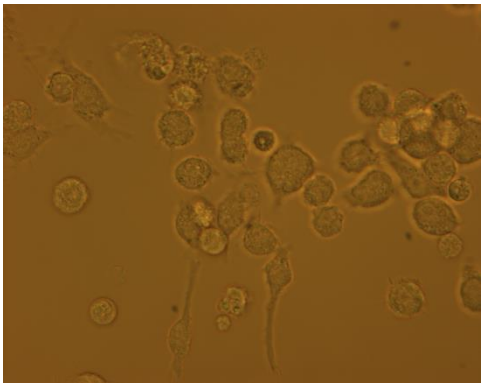
Vdac-1 (100x)	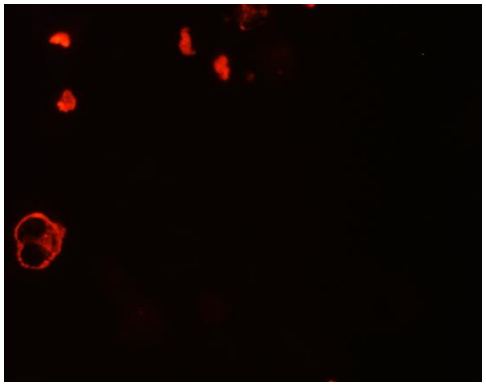	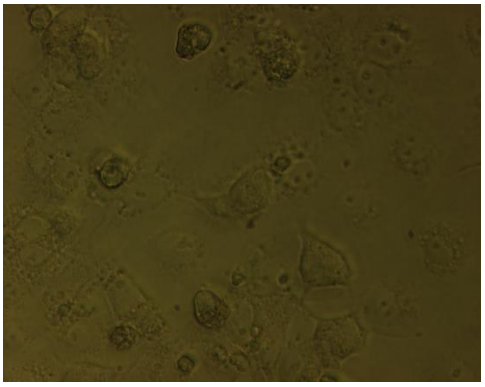
Hsp90 (100x)	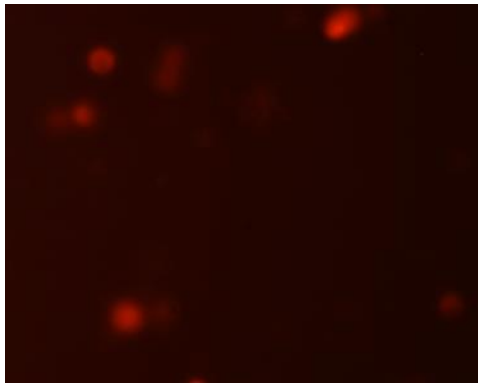	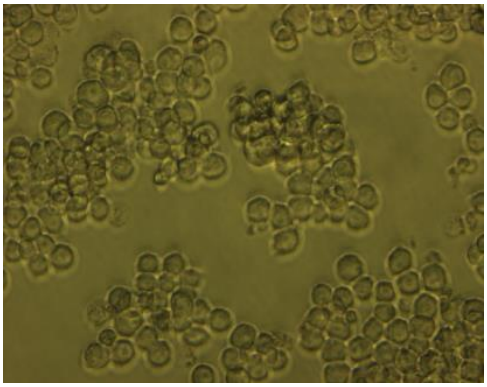

4.2 Function of protein targets: A literature survey

Selected protein targets of BY-POVPE have been cloned into the vector pTagRFP-N1 (Table 4.1). The respective candidates have been identified in total cell lysates and total membrane fractions of RAW 264.7 macrophages after incubation with BY-POVPE (Stemmer *et al.*, 2012). These proteins were chosen because they seem to be particularly relevant to cell death and apoptosis. Here, a short literature review about the functions of PKCδ, 14-3-3ζ, p21 activated kinase, SYK, Stomatin, Histone H4, Vdac-1, Hsp90, Hsp72, CathD and aSMase is given.

Protein kinase C-delta (PKCδ) acts as a pro- or anti-apoptotic kinase, depending on the cell type and stimulus. Chapter 2 provides a detailed study on the contribution of this enzyme to oxPL-induced apoptosis in RAW 264.7 macrophages. Other groups have already shown that PKCδ seems to be a key signaling element in oxLDL-induced apoptosis in vascular smooth muscle cells (Larroque-Cardoso *et al.*, 2013) as well as in J774A.1 macrophages (Giovannini *et al.*, 2011).

Apoptotic signaling of PKCδ is connected to other signaling molecules (Figure 2.10) that are also identified targets of BY-POVPE in macrophages: i.) caspase-3, ii.) 14-3-3ζ and iii.) Cathepsin D. i.) Caspase-3 may be activated by PKCδ-mediated phosphorylation (Voss *et al.*, 2005). ii.) Active caspase-3, on the other hand, can cleave PKCδ (Kato *et al.*, 2009) leading to the formation of an enzyme fragment that promotes apoptosis via 14-3-3ζ monomerization (Hamaguchi *et al.*, 2003). Furthermore, PKCδ can phosphorylate aSMase (Zeidan and Hannun, 2007) leading to its activation and the formation of the apoptotic mediator ceramide. iii.) Ceramide, in turn, binds to the lysosomal aspartic protease Cathepsin D. This interaction induces the cleavage of the pro-enzyme. The active form of Cathepsin D activates components involved in the mitochondrial apoptosis pathway. Several reports have demonstrated that cytochrome c release and caspase activation are downstream of cathepsin D activation. (Pettus *et al.*, 2002)

Spleen tyrosine kinase (SYK) is another protein target of BY-POVPE in RAW 264.7 macrophages. This enzyme has been shown to be activated by mmLDL in macrophages leading to ROS generation (Bae *et al.*, 2009).

Other protein target candidates expressed as RFP fusion proteins were: Vdac-1 and Stomatin. Both are membrane proteins and therefore easily accessible for oxPL if exogenously added to cells. Voltage dependent anion channel 1 (Vdac-1) is involved in mitochondrial apoptosis, since it regulates the release of cytochrome c (Abu-Hamad *et al.*, 2009). Stomatin is a lipid raft protein (Umlauf *et al.*, 2006). No information is available about its possible role in apoptosis.

Many of the identified oxPL target proteins are subject to modification by other lipid electrophiles than POVPC: Hsp90 (Carbone *et al*., 2005), Hsp72 (Carbone *et al*., 2004) and Cathepsin B (Crabb *et al.*, 2002) have been shown to be modified by 4-HNE at specific cysteine residues. Evidence has been provided that these modifications result in decreased enzymatic activities of the proteins. Chapter 3 includes an experiment with the aim to identify the impact of oxPL on the enzymatic activity of molecular chaperones *in vitro* (Figure 3.3).

Elevated intracellular and extracellular levels of molecular chaperones have been found at in atherosclerotic lesions. Upregulation of Hsp expression could contribute to the cellular response to oxidative stress. Soluble extracellular Hsps bind to Toll-like receptors. Thereby they contribute to inflammation in the atherosclerotic lesion by the initiation of an immune response. High titers of autoantibodies against Hsps have been found in the blood of patients with arteriosclerosis (Xu *et al.*, 2012; Xu, 2002; Snoeckx *et al.*, 2001). From these reports, it can be inferred that Hsps play an important role in arteriosclerosis. For these reasons we have included these proteins in our studies to investigate the impact of oxPL on the enzymatic activity of molecular chaperones (see Chapter 3).

In a global proteomic study, Kim *et al.* (2006) identified the cellular proteins that are acetylated at lysine residues. Interestingly, there is a huge overlap between the identified proteins in their study and the protein targets of BY-POVPE we found in RAW 264.7 macrophages: Kim *et al.* identified Hsps from the Hsp90 and Hsp70

families, histones and protein kinase C. Lysine acetylation in these proteins regulates several cellular processes including vesicle fusion, cytoskeleton dynamics and stress response (Sadoul *et al.*, 2011). It is well known that transcriptional regulation is largely mediated by histone acetylation and deacetylation (Grunstein, 1997). Many other proteins are also dynamically acetylated at specific lysines, and thereby influenced with respect to structure and function. For instance, Hsp90 can be acetylated at several lysine residues and its acetylation pattern determines its activation state (Sadoul *et al.*, 2011).

We speculate that the hydrophilic lysine residues, that are prone to acetylation, are available for phospholipid aldehyde modification, too. Lysine acetylation of cellular proteins regulates their function in many cellular processes. It remains to be elucidated to what extent lysine modification by oxPL interferes with enzyme function and activity. Alkylation of proteins by aldehydo-oxPL, e.g. POVPC, not only removes the "free" positively charged lysines at a protein. Modification with aldehydo-oxPL also renders the protein more hydrophobic, functioning as a lipid anchor for association with membranes. Thus, the impact of oxPL modification of proteins is twofold, since it leads to functional consequences on the molecular and supramolecular level.

4.3 References Appendix

Abu-Hamad, S., Arbel, N., Calo, D., Arzoine, L., Israelson, A., Keinan, N., Ben-Romano, R., Friedman, O. & Shoshan-Barmatz, V. 2009, "The VDAC1 N-terminus is essential both for apoptosis and the protective effect of anti-apoptotic proteins", *Journal of cell science,* vol. 122, no. Pt 11, pp. 1906-1916.

Bae, Y.S., Lee, J.H., Choi, S.H., Kim, S., Almazan, F., Witztum, J.L. & Miller, Y.I. 2009, "Macrophages generate reactive oxygen species in response to minimally oxidized low-density lipoprotein: toll-like receptor 4- and spleen tyrosine kinase-dependent activation of NADPH oxidase 2", *Circulation research,* vol. 104, no. 2, pp. 210-8, 21p following 218.

Carbone, D.L., Doorn, J.A., Kiebler, Z., Ickes, B.R. & Petersen, D.R. 2005, "Modification of heat shock protein 90 by 4-hydroxynonenal in a rat model of chronic alcoholic liver disease", *The Journal of pharmacology and experimental therapeutics,* vol. 315, no. 1, pp. 8-15.

Carbone, D.L., Doorn, J.A., Kiebler, Z., Sampey, B.P. & Petersen, D.R. 2004, "Inhibition of Hsp72-mediated protein refolding by 4-hydroxy-2-nonenal", *Chemical research in toxicology,* vol. 17, no. 11, pp. 1459-1467.

Crabb, J.W., O'Neil, J., Miyagi, M., West, K. & Hoff, H.F. 2002, "Hydroxynonenal inactivates cathepsin B by forming Michael adducts with active site residues", *Protein science : a publication of the Protein Society,* vol. 11, no. 4, pp. 831-840.

Giovannini, C., Vari, R., Scazzocchio, B., Sanchez, M., Santangelo, C., Filesi, C., D'Archivio, M. & Masella, R. 2011, "OxLDL induced p53-dependent apoptosis by activating p38MAPK and PKCdelta signaling pathways in J774A.1 macrophage cells", *Journal of molecular cell biology,* vol. 3, no. 5, pp. 316-318.

Grunstein, M. 1997, "Histone acetylation in chromatin structure and transcription", *Nature,* vol. 389, no. 6649, pp. 349-352.

Hamaguchi, A., Suzuki, E., Murayama, K., Fujimura, T., Hikita, T., Iwabuchi, K., Handa, K., Withers, D.A., Masters, S.C., Fu, H. & Hakomori, S. 2003, "Sphingosine-dependent protein kinase-1, directed to 14-3-3, is identified as the kinase domain of protein kinase C delta", *The Journal of biological chemistry,* vol. 278, no. 42, pp. 41557-41565.

Kato, K., Yamanouchi, D., Esbona, K., Kamiya, K., Zhang, F., Kent, K.C. & Liu, B. 2009, "Caspase-mediated protein kinase C-delta cleavage is necessary for apoptosis of vascular smooth muscle cells", *American journal of physiology.Heart and circulatory physiology,* vol. 297, no. 6, pp. H2253-61.

Kim, S.C., Sprung, R., Chen, Y., Xu, Y., Ball, H., Pei, J., Cheng, T., Kho, Y., Xiao, H., Xiao, L., Grishin, N.V., White, M., Yang, X.J. & Zhao, Y. 2006, "Substrate and functional

diversity of lysine acetylation revealed by a proteomics survey", *Molecular cell,* vol. 23, no. 4, pp. 607-618.

Larroque-Cardoso, P., Swiader, A., Ingueneau, C., Negre-Salvayre, A., Elbaz, M., Reyland, M.E., Salvayre, R. & Vindis, C. 2013, "Role of protein kinase C delta in ER stress and apoptosis induced by oxidized LDL in human vascular smooth muscle cells", *Cell death & disease,* vol. 4, pp. e520.

Pettus, B.J., Chalfant, C.E. & Hannun, Y.A. 2002, "Ceramide in apoptosis: an overview and current perspectives", *Biochimica et biophysica acta,* vol. 1585, no. 2-3, pp. 114-125.

Sadoul, K., Wang, J., Diagouraga, B. & Khochbin, S. 2011, "The tale of protein lysine acetylation in the cytoplasm", *Journal of biomedicine & biotechnology,* vol. 2011, pp. 970382.

Snoeckx, L.H., Cornelussen, R.N., Van Nieuwenhoven, F.A., Reneman, R.S. & Van Der Vusse, G.J. 2001, "Heat shock proteins and cardiovascular pathophysiology", *Physiological Reviews,* vol. 81, no. 4, pp. 1461-1497.

Stemmer, U. & Hermetter, A. 2012, "Protein modification by aldehydophospholipids and its functional consequences", *Biochimica et biophysica acta,* vol. 1818, no. 10, pp. 2436-2445.

Umlauf, E., Mairhofer, M. & Prohaska, R. 2006, "Characterization of the stomatin domain involved in homo-oligomerization and lipid raft association", *The Journal of biological chemistry,* vol. 281, no. 33, pp. 23349-23356.

Voss, O.H., Kim, S., Wewers, M.D. & Doseff, A.I. 2005, "Regulation of monocyte apoptosis by the protein kinase Cdelta-dependent phosphorylation of caspase-3", *The Journal of biological chemistry,* vol. 280, no. 17, pp. 17371-17379.

Xu, Q. 2002, "Role of heat shock proteins in atherosclerosis", *Arteriosclerosis, Thrombosis, and Vascular Biology,* vol. 22, no. 10, pp. 1547-1559.

Xu, Q., Metzler, B., Jahangiri, M. & Mandal, K. 2012, "Molecular chaperones and heat shock proteins in atherosclerosis", *American journal of physiology.Heart and circulatory physiology,* vol. 302, no. 3, pp. H506-14.

Zeidan, Y.H. & Hannun, Y.A. 2007, "Activation of acid sphingomyelinase by protein kinase Cdelta-mediated phosphorylation", *The Journal of biological chemistry,* vol. 282, no. 15, pp. 11549-11561.